Available online at www.sciencedirect.com
ScienceDirect
Marine and Petroleum Geology 24 (2007) 341–387
Marine and Petroleum Geology
www.elsevier.com/locate/marpetgeo

Sinuous deep-water channels: Genesis, geometry and architecture

Russell B. Wynn[a,*], Bryan T. Cronin[b], Jeff Peakall[c]

[a]National Oceanography Centre, European Way, Southampton SO14 3ZH, UK
[b]Deep Marine, 9 North Square, Footdee, Aberdeen AB11 5DX, UK
[c]School of Earth and Environment, Leeds University, Leeds LS2 9JT, UK

Received 21 May 2007; accepted 2 June 2007

Abstract

Sinuous deep-water channels display a wide range of geometries and internal architectures. Most modern examples have been documented from large passive-margin fans, supplied by major rivers carrying huge volumes of dominantly fine-grained sediments, e.g. Amazon, Mississippi, Zaire, Bengal, Indus, Rhône and Nile Fans. However, similar examples have also been documented from tectonically active margins, e.g. Magdalena Fan. In most cases, modern sinuous channels comprise the core element of laterally extensive channel–levee systems that often aggrade significantly above a low-gradient (0.1–0.5°) fan surface; individual channels may extend downslope for 100s of kilometres. Typically, channels are subject to frequent avulsions, with only one channel active at any given time. Present highstand conditions have ensured that activity in many modern sinuous channels is much reduced due to the disconnect between fluvial feeder system and canyon head, and some have even been heavily modified or destroyed by major mass-transport deposits. Exceptions include Zaire Fan, where recent activity has provided useful insights into flow processes.

The majority of detailed studies relating to sinuous channels in the subsurface originate from offshore west Africa, where channels typically occur within incisional (confined) slope–channel complexes and often represent the latter stages of channel complex fill. Both dominantly aggradational and laterally migrating styles are recognised, while modern seafloor channels in this region display a similar incisional character, e.g. Cap Timiris Canyon. Morphologic expression of sinuosity is harder to recognise at outcrop, but there are an increasing number of documented examples of lateral accretion deposits, representing point-bar growth, that are currently thought to be diagnostic of sinuous channel forms. Sinuous channel lateral migration, and point-bar growth, appears to be driven by sustained flow of fluvial-sourced (probably hyperpycnal) low-density turbidity currents, although there does appear to be variation in energy conditions, with some outcrop examples showing switches in erosive and depositional phases of activity.

Previous studies have frequently focussed on the obvious gross planform morphologic similarities between fluvial and deep-water sinuous channels, e.g. nature of sinuosity, presence of point bars and cut-off loops. However, we suggest here that the differences between submarine and river channels are of greater significance, in terms of geometry, flow processes, migration style and deposit character. Sinuous deep-water channels typically form initially by a moderate amount of incision followed by rapid initial bend growth (associated with bypass of sediment). Channels that show significant aggradation then reach a point where there is a near cessation of planform movement (ossification), and growth is dominated by vertical aggradation. A new process model is proposed for this developmental sequence that synthesises observations and experiments that were previously paradoxical.
© 2007 Elsevier Ltd. All rights reserved.

Keywords: Sinuous channels; Channel–Levee systems; Turbidites; Submarine fans; Turbidity currents

1. Introduction

In 2005 a conference with the theme of 'Sinuous deep-water channels: genesis, geometry and architecture' was held in Southampton, UK. The aim was to stimulate discussion between researchers of sinuous channels across academia and industry, whether their speciality was modern deep-water systems, outcrop studies, subsurface reservoirs or experimental and numerical flow modelling. The most tangible outcome of this successful and informative meeting was the publication of a series of papers in a special issue of Marine and Petroleum Geology (this issue). This particular journal was an obvious choice

*Corresponding author. Tel.: +44 2380 596 553; fax: +44 2380 596 554.
E-mail address: rbw1@noc.soton.ac.uk (R.B. Wynn).

0264-8172/$ - see front matter © 2007 Elsevier Ltd. All rights reserved.
doi:10.1016/j.marpetgeo.2007.06.001

to host this series; indeed, almost 10% of the references cited in this introductory paper were published in Marine and Petroleum Geology!

The publication of this special issue is particularly timely; sinuous channels host significant hydrocarbon reserves on a variety of continental margins (Mayall et al., 2006); they are major conduits for transfer of sediments (and associated pollutants and organic carbon) from continental shelf to deep ocean (Khripounoff et al., 2003); and understanding mechanics of flows that initiate and shape these impressive seafloor features is a first-order scientific challenge (Peakall et al., 2000a; Corney et al., 2006), with additional implications for submarine geohazard assessment (Bruschi et al., 2006).

The aims of this introductory paper are three-fold: (1) provide an up-to-date summary of the terms and definitions used in study of deep-water sinuous channels, in order to ensure clarity and correct usage, (2) provide an overview of sinuous deep-water channels in modern, outcrop and subsurface systems (Fig. 1), and modelling of the flows that erode and fill them, and (3) discuss some of the outstanding issues in this rapidly moving research field, and suggest ways in which we may develop our understanding of deep-water sinuous channels through future data collection.

1.1. Terminology and definitions

Students of deep-water channels are faced by a potentially bewildering array of terms and definitions, relating to both overall channel morphology (e.g. canyon, channel, fan valley) and erosional and depositional features inside and outside of channels (e.g. levees, inner levees, terraces). Here, we attempt to provide simple definitions for the terms used in this paper that relate to sinuous deep-water channels. We will not discuss the variety of gravity flow processes that generate, maintain and modify submarine channels, as this has been covered in detail elsewhere (e.g. Normark and Piper, 1991; Clark and Pickering, 1996a; Peakall et al., 2000a; Mulder and Alexander, 2001; Kneller, 2003; Mulder et al., 2003; Pirmez and Imran, 2003).

1.1.1. Sinuous deep-water channels

In this study we are concerned with *deep-water* channels, i.e. those that occur on the continental slope and rise beyond the shelf edge (typically in water depths (WDs) >100–200 m and commonly between 1 and 4 km). Channel *sinuosity* is measured as the ratio between the channel axis (centre line) length and the overall down-channel distance for a given section of channel. A sinuosity of 1 therefore represents a straight section of channel, with increasing values representing increasing sinuosity. For the purposes of this paper, we define a truly *sinuous* channel as one that displays a minimum average sinuosity of 1.2. This is comparable to the figure of ~1.15 used by Clark et al. (1992) and Clark and Pickering (1996). It should be noted that maximum sinuosities of relatively straight channels may locally exceed 1.2, and also that some sinuous channels display peak sinuosities well in excess of this figure. Different causes of sinuosity in channels are discussed by Mayall et al. (2006).

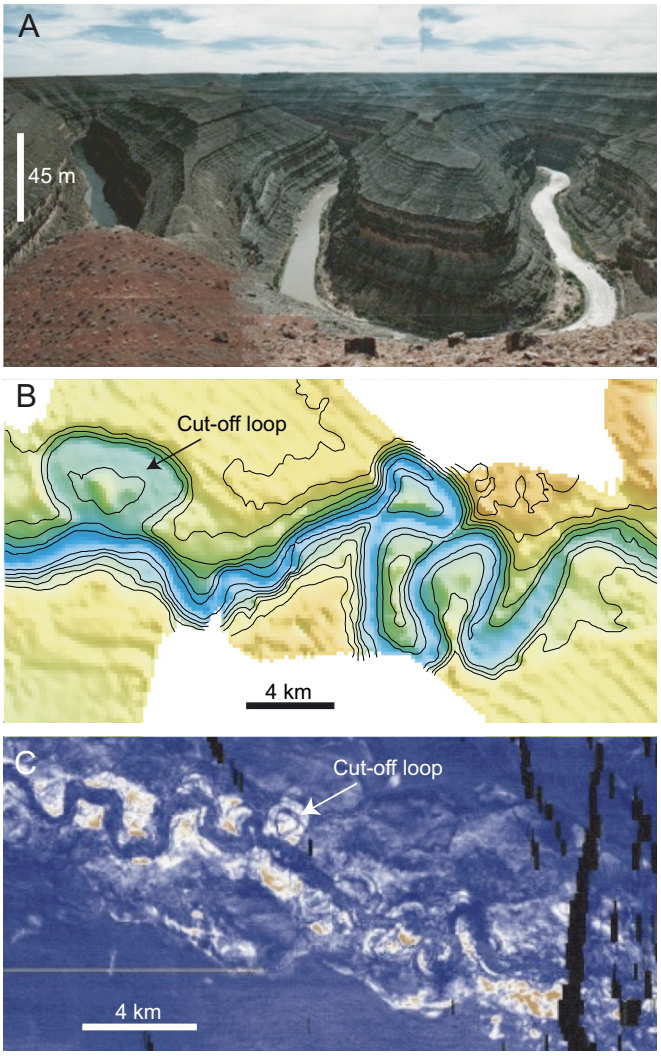


Fig. 1. The nature of submarine channel sinuosity is better understood by comparing all scales of data available, and through use of analogues: (A) entrenched, highly sinuous loop in a subaerial 'badlands' river system of southern Utah, USA; (B) Hydrosweep 3D multibeam bathymetry image, showing highly sinuous planform of Cap Timiris Canyon, offshore Mauritania, at water depths of ~2700 m, (modified from Krastel et al., 2004); (C) 3D seismic horizon slice through subsurface sinuous channel, offshore West Africa; red = high amplitude, blue = low amplitude (Cronin, unpublished data courtesy of Eni Agip S.p.A.).

For an overview of the parameters that are typically measured for sinuous channels, e.g. *radius of curvature* and *wavelength of sinuous loops*, see Flood and Damuth (1987). Channel *migration* is often represented by *swing* (i.e. lateral sinuous loop migration and/or expansion) or *sweep* (i.e. down-system sinuous loop migration) (Peakall et al., 2000a; Posamentier, 2003). It should be noted that, following Peakall et al. (2000a), we have generally avoided use of the term 'meandering' throughout this paper; this

term implies that channels 'wander at random', which is not correct in most cases.

Clear definition of what constitutes a *channel* is not always straightforward, as (1) channels often gradually merge upslope into canyons, (2) they are morphologically highly variable (e.g. Mayall et al., 2006), being V- or U-shaped in cross-section with or without depositional margins (*levees*) and (3) different authors use terms such as 'fan valley' or 'valley' in place of channel. *Canyons* typically occur on the upper slope and connect directly to the shelf edge; they are generally narrow and V-shaped, incised into lithified rock or sediment and display greater cross-sectional areas and higher axial gradients than channels. However, the dividing line between canyon and channel is blurred, and a small number of examples discussed in this paper could be classified as either canyon or channel. Further discussion of channel morphologies can be found in Shepard (1965) and Clark and Pickering (1996a, b).

Channels, and their flanking levees, are commonly referred to as *channel–levee systems* (Flood and Damuth, 1987). These often coalesce and overlap to form *channel–levee complexes*, which are the building blocks of many major *submarine fans*, including those discussed in Section 2.

1.1.2. Features within channels

Channel floors are often incised by a relatively narrow 'inner' channel called the *thalweg*, while coarse-grained channel-fill deposits often generate *high-amplitude reflectors* (*HARs*) on seismic profiles. *High-amplitude reflector packages* (*HARPs*) commonly occur at the bases of channel–levee systems, and represent relatively coarse-grained, unconfined deposits that accumulate in lows between channel–levee systems (Flood et al., 1991); they typically result from channel wall *breaching* and switching (*avulsion*) events. The points where channels separate (*bifurcate*) are sometime called *avulsion nodes*.

Channel floors are host to a complex interplay of erosional and depositional processes; consequently, a range of features can be observed, depending on the level of data resolution available. Large-scale (10s to 100s of metres) *erosional scours* and *depositional bedforms*, e.g. *coarse-grained sediment waves* (Wynn et al., 2002a, b) are often widespread, together with smaller-scale (centimetres to metres) features such as *current ripples, dunes* and *flute marks*. A characteristic feature of sinuous channels are depositional *point bars* on the inside of sinuous loops, which can amalgamate during channel lateral migration to form *lateral accretion packages/deposits* (*LAPs/LADs*: Abreu et al., 2003; Arnott, this issue). In planform these display a concentric pattern referred to as *scroll bars*. *Knickpoints* represent marked changes in the channel longitudinal profile (Heinio and Davies, this issue), and can form in response to avulsion events or rapid changes in *base level* (Pirmez et al., 2000; Kneller, 2003) Sand-rich *nested mounds* on channel floors have been interpreted in terms of two different processes; (1) from anomalously large turbidity currents *overspilling* the channel margin at sharp bends and losing significant momentum (Clark and Pickering, 1996; Peakall et al., 2000a, b) and (2) in response to channel levee/bank collapse (Peakall et al., 2000b, this issue).

1.1.3. Features on channel margins

The inner margins of sinuous channels often display a stepped profile in cross-section due to the presence of *intra-channel terraces*. These may form through a variety of processes, including multiple phases of channel incision and channel margin slumping (Deptuck et al., 2003; Antobreh and Krastel, 2006). *Outer levees* are deposited by flows overspilling the main channel, while the more infrequently described *inner levees* are related to local flow overspill from flows confined within a larger channel complex (Deptuck et al., 2003, this issue; Posamentier, 2003). At sharp bends in sinuous channels, turbidity currents may breach the outer levee leading to development of an unconfined lobate or tongue-shaped deposit in the *overbank* area; these deposits are referred to as *crevasse splays* (Posamentier, 2003). Flow overspill at channel bends may also lead to formation of *erosional scours* (e.g. Fildani et al., 2006) and *fine-grained sediment waves* (Wynn and Stow, 2002). Where focussed overspill beyond outer bends crosses the narrow 'neck' of a sinuous loop, this can lead to incision and eventual cutting off of the loop (Fig. 1b and c). These abandoned *cut-off loops* are often filled with fine-grained sediments that have overspilled from the adjacent active channel.

2. A review of sinuous deep-water channels research

The majority of studies relating to sinuous deep-water channels have been carried out within the last decade, largely as a response to industry need for analogue data in hydrocarbon reservoir characterisation. Most published studies of sinuous channels come from the present-day seafloor or, occasionally, from outcrops with extensive exposure and dissected topography. However, there is also a rapidly growing literature on sinuous channels in the subsurface, largely based upon industry three-dimensional (3D) seismic data. In addition, experimental and numerical modelling of channelised gravity flows has been carried out by a number of research groups.

Comparison of data collected in these widely different fields can be challenging, due to marked differences in scale and data resolution. For example, published images of modern sinuous channels, both in planform and cross-section, are often highly vertically exaggerated (typically $>25\times$ and sometimes $>150\times$, e.g. Schwenk et al., 2003). As a consequence the reader should always bear in mind that V- or U-shaped channels displayed in seismic sections may actually have very subtle seafloor expression in reality (see discussion in Curray et al., 2003). Conversely, channels exposed in outcrop are typically affected by compaction

during burial and diagenesis; this can be further accentuated by differential compaction, for example where a coarse-grained channel fill is surrounded by fine-grained levees (e.g. Nilsen et al., 1994), or where a channel fill contains discontinuous coarse- and fine-grained elements such as point bars and sediment waves. Channels used in laboratory experiments are typically on the scale of a few metres long, whereas those in nature are often several hundred kilometres long; this is five orders of magnitude difference, and leads to obvious issues of flow scaling (Parsons et al., 2003; Shanmugam, 2003; Peakall et al., this issue).

Here, we explore the strengths and weaknesses of the various types of data relating to deep-water sinuous channels, and review previous studies by focussing on classic localities around the world (Fig. 2).

2.1. Modern sinuous channels

Most modern sinuous channels are located on passive-margin fans, and transfer sediment from major rivers to large ocean basins (Shanmugam and Moiola, 1988). The extensive length (10s to 100s of kilometres) of most of these channels means that comprehensive analysis of channel morphology, evolution and sedimentology is restricted to a small number of intensively studied systems, e.g. Amazon, Mississippi, Zaire, Bengal, Indus and Rhone Fans.

The examples listed above have all benefited from use of high-quality integrated geophysical and sedimentological datasets; these data include all or most of the following: (1) planform mapping of channel morphology and sediment facies using multibeam bathymetry and side-scan sonar, (2) cross-sectional imaging of channel architecture and evolution using seismic profiling and (3) sampling of channel sediments through shallow coring or deeper ODP drilling.

A major disadvantage facing researchers of modern sinuous channels is that they are mostly inactive at the present day, hence actual processes of sediment delivery cannot usually be directly observed. Zaire Fan is a notable exception (Khripounoff et al., 2003). In addition, detailed analysis of intra-channel architecture is usually limited by geophysical data resolution and lack of core calibration, consequently outcrop-scale bedforms and erosional features are rarely identified but are likely widespread. We now review six classic examples of modern sinuous channels on major fans (see Fig. 2 for locations), and document relevant background information relating to feeder system and regional setting. This background is important as it provides contextual environmental

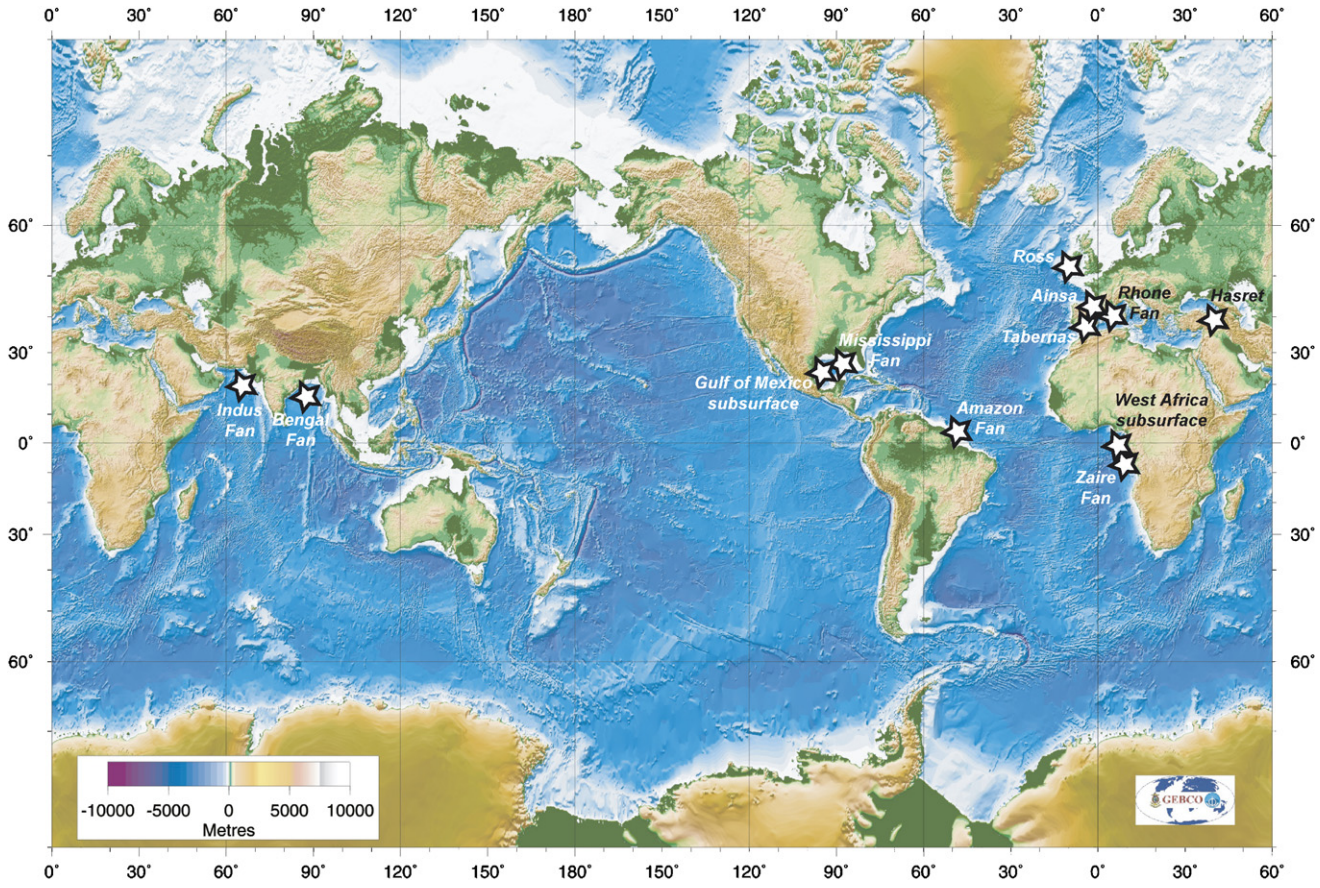


Fig. 2. Map showing locations of key case studies discussed in this paper, including six major modern fans and a number of world-class outcrop areas. Map based upon GEBCO global bathymetry (http://www.noc.soton.ac.uk/gg/gebco/gebco_maps.php).

information, and also allows comparison between different fans. Selected examples of sinuous channels from other, less well-studied systems, are included at the end of this section.

2.1.1. Amazon Fan

The Amazon Fan (Fig. 2) is one of the largest and most intensively studied deep-water fan systems in the world. It is fed by the mighty Amazon River, which sits within the world's largest river basin (7,050,000 km^2), discharges ~20% of all water carried to the oceans (Franzinelli and Potter, 1983; Curtin, 1986), and has an annual sediment load of $11–13 \times 10^8$ ton/year (Meade et al., 1985). The Amazon Fan covers an area of ~330,000 km^2, has a total sediment volume in excess of 700,000 km^3, and extends seawards for over 800 km (Damuth and Kumar, 1975; Damuth and Flood, 1984, 1985; Pirmez and Imran, 2003). Average fan gradients decrease downslope from 0.8° on the upper fan, to 0.3° on the middle fan and 0.1° on the lower fan (Damuth and Flood, 1984, 1985). The main submarine feeder conduit is the Amazon Canyon (Fig. 3), which is up to 600 m deep and incises landwards to at least the 75 m isobath. On the upper fan, at a WD of 1400 m, the canyon abruptly opens out to a single leveed distributary channel (the Amazon Channel), while further leveed distributary channels bifurcate from this main channel between 2000 and 3000 m WD (Damuth and Kumar, 1975; Damuth et al., 1983a). The mud-rich, net-aggradational, middle fan is characterised by two main channel–levee complexes (Western and Eastern Levee Complex), each comprised of numerous overlapping channel–levee systems. The smooth sand-rich lower fan is crossed by small incisive distributary channels that lack levees, and ultimately terminate as sandy lobes on the Demerara Abyssal Plain at a WD of ~4800 m (Damuth and Kumar, 1975; Damuth and Flood, 1984, 1985; Damuth et al., 1988). Two major mass-transport deposits (MTDs) originate on the upper fan surface (Fig. 3) and each cover an area of $>15{,}000\ km^2$; in places they destroy and/or bury channel–levee systems (Damuth and Embley, 1981; Maslin and Mikkelsen, 1998; Maslin et al., 2005). Two older buried MTDs are also visible on seismic profiles (Flood et al., 1995, 1997; Maslin and Mikkelsen, 1998; Maslin et al., 2005). The upper parts of MTDs consists of hummocky slump or slide deposits while, further downslope, thin debris-flow deposits extend for up to 300 km. Smaller failures are present on levee backslopes (Damuth et al., 1988).

Details of Amazon Fan evolution and stratigraphy are outlined in numerous studies (Damuth and Kumar, 1975; Damuth et al., 1983b, 1988, 1995; Damuth and Flood, 1984; Manley and Flood, 1988; Flood et al., 1991; Lopez, 2001; Kolla, this issue), including results of ODP Leg 155 (Flood et al., 1995, 1997; Maslin and Mikkelsen, 1998; Rimington et al., 2000). Amazon Fan has been largely inactive throughout the Holocene sea-level highstand, but was previously active during times of lowered sea level when the Amazon River was directly connected to Amazon Canyon. High-frequency, mixed sediment load, low-density turbidity currents, triggered by failure of shelf-edge deltas, are thought to be the primary process responsible for sediment transport though fan channels (Damuth et al., 1988; Piper and Normark, 2001; Pirmez and Imran, 2003). Only one distributary channel on each levee complex is active at any given time; subsequent channels originate from avulsion events, mostly in the middle fan region (for a detailed description of avulsion processes on Amazon Fan see Kolla, this issue). Channel avulsions are related to deep levee breaches or major channel wall failures on the outside of sinuous loops, induced by high-energy sand-rich flows (Damuth et al., 1983a; Flood et al., 1991; Kolla, this issue). Avulsions lead to initial deposition of elongate sand bodies up to 10s of metres thick, which appear on seismic profiles as HARPs; mud-dominated channel–levee systems then aggrade on top of the HARP unit, with aggradational sand-rich channel axes also producing a HAR response on seismic profiles (Flood, 1987; Flood et al., 1991, 1995, 1997). This evolution leads to development of a series of overlapping channel–levee systems (Fig. 3) that coalesce to form a levee complex that grows upwards and outwards (Damuth et al., 1983b).

Initial studies of Amazon Fan, using seismic profiles and sediment core data, provided information on gross planform distribution, cross-sectional morphology and sedimentology of distributary channels, which are typically 'perched' on top of a broad levee system (Damuth and Kumar, 1975). However, it required multibeam bathymetric and GLORIA long-range side-scan sonar mapping to reveal that most distributary channels on the middle and lower fan (below 2500 m WD) are highly sinuous (Fig. 3), with cut-offs and abandoned sinuous loops indicating significant lateral migration (Damuth et al., 1983a, 1988). Sinuosities are in the order of 1.1–2.95, with peak values (1.6–2.95) occurring on the middle fan between 3000 and 4000 m WD (Flood and Damuth, 1987; Flood et al., 1991; Pirmez and Flood, 1995). Quantitative analysis of channel parameters on the middle and lower fan, based largely upon GLORIA data, measured channel widths of 0.3–1.4 km, sinuous loop wavelengths of 2–15 km and radius of curvatures of 0.5–7 km (Flood and Damuth, 1987). Channel width and radius of curvature are strongly positively correlated with wavelength of sinuous loops. Channel dimensions and levee height both generally decrease downslope, for example channel cross-sectional area decreases from 100,000 m^2 at 2000 m WD to 10,000 m^2 at 4500 m WD; this is interpreted to relate to a downslope decrease in turbidity current flow thickness and volume (Flood and Damuth, 1987; Pirmez and Imran, 2003). Local increases in 'valley slope' (valley is defined as the general down-fan trend of a channel segment) lead to increased sinuosity; this enables maintenance of a relatively constant channel axis slope that gradually decreases down-fan.

Recent numerical modelling (Pirmez and Imran, 2003) based on measured morphologic parameters of the 'active' Amazon Channel (Pirmez and Flood, 1995), together with

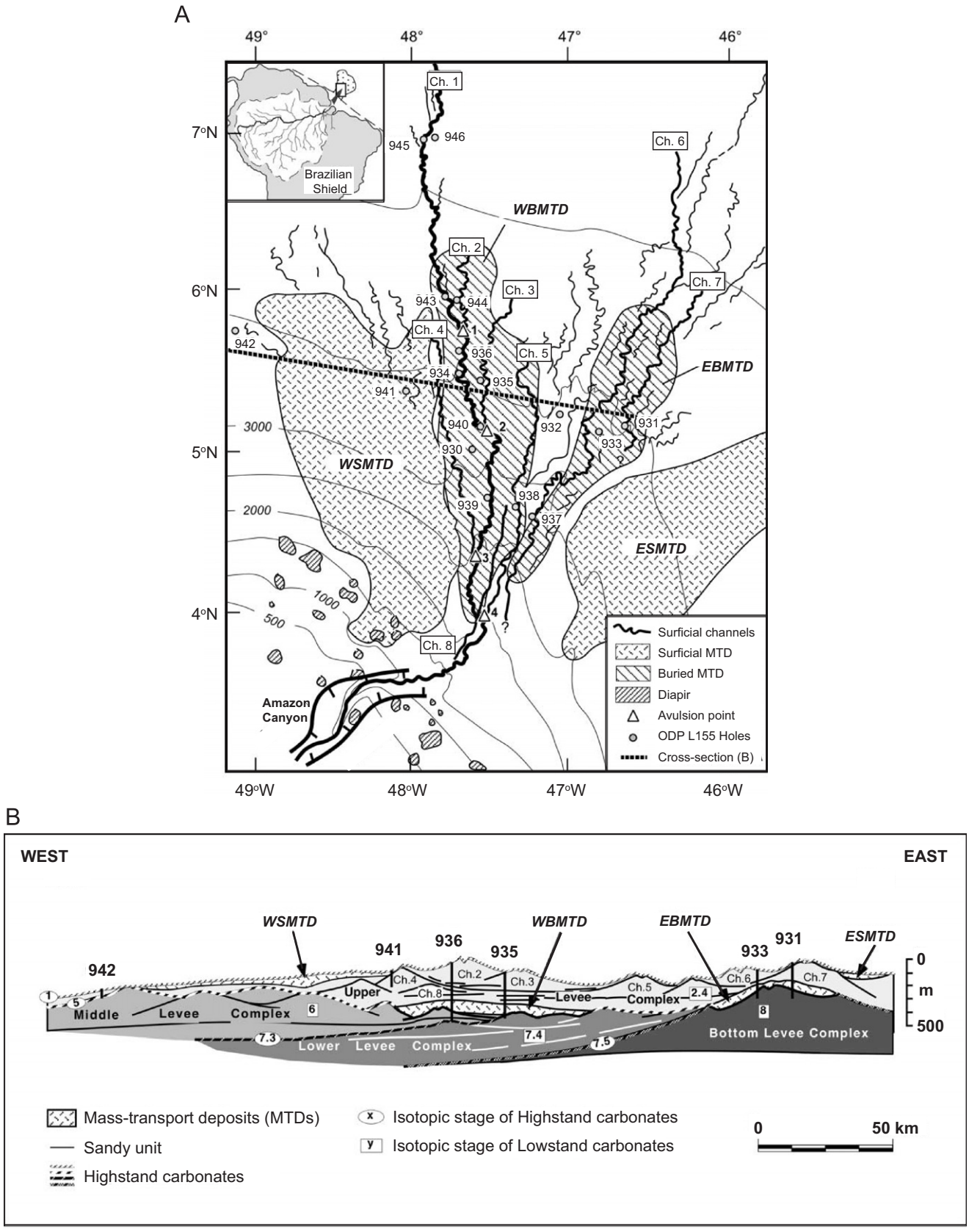


Fig. 3. Map of Amazon Fan (A), showing sinuous channel morphology and dominance of MTDs. Locations of 17 sites drilled during ODP Leg 155 are shown. Inset shows location off South America (small box) and surface area of Amazon River relative to Amazon Fan. (B) Schematic cross-section across Amazon Fan, through selected ODP Leg 155 sites. Note the major channel–levee complexes and the surficial and buried MTDs. Reproduced from Lopez (2001) with permission of Elsevier.

insights gained from analysis of overbank sediment waves (Normark et al., 2002), has provided new insights into turbidity current characteristics on Amazon Fan: (1) flow durations are likely to be in the order of at least tens of hours and up to a few days, with recurrence intervals for individual flows of 1–2 years, (2) turbidity currents passing through Amazon Canyon are probably relatively thin and slightly supercritical, with average velocities of 2–4 ms^{-1} and initial mean flow concentrations of ~1%, (3) flow thicknesses initially increase dramatically in the canyon, leading to significant overspill onto levees once the channel is reached; this reduces flow volume, leading to a gradual decrease in flow velocity (to 0.5–1 ms^{-1}) and flows becoming subcritical across much of the fan, (4) turbidity currents are silt-dominated (~90–95% silt), (5) overbank flows are likely to be initially supercritical, but rapid water entrainment and thickening lead to a reduction in velocity and abrupt deposition of sediment, hence the relatively sharp rate of levee thinning away from the channel, (6) overbank flow deposits are of fairly uniform thickness (10s of centimetres), suggesting that individual flows are rather similar to each other, (7) flows are well-stratified, with sand confined to the lower 20–30 m of the flow, and within 1–2 km laterally of the channel axis.

2.1.2. *Mississippi Fan*

The Mississippi Fan (Fig. 2) shares many characteristics with Amazon Fan, in terms of scale, feeder system and gross morphology. It covers an area of at least 300,000 km^2, has a volume of at least 290,000 km^3, and is over 600 km long (Fig. 4); it was constructed rapidly during the Plio-Pleistocene, and is covered by a thin veneer of Holocene pelagic/hemipelagic sediments (Bouma et al., 1984, 1985a, b, 1989; Feeley et al., 1985; Pickering et al., 1986; Twichell et al., 1991). Sedimentation rates were as high as 6–11 m per 1000 year during Pleistocene glacials (Kohl and DSDP Leg 96 Shipboard Scientists, 1985; Stelting et al., 1985), with the ancestral Mississippi River being the dominant feeder system (Huang and Goodell, 1970; Davies, 1972). The Mississippi Fan comprises a series of large, compensation-stacked, channel–levee systems, the youngest of which can be seen covering a large proportion of the modern seafloor in the eastern Gulf of Mexico, before ultimately terminating on the Florida Abyssal Plain at >3400 m WD. The fan surface is heavily modified by at least one large early Holocene MTD (Fig. 4), which is up to 300 km long and 130 km wide (Walker and Massingill, 1970; Bouma et al., 1985a, b; Kastens and Shor, 1985; Twichell et al., 1991).

The main feeder of the modern Mississippi Fan is the Mississippi Canyon, located some 60 km west of the modern Mississippi Delta. The canyon head is located at 60 m WD and canyon widths are 12–25 km. On the upper fan, at 1200 m WD, the canyon passes downslope to the Mississippi Channel, which is partly infilled in its upper reaches by a major MTD (e.g. Kastens and Shor, 1985). On the convex-upwards middle fan, below 2000 m WD, the aggradational Mississippi Channel is 2–4 km wide and 25–45 m deep. It is perched upon a broad levee system, some 50 km wide and 200 m high; crevasse splays are present on outer bends in some places. Slope angles in this section vary between 0.5° and 0.25° (Bouma et al., 1984, 1985a, b; Kastens and Shor, 1985, 1986; Pickering et al., 1986). Early seismic-based studies provided information on the cross-sectional morphology of Mississippi Channel (Stuart and Caughey, 1976; Moore et al., 1978) but, as with Amazon Fan, it was not until planform mapping of the fan surface was undertaken with GLORIA sidescan sonar, that the sinuous nature of the channel was fully revealed (Garrison et al., 1982; Kastens and Shor, 1985, 1986; Wen et al., 1995). Relative to Amazon Fan, sinuosity on Mississippi Fan is generally lower (maximum 1.7) and sinuous loops are smaller in dimensions (Kastens and Shor, 1986).

Kastens and Shor (1985) presented site survey data across a single sinuous loop on the middle Mississippi Fan at ~2500 m WD. HARs are visible at 200–500 m depth below the channel floor, and crevasse splays can be seen cutting levees on the outsides of bends. There is some evidence that during HAR deposition, sinuosity progressively increased through time; for example, a different study of the same sinuous loop by Kastens and Shor (1986) showed sinuosity increasing from 1.1 at 320 m depth to 1.5 at 200 m depth, with a concurrent down-channel migration of 1 km. Geophysical data indicate that HAR deposition was interrupted by deposition of at least two major MTDs with a total thickness of ~100 m (Kastens and Shor, 1985). Consequently, present-day levee relief is subdued, and pressure ridges are visible on the surface of the MTD where it has become confined against levee topography.

Subsequent DSDP drilling of the aggradational fill of the sinuous Mississippi Channel on this section of the middle fan produced an overall fining-upwards sequence some 200 m thick, with a basal gravel-rich lag (corresponding to the uppermost 6–10-km-wide HARs on seismic profiles) overlain by interbedded sands and muds, overlain in turn by muds and clays (DSDP Leg 96 Scientific Party, 1983; Bouma et al., 1985a, b; Stelting et al., 1985). Detailed analysis of seismic profiles, taken across the single sinuous loop in the vicinity of sites 621 and 622, show that the channel thalweg migrated 1.5–2 km laterally, 1.2 km downslope, and aggraded about 175 m between deposition of basal HARs and gradual channel abandonment prior to MTD deposition (Stelting and DSDP Leg 96 Shipboard Scientists, 1985).

Further downslope, on the lower fan below 3100 m WD, the Mississippi Channel decreases in sinuosity and cross-sectional area, and feeds a network of progressively smaller, low-sinuosity, distributary channels that extend across a series of depositional lobes. These lobes are 50–100 km wide, 100–200 km long, and up to 50 m thick (Twichell et al., 1991, 1992, 1995). Distributary channels show evidence for frequent lateral shifts, suggesting that only one channel was active at any given time (O'Connell

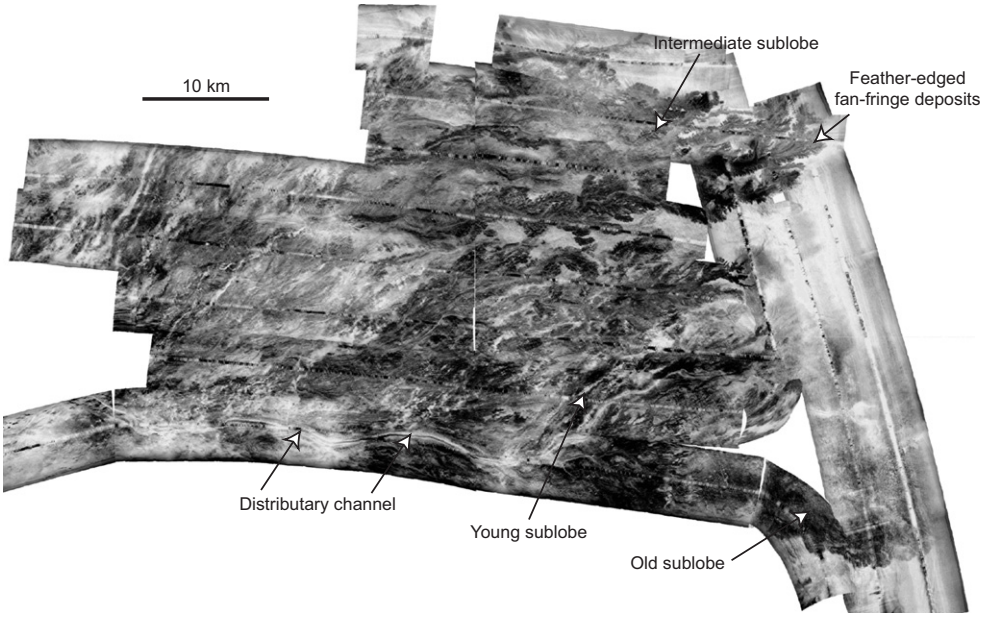


Fig. 4. SeaMARC 1A sidescan sonar mosaic across a depositional lobe on the Mississippi Fan. This lobe emanates from the highly sinuous Mississippi Channel, and comprises a series of low-sinuosity distributary channels feeding high-backscatter lobe deposits with irregular 'feather-edged' fringes. This geometry, combined with core data, reveal that these lobes are largely comprised of debris-flow deposits, indicating that the latest stage of Mississippi Fan channel activity has likely been dominated by debris flow rather than turbidity current processes. Dark tones = high backscatter, light tones = low backscatter. Raw image data from Twichell et al. (2005).

et al., 1985, 1991b). High backscatter lobe deposits show an irregular 'finger-like' margin indicative of rapid freezing of flows, suggesting that channelised debris flows may have been an important process supplying sediment to the distal-most Mississippi Fan (Twichell et al., 1991, 1992, 1995; Nelson et al., 1992; Schwab et al., 1996).

Seismic-based studies of the entire western Mississippi Fan have recognised a remarkable total of 17 channel–levee systems (including the youngest described above); intriguingly, these systems show marked variations in the degree of bifurcation (avulsion), sinuosity, aggradation and lateral migration (Weimer and Buffler, 1988; Weimer, 1989, 1990, 1991). It appears that a number of controlling factors have influenced channel–levee development on the Mississippi Fan, and that the youngest and most intensely studied system may not be representative of the fan as a whole.

About 150 km to the northeast of the Mississippi Channel is the poorly known DeSoto Channel, which runs roughly parallel to the base of the Florida Escarpment and is not connected to Mississippi Canyon (Twichell et al., 1991). The DeSoto Channel is 0.5–1 km wide, 10–20 m deep and is visible for at least 200 km, although its proximal and distal sections are apparently buried. The channel is highly sinuous, with values of about 2.1 (Clark and Pickering, 1996).

2.1.3. Zaire Fan

The Zaire Fan (Fig. 2) off west Africa is another huge (~300,000 km^2) passive margin submarine fan that is dominated by fine-grained sediments supplied by a major river; the fan extends ~800 km downslope from the shelf edge, terminating at >5200 m WD on the Angola Abyssal Plain (Van Weering and Van Iperen, 1984; Droz et al., 1996, 2003). The Zaire (formerly Congo) River has the second largest drainage area and fluid discharge in the world after the Amazon River. However, the annual suspended-sediment load is relatively low at 55×10^6 ton/year (Wetzel, 1993), which is about 20 times lower than Amazon River. The Zaire Fan differs from both Amazon and Mississippi Fans in that the main feeder conduit, the Zaire Canyon, cuts back across the shelf and penetrates some 30 km up the Zaire River estuary (Heezen et al., 1964); consequently the canyon has remained active through the Holocene to the present day. Recent gravity flow activity is evidenced by submarine cable breaks and current meter records linked to turbidity currents mostly initiated by Zaire River flooding (Heezen et al., 1964; Khripounoff et al., 2003), and also by thick Holocene turbidite deposits on the fan surface (Van Weering and Van Iperen, 1984). The relatively dilute input flow via the Zaire River and Canyon, active throughout the Holocene, appears to be a key factor in the more incisional nature of the active channel on Zaire Fan, compared to the highly aggradational youngest channel on Amazon Fan (Babonneau et al., 2002).

The Zaire Fan is composed of more than 80 stacked channel–levee systems emanating from Zaire Canyon, most of which are now abandoned (Droz et al., 1996; Savoye et al., 2000). These channel–levee systems are grouped into three individual fans (northern, southern and axial) that together make up the Zaire Fan. Only one channel–levee

system is believed to be active at any given time, with avulsion events leading to channel abandonment and switching. MTDs are of relatively minor importance on Zaire Fan, comprising less than 10% of the fan deposit (Droz et al., 2003).

The main feeder is the Zaire Canyon, which is deeply incised (up to 1300 m) into the outer shelf and upper continental slope, and has a maximum width of ~15 km (Heezen et al., 1964; Shepard and Emery, 1973). The lower canyon curves around a diapiric salt province to the south, before gradually opening out into the active Zaire Channel at 3300 m WD; this channel sits on top of the youngest channel–levee system and is located in the axial fan (Droz et al., 1996). The presence of an incisional thalweg along much of the active channel ensures that flows are largely confined and consequently bypass much of their sediment load, with intra-channel sedimentation largely restricted to terraces (Fig. 5: Babonneau et al., 2004). Significant channel aggradation on Zaire Fan is only observed in palaeo-channels, as the active channel is open (Babonneau et al., 2002).

The sinuous axis of the entire active Zaire Channel, from canyon head to terminal lobe, is some 1200 km long, with an average sinuosity of 1.58 (Babonneau et al., 2002). The overall channel depth profile is smooth and concave-upwards, suggesting the system is close to equilibrium profile. Channel dimensions, sinuosities and slope angles progressively decrease downslope. Between 3300 and 4100 m WD the channel is generally 1.5–2 km wide and 150–250 m deep, with slopes of 0.1–0.2°; intra-channel terraces are common (Fig. 5) and sinuosity averages 1.7 (although is locally highly irregular). Further downslope, between 4100 and 4800 m WD, the channel is 1–1.5 km wide and <150 m deep, with slopes of 0.05–0.15°; terraces become scarcer and less continuous, while sinuosity becomes more regular and gradually decreases to <1.1 (Babonneau et al., 2002).

Quantitative analysis of sinuosity has been undertaken at two scales: a 10 km reach best captures sinuosity of large loops, and shows peak values >2 are largely confined to ~3000–3500 m WD, while a 2 km reach best captures sinuosity of small loops, and shows irregular values <2 above 3750 m WD, decreasing progressively downslope beyond this. Wavelengths of sinuous loops are relatively short (average 3 km) above 4000 m WD, but progressively increase downslope beyond this to values >5–10 km (Babonneau et al., 2002). Wavelength and sinuosity therefore display an inverse relationship. Detailed SAR high-resolution side-scan sonar analysis of a sinuous loop at 4100 m WD (Fig. 5) reveals that the outer bank is comparatively steep and erosional, whereas the inner bank shows multiple small terraces (Babonneau et al., 2002). The channel floor is very flat.

Channel levees are relatively small and highly symmetrical (Migeon et al., 2004), presumably because the influence of Coriolis force on flow overspill is reduced this close to the Equator (~6°S). Levee development begins in the upper channel where channel depths are <250–300 m; this therefore likely corresponds to maximum thickness of flows passing through the channel (Babonneau et al., 2004; Migeon et al., 2004). Observations of a recent turbidity current showed that at ~4000 m WD individual flows can have velocities $>1.2\,ms^{-1}$ at heights of 150 m above the channel floor (Khripounoff et al., 2003). Progressive overspill of fine-grained suspended load is interpreted to result in a progressive downslope increase in flow concentration, and a corresponding decrease in flow thickness (Babonneau et al., 2002). Fine-grained sediment waves are widely observed on levee backslopes, and are related to turbidity current overspill. They are particularly common beyond sharp bends in the channel, or on the outside of sinuous loops (Savoye et al., 2000; Migeon et al., 2004).

Several knickpoints are visible along the axial channel profile, and are related to avulsions (Babonneau et al., 2002). New channel sections associated with avulsions initially show reduced sinuosities, as they are relatively straight and steep. However, in an attempt to regain equilibrium profile (Flood and Damuth, 1987; Pirmez and Flood, 1995), channel sinuosity increases through time near avulsion points, and eventually these areas show sinuosity peaks in the overall channel profile. Consequently, local increases in channel slope gradient lead to locally increased sinuosities. Further analysis of avulsions on Zaire Fan is presented in Kolla (this issue).

Seismic profiles show that the channel axis is usually underlain by laterally extensive HARPs, while intra-channel deposits include HARs, local MTDs and inner levees (Droz et al., 1996, 2003; Babonneau et al., 2004). Basal transparent units, interpreted to be MTDs related to levee breaching, are occasionally observed beneath HARPs. The active channel floor is hard and sandy, while levees are composed of fine-grained turbidites (Van Weering and Van Iperen, 1984; Droz et al., 1996, 2003; Savoye et al., 2000; Gervais et al., 2001; Migeon et al., 2004). Distally, the Zaire Channel terminates in a depositional lobe complex, fed by a series of small distributary channels. The most recent lobe is sand-rich, highlighting the high efficiency of sand transport in this system (Savoye et al., 2000).

2.1.4. Bengal Fan

The Bengal Fan (Fig. 2) is the largest submarine fan in the world (Curray and Moore, 1971; Emmel and Curray, 1984, 1985; Curray et al., 2003), and is supplied by the sediment-laden, confluent, Ganges and Brahmaputra Rivers, which drain much of the Himalayan Mountains. The fan extends from the Ganges Delta south across the Bay of Bengal for about 3000 km, has a maximum width of 1430 km, and covers an area of $2.8–3.0 \times 10^6\,km^2$. The total fan sediment volume is $12.5 \times 10^6\,km^3$ (Emmel and Curray, 1984, 1985; Curray et al., 2003). As with other large fans, Bengal Fan is composed of numerous large, stacked and overlapping, channel–levee systems (Fig. 6), which may be up to 50–60 km wide and 800–1000 m thick. Unfortunately,

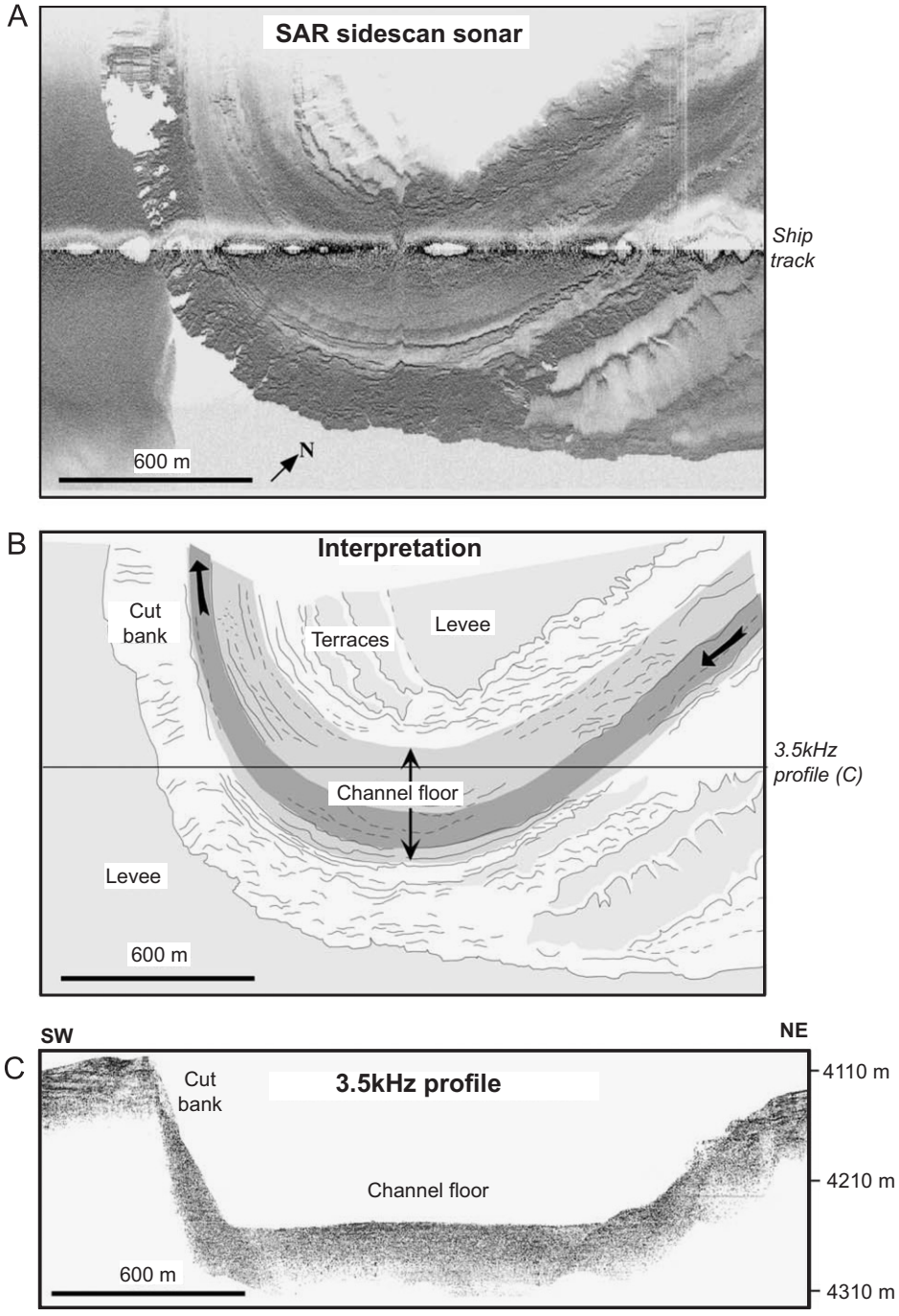


Fig. 5. SAR sidescan sonar image (A), interpretation (B) and 3.5 kHz profile (C) crossing the active channel on the middle Zaire Fan at ~4100 m WD. Note the prominent cut bank on the outer bend, the multiple terraces on the inner bend, and the relatively flat channel floor. Reproduced from Babonneau et al. (2002) with permission of Elsevier.

partly due to its immense size, detailed channel planform morphology and sediment distribution is poorly understood for large sections of Bengal Fan. Nevertheless, existing data allow us to make some comparisons with the more intensively studied fans discussed above.

Although the modern Bengal Fan surface is composed of numerous channel–levee systems, only one channel is presently connected to the main feeder canyon, which has been the dominant feeder for the last 125 ka. The canyon extends landwards to the inner shelf at 38 m WD, reaches a depth of ~700 m where it incises into the outer shelf, and has a length of about 160 km (Curray et al., 2003; Kottke et al., 2003). The active channel, presently connected to the canyon at about 1400 m WD and extending for over 2220 km downslope, has been largely cut-off from fluvial sediment supply during the late Holocene highstand, but is still fed by small turbidity currents (Emmel and Curray, 1984, 1985; Hübscher et al., 1997; Curray et al., 2003). The channel is believed to have formed at ~12 ka and was filled rapidly until sea-level rise slowed at 6–6.5 ka, with reduced

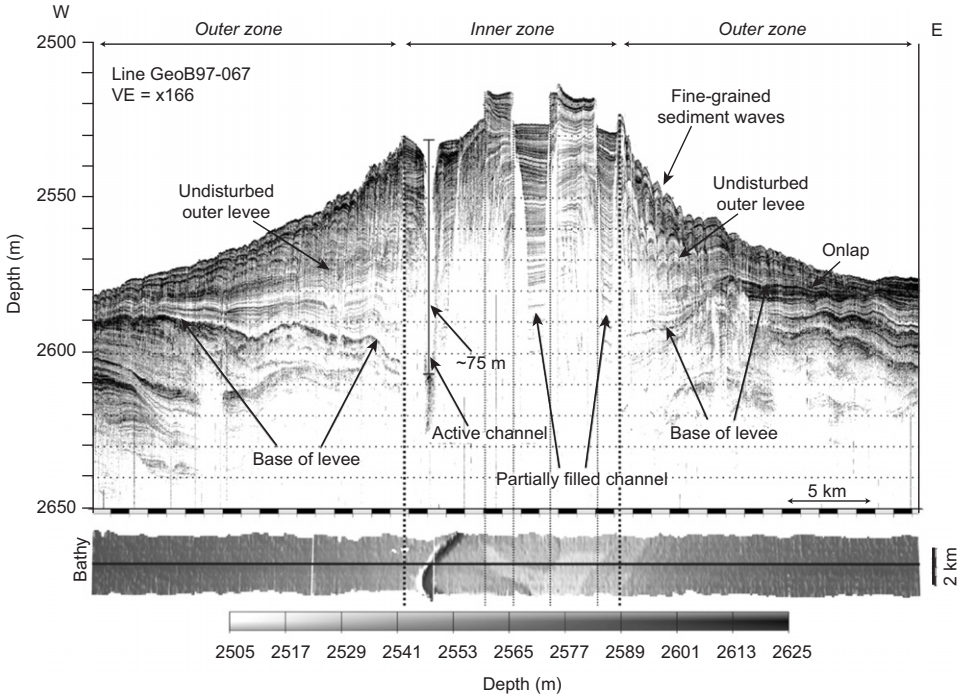


Fig. 6. High-resolution Parasound seismic profile and Hydrosweep multibeam bathymetry swath across the active channel–levee system of middle Bengal Fan. Note the highly sinuous abandoned and partially filled channel, and widespread presence of fine-grained sediment waves on outer levees. Also note the extreme vertical exaggeration (× 166). Reproduced from Schwenk et al. (2003) with permission of Elsevier.

deposition continuing to the present day (Weber et al., 1997; Curray et al., 2003).

On the upper fan the active channel is elevated above the fan surface (Fig. 6) and has a maximum depth of 325 m, levee crest-to-crest widths of up to 20 km, and an axial thalweg slope of 0.14°, compared to the general upper fan slope of 0.33° (Emmel and Curray, 1981a, b, 1984, 1985; Curray et al., 2003). Large levees are developed and intra-channel terraces are common. On the middle fan, from 2250 to 2900 m WD, the channel thalweg incises about 100 m into the fan surface, and both thalweg and fan slopes average ~0.1°, which is markedly lower than equivalent slopes on e.g. Amazon and Zaire Fans. HARPs occur beneath and between channel–levee systems, but large MTDs are apparently absent, although detailed surveying of the uppermost fan is required to confirm this (Schwenk et al., 2003, 2005). On the lower fan, slope angles drop to <0.06° and channel widths are <3.5 km, but incision depths remain at a few 10s of metres (Emmel and Curray, 1981a, b, 1984, 1985; Redbourn et al., 1993; Curray et al., 2003). Right-hand levees (looking downstream) typically show enhanced growth on the upper and middle fan due to the effects of Coriolis force, but are equal in size on the lower fan due to proximity to the Equator (Emmel and Curray, 1981b, 1984, 1985). Fine-grained sediment waves are present on levee backslopes on the middle fan (Fig. 6), and localised small MTDs can sporadically be seen (Hübscher et al., 1997).

Channel avulsions are documented in numerous sections of the upper and middle fan, and are thought to relate to levee breaching around tight sinuous loops (Emmel and Curray, 1981b; Schwenk et al., 2003, 2005). A detailed study of the active channel on the middle fan revealed that channel avulsions have occurred, on average, once every 750 years (Schwenk et al., 2003). Abandoned channel segments are filled extremely rapidly (Fig. 6), often before the next avulsion, and HARPs are deposited in inter-channel–levee lows immediately following avulsions (Schwenk et al., 2005). Bengal Fan differs from many other modern fans in that, further downfan, newly avulsed channels tend to reoccupy and rejuvenate pre-existing channels. Consequently, numbers of channels on the fan surface peak on the middle fan, but decrease on the lower fan (Curray et al., 2003).

Lateral channel migration on Bengal Fan was first recognised in cross-sectional profiles by Curray and Moore (1971), while low continuity of channels in closely spaced profiles on the lower fan suggested a high degree of sinuosity (Redbourn et al., 1993). However, it was not until the use of Hydrosweep multibeam bathymetry that the true nature of channel sinuosity on Bengal Fan was revealed (Hübscher et al., 1997; Schwenk et al., 2003, 2005). Detailed study of the middle fan, between 2480 and 2680 m WD (slope angle ~0.04°), has revealed that outer levees are of low sinuosity and are relatively stable, whereas the active thalweg is highly sinuous and unstable, suggesting increased sinuosity development through time via thalweg outer bank erosion and lateral thalweg migration (Hübscher et al., 1997; Schwenk et al., 2003). Sinuosities in this section are highly variable, with values falling between

1.05 and 3.5, and an average of 2. Point-bar deposits, up to 1 km wide and 2 km long, are visible on the insides of sinuous loops in some places (Schwenk et al., 2003). Cut-off loops are particularly common (e.g. >20 over a channel length of 90 km) and contain variable amounts of fill (Fig. 6; Schwenk et al., 2003); interestingly, these features, when seen in cross-section, were originally interpreted as inner levees by Hübscher et al. (1997). Enhanced spillover on the outside of sinuous loops leads to development of localised tongue-shaped sediment wedges on levees (Schwenk et al., 2003), in addition to the larger lateral levee wedges that represent more continuous overspill. Chaotic, dipping, high-amplitude reflectors (CHARs) represent channel axis aggradation and lateral migration; these migrations appear to have occurred continuously based upon seismic profile data. Further details on the evolution of channel–levee systems are discussed in Schwenk et al. (2003, 2005).

Shallow core data are sparse but, when compared with shallow seismic data, suggest that the floor of the active channel is sand-dominated with HAR and CHAR development, and that sand can be transported to the lower part of the lower fan (Emmel and Curray, 1984, 1985; Schwenk et al., 2003). Much of the fan surface is covered by muddy fine-grained turbidites a few 10s of centimetres thick (Stow et al., 1989; Weber et al., 1997). Deeper drilling of the distal-most Bengal Fan, during ODP Leg 116, recovered a 2–6 m thick sequence of pelagic and turbiditic mud, overlying 100s of metres of interbedded silt-mud turbidites (Stow et al., 1989). Individual turbidite beds are up to 2.5 m thick and contain occasional coarse (sand-sized) quartz grains; this suggests that, even 2500 km from source, turbidity currents were still capable of carrying significant sediment loads, and were most likely initiated by large-scale slumping of pro-delta sediments (Stow et al., 1989; Redbourn et al., 1993). Estimates of turbidity current flow velocities through the active channel (during periods of lowered sea level) are in the order of 10 ms^{-1} on the upper fan to 4 ms^{-1} on the lower fan (Curray et al., 2003). This progressive downslope decrease in flow velocity is typical for a system where the overall channel slope is close to equilibrium profile.

2.1.5. Indus Fan

The Indus Fan in the Arabian Sea (Fig. 2) is another major passive margin fan, being 1500 km long, up to 960 km wide, and covering an area in excess of 1.1×10^6 km^2 (Naini and Kolla, 1982; Kolla and Coumes, 1984, 1987; McHargue and Webb, 1986; Droz and Bellaiche, 1991; McHargue, 1991; Clift et al., 2001). Fan sediments are supplied by the Indus River, which ultimately drains the eastern Himalayan Mountains and transports sediment to the Indus Canyon. This canyon cuts back across the shelf to 20–30 m WD, and averages 8 km wide and 800 m deep. At 1400 m WD the canyon widens to 20 km and is 325 m deep; in this area it passes to a channel–levee system on the upper fan, which forms part of a larger channel–levee complex. As with other fans described above, only one canyon–channel system has been active on Indus Fan at any one time (McHargue and Webb, 1986; Kolla and Coumes, 1987; Kenyon et al., 1995a; Von Rad and Tahir, 1997).

The upper Indus Fan, down to 3400 m WD, shows an overall slope angle of 0.11°–0.14°, decreasing to 0.05° on the lower fan below 3800–4000 m WD (Kolla and Coumes, 1984, 1987). Channels on the upper fan are up to 10 km wide and 200 m deep, and have well-developed levees up to 40 km wide and 600 m thick. Levee development is enhanced on the right-hand side (looking downslope) due to Coriolis forces acting on overspilling turbidity currents. Intra-channel terraces are common. Channels on the convex-upward middle fan are smaller, with depths up to 30–40 m and relatively small levees (Fig. 7), while the lower fan is characterised by numerous small channels (<1.5 km wide and <5 m deep) with or without small levees (<20 m high). Large MTDs have not been recognised on Indus Fan, but small-scale slumping is common within channels and on levee slopes on the upper and middle fan (Kolla and Coumes, 1984, 1987; Droz and Bellaiche, 1991; Kenyon et al., 1995a).

Initial crossings of channels on the middle fan, with shallow seismic profiles, revealed tight channel spacing which was thought to be evidence for high sinuosity (McHargue and Webb, 1986; Kolla and Coumes, 1987). In addition, lateral channel migration is visible on profiles, occurring through erosion of the outer cut bank and point-bar deposition on the inner bank. Lateral migration of the channel axis and width of the thalweg sinuous belt appears to decrease through time, while vertical aggradation increases. This is presumably a function of decreasing flow volume, velocity and/or frequency. Channel abandonment through avulsion at two nodal points (one beyond the Indus Canyon and the other on the middle fan) have also been recognised, with levee breaching or retrogradational channel filling being the suggested mechanism (Kolla and Coumes, 1984; McHargue and Webb, 1986; McHargue, 1991; Kenyon et al., 1995a; Kolla and Schwab, 1995; Prins et al., 2000). Increased understanding of the planform morphology of sinuous channels on Indus Fan has been provided by GLORIA sidescan sonar imagery (Kenyon et al., 1995a). High backscatter channels show sinuosity values up to 3 (Fig. 7), with peak sinuosities occurring on the middle fan and values decreasing down-fan as gradient decreases.

Surficial sediments on Indus Fan comprise a Holocene drape underlain by mostly fine-grained turbidites, representing dominant levee sediments. Significant sands are only present in channels on the upper and middle fan (represented by HARs on shallow seismic profiles), and in interchannel–levee lows (HARPs), but become commoner in the lower fan area where depositional lobes are developed (McHargue and Webb, 1986; Kolla and Coumes, 1987; Droz and Bellaiche, 1991; Kenyon et al., 1995a; Von Rad and Tahir, 1997; Prins and Postma, 2000).

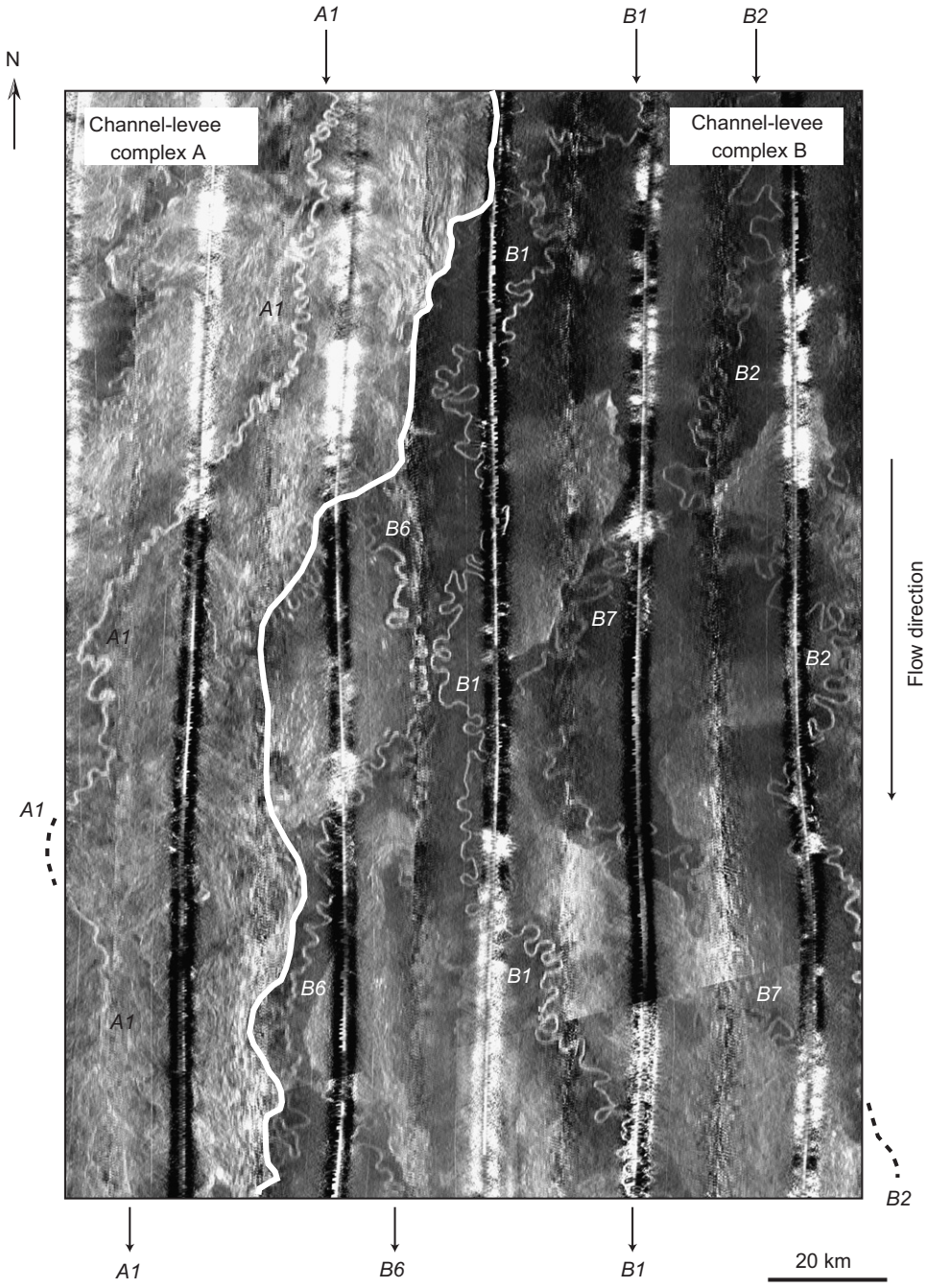


Fig. 7. GLORIA sidescan sonar image showing numerous highly sinuous channels on the middle Indus Fan. The youngest channel (A1) shows the highest backscatter and forms part of the youngest channel–levee complex A; it is bounded by moderate backscatter levees (thick white line marks eastern boundary of levee). Channels B1, B2, etc. form part of older channel–levee complex B, which is covered by several metres of hemipelagic sediments and shows lower backscatter. Channel numbers shown in italics. Light tones = high backscatter. Modified from Kenyon et al. (1995a).

Seismic profiles suggest that overall fining-upward sequences are present in channel fills on the upper and middle fan, but that a more complex pattern may occur in the lower fan (Kolla and Coumes, 1987; Kolla and Schwab, 1995).

2.1.6. *Rhône Fan*

The Plio-Quaternary Rhône Fan is the largest fan in the northwest Mediterranean Sea (Fig. 2), and extends seawards for some 300 km before terminating on the Balearic Abyssal Plain at ~2600 m WD (Menard et al., 1965; Droz and Bellaiche, 1985; Normark et al., 1985). The total fan area is hard to estimate as the lower fan boundary is poorly defined, but is in the order of 10^5 km^2. Fan sediments are dominantly supplied by the Rhône River, which during lowstand conditions transported material derived from the Alps directly to the head of the Petit-Rhône Canyon. As with other major fans, the Rhône

Fan is composed of at least eight stacked channel–levee systems, each up to 100 m thick and 70 km wide (Bellaiche et al., 1981, 1984; Droz and Bellaiche, 1985). HARs, representing coarse-grained sediments, are confined to channel floors, while wedge-shaped stratified units correspond to fine-grained levees (Droz and Bellaiche, 1985; O'Connell et al., 1995). Salt diapirs have significantly affected the morphology of the middle and lower fan, and MTDs are common (Bellaiche et al., 1984, 1986a, 1990). The two most recent (probably late glacial) MTDs cover a large portion of the fan surface either side of the Rhône Channel, with that on the eastern side covering an area of 5100 km^2, having a volume of 170 km^3, a maximum thickness of 160 m, and a run-out distance of 170 km, and that on the western side having a volume of 260 km^3, a maximum thickness of 100 m, and a run-out distance of 150 km (Droz and Bellaiche, 1985; Bellaiche et al., 1986a, 1990; Gaullier et al., 1998; Droz et al., 2001). Older buried MTDs are believed to have triggered abrupt avulsion events on the fan.

The Petit-Rhône Canyon comprises a broad, slightly sinuous valley with a more highly sinuous thalweg, bordered by numerous scallop-shaped intra-channel terraces, interpreted to be slump scars (Bellaiche et al., 1984; Droz and Bellaiche, 1985; D'Heilly et al., 1988). Axial slope angles are about 1.5–2° in the canyon. Turbidity currents passing through this area have been estimated to be flowing at velocities of a few ms^{-1}, possibly up to 15 ms^{-1} or more, based on simple numerical modelling (D'Heilly et al., 1988).

The canyon passes downslope to the Rhône Channel on the convex-upwards upper fan; this channel is 2–5 km wide and is perched up to 500 m above surrounding seafloor, on asymmetrical levees 50–75 m high. Axial slope angles in this area are 0.4–0.5°. Multibeam bathymetry surveys have revealed the highly sinuous character of the Rhône Channel (sinuosity up to 1.4–1.5) and the presence of crevasse splays, cut-off loops and a spectacular incisional thalweg (Bellaiche et al., 1984, 1986b). The size of sinuous loops progressively decreases downfan. The channel thalweg is 200–800 m wide and 40–50 m deep, and displays cuspate, scalloped and gullied walls with scattered slump deposits on the thalweg floor (Bellaiche et al., 1981; O'Connell et al., 1991a, 1995). Terraces flanking the thalweg may be partly depositional and similar therefore to inner levees (Torres et al., 1997). Small slumps and overbank sediment waves are visible on levee backslopes (Kenyon et al., 1995b; O'Connell et al., 1995; Torres et al., 1997; Dennielou et al., 2006). Cores recovered from the Rhône Channel in this area contain stacked, thin-bedded, sand-mud turbidites, which are coarser closer to the thalweg (Mear, 1984).

The most recent avulsion of the Rhône Channel (Fig. 8), formed through levee breaching, has resulted in development of a depositional lobe called the Rhône 'neofan', which is up to 70 m thick, covers an area of at least 1430 km^2 and has a volume of about 25 km^3 (Bellaiche et al., 1984; Mear, 1984; D'Heilly et al., 1988; O'Connell et al., 1991a, 1995; Torres et al., 1997; Gaullier et al., 1998; Droz et al., 2001; Bonnel et al., 2005; Dennielou et al., 2006). The newly avulsed 'neochannel' feeding the neofan is relatively straight (sinuosity of 1.1), up to 210 m deep and has an axial slope of up to 0.6° at the avulsion point, compared to a slope of 0.3° for the abandoned Rhône Channel immediately downslope of the avulsion point (Torres et al., 1997). Enhanced thalweg entrenchment and knickpoint development about 20 km upslope of the avulsion point also indicate that the neochannel has yet to regain equilibrium profile (O'Connell et al., 1995; Torres et al., 1997). The neochannel passes downslope into a series of small distributary channels crossing the neofan surface

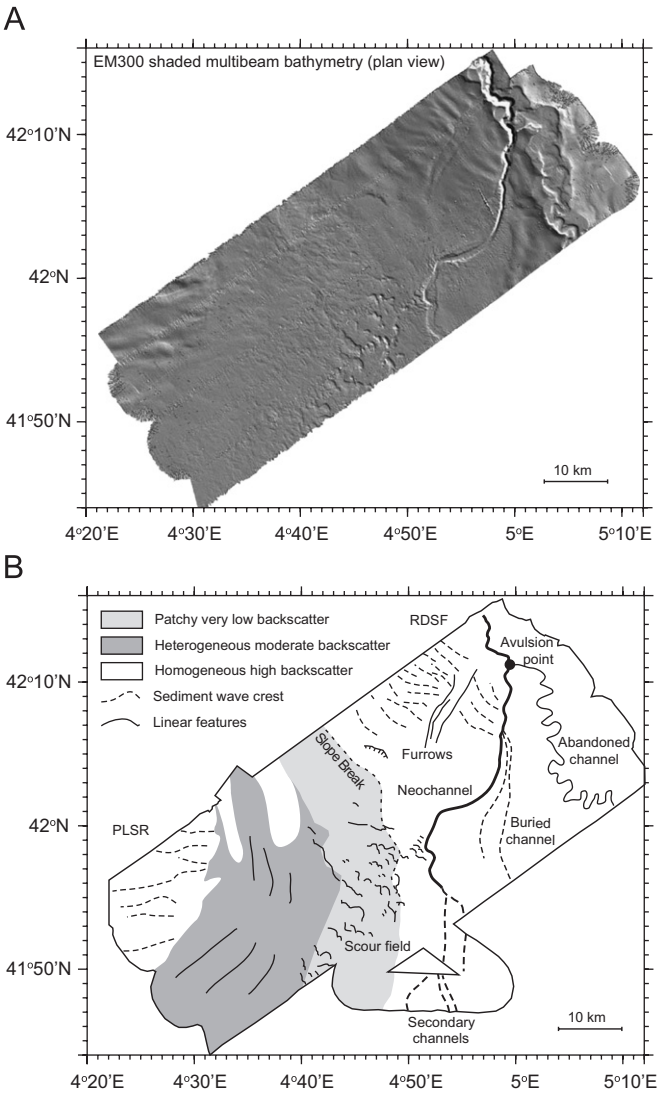


Fig. 8. Shaded EM300 multibeam bathymetry (A) and line drawing interpretation (B), showing the most recent avulsion of the Rhone Channel. Backscatter distribution is interpreted from EM300 backscatter (not shown). Note the presence of giant scours beyond the sharp bend of the relatively low-sinuosity 'neochannel', and the subdued expression of the abandoned high sinuosity channel downstream of the avulsion node. Reproduced from Bonnel et al. (2005) with permission of Elsevier.

(Fig. 8). Seismic profiles through the neofan show well-developed HARPs overlain by a lower amplitude levee-shaped deposit (Torres et al., 1997; Bonnel et al., 2005), while cores recovered from the neofan surface contain either homogeneous, well-sorted, medium-grained sands with an outer shelf origin, or stacked fine-grained turbidites with thin sand-silt bases (Mear, 1984; Droz et al., 2001). Flows are thought to have been more sand-rich during formation of the neofan than previously, as the sediment source switched from fluvial, possibly hyperpycnal, flows to shelf-edge failures and intra-channel erosion (Torres et al., 1997; Bonnel et al., 2005). Giant km-scale erosional scours incised into the neofan surface appear to have resulted from significant spillover at a sharp bend in the neochannel (Fig. 8; Kenyon et al., 1995b; Wynn et al., 2002a; Bonnel et al., 2005).

Beyond the avulsion point, on the middle Rhône Fan, slope angles decrease to 0.3° and a number of smaller distributary channels emanate from the main (abandoned) channel. The offset stacking of different channel–levee systems in this section points to this being an area of frequent avulsion; in contrast channel–levee systems on the upper fan are stacked vertically, indicating limited avulsion (Bellaiche et al., 1984). Channel morphology is hard to trace on the lower fan due to the presence of abundant salt diapirs (Bellaiche et al., 1984), but there appears to be a network of numerous shallow distributary channels indicating progressive downslope–channel bifurcation (Droz and Bellaiche, 1985).

2.1.7. Other examples

Away from the well-studied passive margin fans, there are an increasing number of published examples of sinuous channels on the modern seafloor, following the upsurge in use of planform imaging tools such as multibeam bathymetry and side-scan sonar. However, the very first well-documented sinuous loop in the deep ocean was reported by Shepard (1966) from the deeply entrenched Monterey Canyon, using closely spaced 2D profiles alone. More recent studies of the 'Shepard Meander' have shown this to be an important site in understanding flow overspill processes on the outside of sinuous loops, with both sediment waves and erosional scours in the overbank area being attributed to development of cyclic steps within the flow (e.g. Fildani et al., 2006).

The first imaging of an actual cut-off loop in a deep-water channel was reported by Lonsdale and Hollister (1979) from the Reynisdjup Channel south of Iceland. Their study indicated that flows are capable of cutting across the inner neck of sinuous loops, leading to deposition of dominantly fine-grained turbidites in the progressively abandoned cut-off loop. The location of focussed erosion across the 8-km-wide neck of the cut-off loop is related to a tight left-hand bend immediately upstream in the channel, leading to flow super-elevation in an area where centrifugal and Coriolis forces combine. Spillover flows are responsible for generating km-scale scours and large erosional grooves in the eroded neck area. Earlier phases of spillover also led to development of a crevasse splay, some 2 km wide and 25 m deep, incised into the 60 m-high outer bank of the sinuous loop. Features interpreted to be scroll bars are visible on the inner bank of the cut-off loop while, downstream of the cut-off loop, a 20 m-thick acoustically transparent lens of sediment on the next inner bend is interpreted to be a point-bar deposit.

Kenyon et al. (1975) used long-range side-scan sonar to image sinuous channels on the Nile Fan. These channels are 0.5–1 km wide and occur on slopes of ~0.4°; measured wavelengths of sinuous loops varied between 1.5 and 8 km. Surprisingly, it was over 15 years before these channels were revisited, when Mascle et al. (2001) published the first detailed multibeam bathymetry maps of the Nile Fan surface. They showed that the western channels were apparently more active than those on the eastern fan, with levees over 100 m high, and high channel sinuosity with occasional cut-off loops. As with other major fans, large-scale MTDs are visible on the upper fan interspersed with channels, these slope failures have left exposed headwall scarps up to 100 m high at about 2000 m WD.

Initial studies of Magdalena Fan using 2D seismic profiles (Kolla and Buffler, 1983/1984; Kolla et al., 1984), showed that channels on this fan displayed many similarities to those on Amazon Fan. An increase in the number of channels on the middle fan, was interpreted to be a result of high channel sinuosity with consequent levee breaching and avulsion. Multibeam bathymetric mapping of Magdalena Fan (Ercilla et al., 2002; Estrada et al., 2005) later confirmed the high sinuosity (up to 1.6) of the most recently active channel, and the increased number of channels downfan resulting from successive avulsions. Channel sinuosities generally increase downfan as slope angle decreases, with peak values occurring on slopes of about 0.4°. Quantitative analysis of channel parameters has been carried out, but are focussed on longitudinal channel and levee depth profiles rather than parameters of sinuosity (Estrada et al., 2005). It should be noted that although Magdalena Fan occurs on a tectonically active margin, the overall fan and channel morphology are remarkably similar to major passive margin fans, e.g. Amazon Fan. In addition, an abundance of MTDs cover much of the upper fan, and are responsible for widespread destruction of channels (Ercilla et al., 2002; Estrada et al., 2005).

Although this review is mostly concerned with sinuous channels rather than sinuous canyons, special note should be made of a sinuous canyon system that has been spectacularly imaged by Hagen et al. (1994) in the tectonically active domain of the Peru–Chile forearc. This canyon is up to 350–1100 m wide and 150–250 m deep as it crosses the East Arequipa (forearc) Basin, but becomes more deeply incised as it breaches the forearc structural high. Within the basin, low levees that are 10–60 m high and 500–1500 m wide border the canyon, and overbank sediment waves with wavelengths of 400–800 m and wave heights up to 5 m are widespread. The canyon in this area

exhibits numerous arcuate intra-canyon terraces and several cut-off loops can be observed on side-scan sonar images. Canyon sinuosities average about 2, but exceed 3 in certain areas. Sinuous loop wavelengths are in the region of 1–6.5 km, and amplitudes fall between 100 and 1600 m. Sinuosity increases as slope angle increases, to a threshold slope value of about 0.8°; on progressively steeper slopes, sinuosity values begin to decrease. Tributary canyons that feed into the main canyon display lower sinuosity even though they are crossing comparable slopes, suggesting that turbidity current flow parameters, e.g. volume and grain size, are providing an additional control on sinuosity.

Another incised but highly sinuous 'canyon' is the Cap Timiris Canyon offshore Mauritania (Antobreh and Krastel, 2006). The upper ~290 km, down to 3050 m WD, has been mapped with multibeam bathymetry, and shows an overall sinuosity of 1.4 and local sinuosity peaks reaching 4.2 (measured over a 40 km length). Sinuosity appears to have progressively increased through time, and is spatially controlled by slope angle and underlying fault structure. Downslope migration of sinuous loops is also observed. Intra-canyon terraces (interpreted to be formed by at least three different processes) and cut-off loops are well developed (Fig. 1b), although due to the deep entrenchment (>100 m) levees are poorly developed or absent.

The Almeria Canyon, located on the active Alboran margin of the western Mediterranean Sea, is also a fault-controlled, deeply entrenched sinuous conduit (Cronin et al., 1995). Sinuosity varies from 1.2 to 2.0, which is unusually high given that present-day slope angles are approaching 1°. This highlights the likely influence of structural control on this system, with the sinuous planform developed prior to tectonic tilting. On side-scan sonar records, arcuate intra-canyon terraces are visible, related to canyon-wall slumping, and overspill splay channels and vertical furrows on the outer (cut) banks of sinuous loops can also be observed.

Finally, Popescu et al. (2001) have documented a network of highly sinuous channels on the Danube Fan. This system differs from all those described above, in that the Black Sea was believed to have been a freshwater lake during sea-level lowstands when channels were active. The fan is composed of stacked channel–levee systems, with HAR development in the channel axes and lower-amplitude wedges representing flanking levees. A well-developed distributary channel network on the middle fan is believed to have formed through multiple levee breaching and channel avulsion events, with only one channel active at any one time. Coriolis-induced development of an enlarged right-hand levee (looking downslope) is believed to be responsible for the continued breaching of the lower left-hand levee and four successive channel avulsions to the left. Basal HARPs underlie each channel–levee system and intervening MTDs are scattered throughout the fan stratigraphy. Sampling of a near-surface HARP unit produced well-sorted, slightly normally graded fine sand containing mud clasts. Overall the Danube Fan is morphologically similar to typical large submarine fans, e.g. Amazon Fan, but further sampling would be useful to see if there is a greater input from hyperpycnal flows in the freshwater lowstand-active environment of the Black Sea.

2.1.8. Synthesis of modern deep-water sinuous channels

(1) Most examples of modern sinuous channels are located on major passive margin fans that are fed by huge rivers with a large-volume, mixed (but dominantly fine-grained), sediment load. Consequently, many sinuous channels are presently inactive, or activity is much reduced, as highstand shelf flooding isolates canyon heads from feeder river systems.
(2) Modern sinuous channels often extend for 100s of kilometres downslope and occur on relatively low-angle slopes (0.1–0.5°); they form a core element of laterally extensive mud-rich channel–levee systems, which in turn stack and overlap to form channel–levee complexes. Many channels aggrade to heights significantly higher than the surrounding fan surface.
(3) Deep-water sinuous channels are dominantly fed by high-frequency or semi-continuous, low-density turbidity currents, some of which may be hyperpycnal at times of peak fluvial discharge.
(4) Networks of sinuous channels on major fans typically emanate from a single feeder canyon or channel. Due to frequent avulsion, only one channel in a particular channel–levee complex is active at any one time. Avulsion events can lead to HARP development in lows between channel–levee systems, with subsequent channel fill showing an overall fining-upwards sequence as sand is increasingly efficiently transported to the fan fringes. Sinuosity also typically increases upwards through this evolutionary sequence.
(5) Features indicating lateral migration, such as cut-off loops and scroll bars, are commonly observed in modern sinuous channels. The more incisional channels also display a wide variety of terrace morphologies.
(6) Many sinuous channels on major fans are modified or destroyed by large-scale MTDs, while smaller-scale mass-wasting can significantly modify channel margins and levees.

2.2. Outcrop sinuous channels

Until the early 1990s there was a general lack of understanding of the complexity of fills of submarine channels. This was in part due to the incompatibility of modern datasets (planform datasets of essentially empty channels, with few examples of channel fills) with ancient deposits from 2D outcrop or 1D core through channel fills. The root of the problems of comparison and modelling lay in the scales of analysis, and much of the frustration came from a lack of characterisation of channel fills in ancient

sequences. May et al. (1983) recognised a number of different channel fill styles from the Torrey Pines area of the San Diego Embayment: (1) hemipelagic fills, (2) draped and plugged fills, (3) turbidites and tidally induced deposits and (4) thinning and fining-upwards fills. Mutti and Normark (1987) described three channel fill types: (1) erosional channels, (2) depositional channels and (3) mixed channels, and suggested that the processes leading to channel formation and channel filling may represent genetically independent processes. Shanmugam and Moiola (1988) described five different types of submarine channel fill deposits: (1) thinning-upwards turbidites, (2) slump fills, (3) debris-flow filled channels, (4) hemipelagic fills and (5) combination fills. All of these models focussed on vertical characterisation and channel fill facies. Even today, the broad consensus for deep-water channel fills is that they have broadly fining-upwards turbidite fills.

One of the main advances in outcrop channel fill modelling came from Cook (1993) and Cook et al. (1994) who recognised five main types of channel fill end member, separated on the basis of fill geometry: (1) onlap geometry, (2) convergent geometry, (3) internally scoured geometry, (4) oblique (lateral accretion) geometry and (5) massive (non-bedded) geometry. These geometries were thought to be ultimately controlled by the erosive versus depositional nature of individual flows passing through the channels. Thus, for the first time there was an indication that ancient channel fills might not all be passively infilled 'erosional vacuities', with sand-prone channels presented as elliptical cross-sections of shoestring-shaped bodies at outcrop. Mutti (1985) had already discussed facies variation from channel axis sands (amalgamated, coarser-grained turbidites) passing laterally into channel margin thin-bedded turbidites from exposures in the Spanish Pyrenees and the Italian Apennines. Cronin (1994) and Clark and Pickering (1996) documented ranges of channel fills from across the world, although truly sinuous examples continued to be elusive at outcrop.

Sinuous submarine fan channels were interpreted from the Tesnus Formation, Marathon Basin, East Texas (Wuellner and James, 1989). There, fining-upwards trends were noted above erosive channel bases. The migratory channels and associated facies were in the order of 30–100 m thick. Individual channels, formed by migration of a single channel, are approximately 0.5–1.5 km wide and 10–20 m thick. The migratory nature of the channels was interpreted from fining-upwards trends where, if the channel axis shifted laterally, the progressively thinner and finer channel-margin sands would have then been deposited over thicker channel-axis sands. In contrast to interpreted braided submarine channels from the same formation, the sinuous channel deposits were thought to have undergone a more systematic and gradual change from amalgamated (axial) sandstones to pelagic mudstone. The model developed for depositional processes active in and adjacent to a sinuous submarine fan channel is shown in Fig. 9 (Wuellner and James, 1989), although they did not specifically refer to lateral accretion. This arrangement of trends would lead to a 'pod-like' rather than 'sheet-like'

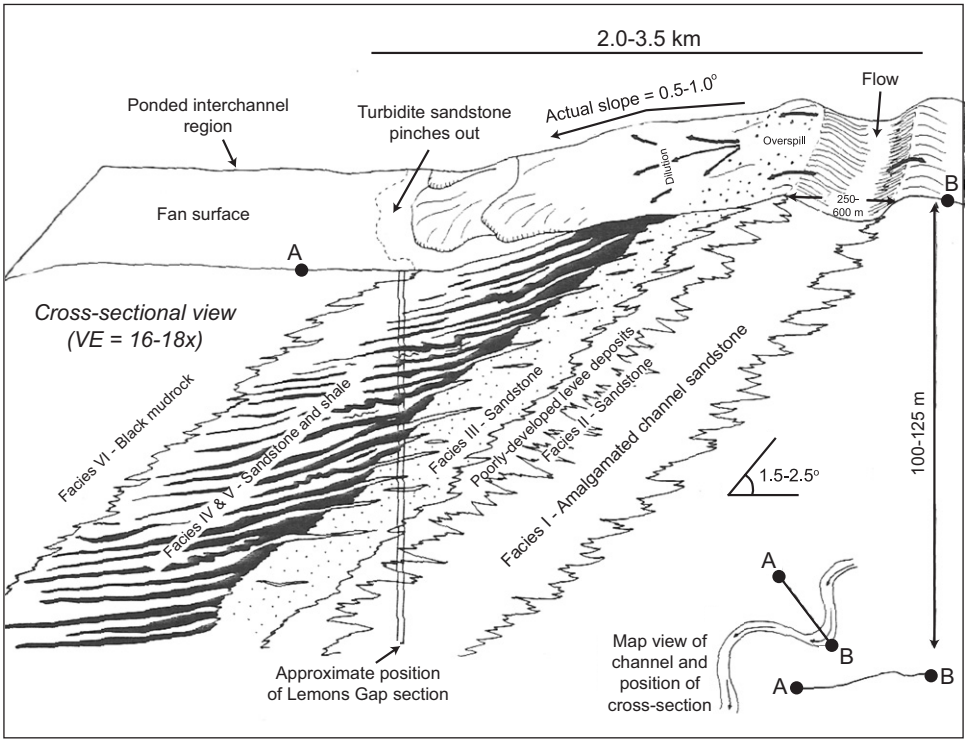


Fig. 9. Variation in channel fill and associated facies in the vicinity of sinuous channels in the Tesnus Formation, Marathon Basin, East Texas. This is one of the first documented examples of sinuous channels at outcrop. Reproduced from Wuellner and James (1989) with permission of Elsevier.

sandbody morphology. The development of sinuous channels in this part of the sedimentary record within the Marathon Basin is thought to have been favoured by (1) low slope gradients, (2) highly efficient (i.e. high suspended load, or muddy) turbidity currents (Ghibaudo, 1980) and (3) continuous turbidity current flow (Damuth et al., 1983a).

The fining-upwards trends attributed to outcrop sinuous channels was not thought to be in itself a strong enough principle for their recognition. Hiscott (1980) noted that sinuous channel deposits may lack accretionary foresets, as until that time there had been no incontrovertible examples documented. One of the first examples was that of Bouma and Coleman (1985), who documented large-scale foresets from the upper Eocene of the Alpes Maritimes of south-east France. The Solitary Channel of Kleverlaan (1982) was discovered to have large-scale accretionary surfaces in its fill by Cronin (1995), indicating the possibility of truly sinuous form, although it was not until later that the architecture of that example was truly understood. The root of the problem lay in what workers were expecting to find: linear sand-prone fairways. Although these do exist, spectacularly in the case of the Brushy Canyon Formation of West Texas (Beaubouef et al., 1999), relatively few examples were identified.

The key insights came from the upsurge of 3D subsurface data, which documented the existence of highly sinuous channels with a similar distribution of sand to sinuous fluvial channels. Sand was found in five main areas: (1) occasionally on the floors of channel cuts, though rarely, (2) in point bars (generally fining-upwards sequences), (3) as thin beds in the levees, (4) as crevasse splays or (5) as frontal splays, through which younger channels then cut through or diverted around. Thus, what we should expect to find at outcrop were vertical and lateral associations between thin beds of the levees, thicker sands within frontal splays and crevasse splays in the overbank and, most critically, mud-prone channel fill plugs separating lenticular sand-prone point bars. This is in stark contrast to the expected shoestring-shaped linear channel bodies that were sought for so long at outcrop. Now we have some excellent documented examples of these types of association at outcrop, and these are discussed below.

2.2.1. Ross Formation, Clare Basin, Namurian, western Ireland

One of the first examples of lateral accretion to be documented in detail from an ancient submarine channel was relatively recent, with the recognition of a number of contrasting architectural styles in turbidite channels of the middle and upper Ross Formation, in the Namurian of western Ireland. The basin fill was initially described by Hodson (1954) and some of its more spectacular features (such as sand volcanoes and synsedimentary deformation features) were documented in detail by Gill and Keunen (1958) and Gill (1979). Research specifically on the Ross Formation came later, with a reappraisal and further documentation of the lower and middle parts of the succession in particular (Chapin et al., 1994; Elliott, 2000a, b; Elliott et al., 2000; Lien et al., 2003; Martinsen et al., 2003).

The lower parts of the Ross Formation are primarily composed of either thin-bedded sheet turbidites or thick-bedded, amalgamated sheet turbidites. Thinning- and thickening-upwards trends are usually absent on a scale of 5–10 m, but on a scale of 2–5 m a clear alternation of thin-bedded turbidites with thicker beds and then a draping heterolithic package is observed (Elliott et al., 2000). These two architectures are interpreted as being of lobe association.

In the middle part of the Ross Formation, where alternations between sheet and more channelised elements were observed by a number of authors (e.g. Collinson et al., 1991; Chapin et al., 1994), aggradational amalgamated channels were recognised by Elliott (2000a, b) and Elliott et al. (2000). These channels were associated with megaflute surfaces and mud-filled scours (possibly gullies), which marked the initiation of aggradational channels by large-volume, low periodicity, bypassing flows. Above these channels, lateral accretion surfaces were documented in other channel bodies. For example, detailed images from part of the sinuous channel belt exposed at Rehy Cliffs on the Shannon Estuary (Fig. 10) have proved extremely informative (e.g. Elliott, 2000a, b; Elliott et al., 2000; Abreu et al., 2003; Lien et al., 2003). The line drawing by Elliott et al. (2000) elegantly illustrates the westwards migration of the complex, with a sinuous channel belt some 380 m wide and 7.5 m deep, individual lateral accretion surfaces with lengths of 85 m, and an estimated individual channel width of 130 m. Elliott et al. (2000) described in detail the form and architecture of the observed point bars, and a reduced version (with added observations from the second author) is reproduced here. The channel fill comprises interbedded sandstones and mudstones/siltstones that display westerly dipping depositional surfaces in three sectors of the channel fill. Bed thicknesses, defined by the dipping surfaces, range up to 1.0–1.5 m, although this is largely due to amalgamation of thinner beds. Individual sandstone beds are well defined and have a flattened lens shape, tapering both up- and down-dip. Each lens shingles downdip. Thicker (>1 m) sandstone beds (made up of amalgamated thinner beds) have erosional bases and are separated by thinner fine-grained turbidites. Matrix-supported intraformational mud-clast breccias are found nested within the sandstone packages. Dipping surfaces locally show parallel sets with a systematic decrease in bed thickness up-dip, but less regular bedding styles are also found. These include inclined erosional surfaces, some with onlapping aggradational beds, while some areas also show horizontal erosion. A solitary slump is recognised, and the upper part of the channel belt is characterised by horizontal, thin-bedded turbidites.

The channels are interpreted to be sinuous, and occur just below a marine band (a condensed interval) associated with relative sea-level rise (Lien et al., 2003). The sinuous

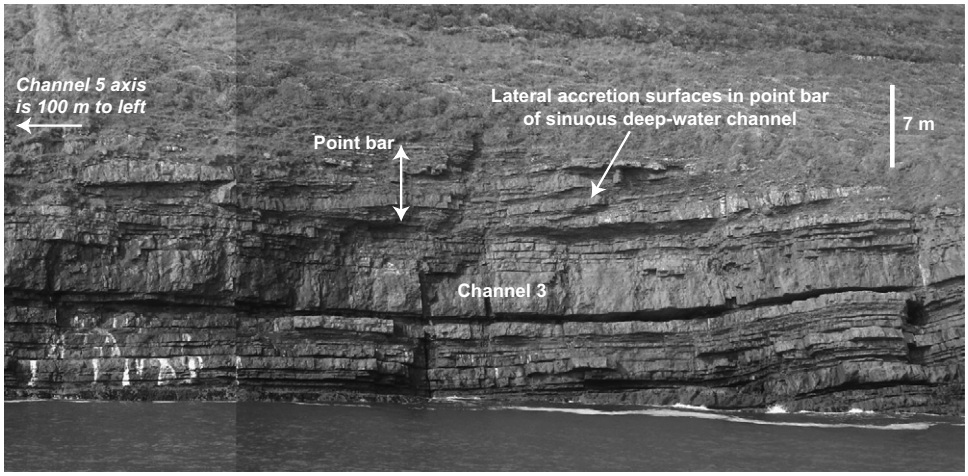


Fig. 10. Detailed image showing lateral accretion surfaces in uppermost of five channels observed in the Ross Formation at Rehy Cliff, northern Shannon Estuary. Channel 5 (terminology of Elliott et al., 2000) is interpreted as a sinuous deep-water channel.

channel elements were thus associated with decreasing input of large-volume, coarse-grained turbidity currents in the basin, and an increasing input of fines (silt and clay), just before the 'shutdown' of the turbidite system. What is notable about the channel body in Rehy Cliff is that the point-bar deposits are not marked by continuous lateral migration interrupted by clay drape development, but are considerably more episodic in character, as documented above. The alternations in erosion and deposition within the point bar, and the vertical aggradation and localised onlap of turbidites against some lateral accretion surfaces in particular, are characteristic features of this well exposed deep-water channel (Elliott et al., 2000).

Although there is undoubtedly more complexity to the architecture of the channel seen at Rehy Cliff, and variations in the volume of flows, the direct link to a fluvial source is supported here. For example, although (1) the sediment source is second cycle, and therefore compositionally and texturally mature, and (2) the nature of the exposure does not always favour a clean surface, there is still an overall lack of obvious sedimentary structures, such as grading. Many of the turbidite beds are predominantly Bouma T_a with a capping Bouma T_b. Plant material is very common throughout, including intact silicified logs of *Lepidodendron* (particularly though not exclusively in the intraformational conglomerates), as well as disseminated layers of plant material towards the top of turbidite beds. In situ growth of *Lepidodendron* has been described from the youngest of the five deltaic cyclothems (Tullig) by Wignall and Best (2002). This preponderance of plant material and, tentatively, the lack of grading, suggests a direct sourcing of much of the Ross Formation from a deltaic origin. Organic material is readily recycled by vigorous, migrating distributary channels in a lower delta plain, and then transported downslope and into more distal settings via hyperpycnal flows once a critical threshold in discharge is reached during river flood. An increase in supply of fine sediments into the system, with a concurrent change to a mixed feeder fluvial style (as noted by Elliott et al., 2000), will likely increase the possibility of sinuous channel development in deep water. Elliott et al. (2000), in describing accretion units related to deep-water channels in the Ross Formation, implied that during periods of lowered sea-level the sedimentation rate was so high that sediment could have been supplied to the deep-water fan system by quasi-continuous hyperpycnal currents emanating from the delta mouth.

In summary, a particularly excellent example of a sinuous channel belt is exposed in the upper part of the (Namurian) Ross Sandstone Formation in western Ireland. The channel complex exhibits prominent low-angle cross-stratification with a variety of lithofacies and stratal relationships, implying a complex development with alternating phases of erosion, deposition, accretion, aggradation and bypass (in no particular order) that differ markedly from fluvial point-bar architecture.

2.2.2. *Solitary Channel, Tabernas Basin, southern Spain*

One of the best-documented examples of low-angle cross-stratification in a deep-water channel exposure is that of the Solitary Channel in south-east Spain. This narrow, elongate Neogene intramontane basin was one of a series of basins connecting the Mediterranean Sea to the Atlantic Ocean in pre-Messinian time. The basin fill is ~900 m thick (Kleverlaan, 1989) and is composed of a deep-water fan complex overlain by shallow marine deposits (only the upper and lower 50 m of section are not related to 'submarine fan' deposits). Kleverlaan (1982, 1989) described three different systems with contrasting architectural style, two with recognisable radial geometries and one linear system. Two of these systems have been described subsequently in some detail. The radial Sandy System is one of these, and is particularly sand rich. The Mixed System also has a radial geometry but is characterised by significantly lower sand:shale ratios, and by frequent slumping, but has not been documented in as much detail.

Both of these systems were thought to have been sourced from the northern margin of the basin. The Solitary System is the linear and isolated system and forms the focus of this section.

The Solitary Channel (as it is now called) was known to consist of one long channel completely isolated within basinal (sand-starved) mudstones. It is mapped as having a linear planform. The fill is a mixture of both lenticular and sheet-dominated packages of sandstones and pebbly sandstones, up to 150 m wide and 10–25 m thick, enveloped in marl, and extending 2 km beyond the other two systems. Cronin (1994, 1995) examined the Solitary Channel fill architecture in some detail, and recognised a four-fold channel fill; his lowermost Unit A was described as a 'clinoform surface unit', initially interpreted as both bedforms and lateral accretion surfaces. These larger surfaces dip up-system and become finer-grained in that direction, towards the west. Subsequently, Haughton (2000) described the Solitary Channel as having a west–east and not east–west orientation, having recognised cross-bedding and other palaeocurrent indicators (32 unambiguous flute marks) that eluded previous authors. He interpreted the large-scale clinoforms as representing back-filling of the channel with progressively finer sediment. In the axial parts he also recognised second-order inclined stratification within the channel fill, initially interpreted as lateral accretion by Cronin (1995), which he described as inclined bundles dipping at up to 10° (relative to bedding in the marls surrounding the sand body), with azimuths at a high angle to the overall sand body trend. Thin-bedded 'marginal sections' composed of bundles of lenticular, sharp-based sandstones 0.1–0.25 m thick, are arranged in low-angle, shingled to sigmoidal packages, and seen in sections at a high angle to the inferred palaeoflow. These were interpreted as inclined bed stacks extending tens of metres transverse to initial small-scale channel incisions, with some showing a change from initial lateral offset to aggradational infilling of these small channels.

With the correct channel orientation documented by Haughton (2000), Pickering et al. (2001) used anisotropic magnetic susceptibility data to confirm this interpretation, but also reinterpreted the larger-scale inclined stratification as being a new type of deep-water bedform produced by back-filling of the channel, as a means of accounting for their odd orientation in relation to palaeoflow. Subsequently, Abreu et al. (2003) used the Solitary Channel as an outcrop analogue, including using seismic forward modelling, to compare with LAPs from the Girassol and Dahlia fields offshore Angola. From their paper the term LAPs was introduced, but was defined from seismic data rather than outcrop. Arnott (this issue) uses the new term LADs, exclusively for LAPs and their sedimentary facies specific to outcrop, due to the degree of scale incompatibility. Abreu et al. (2003) documented several examples of LAPs/LADs from the Solitary Channel, and current consensus is that these packages are classic deep-water point bars. In this section we thus revert to the descriptions of Cronin (1994), and use the vertical expression of Unit A in one logged section as being representative of a classic fining-upwards deep-water point bar (Fig. 11).

Unit A comprises a sequence of thick (>1.5 m) erosive- or sharp-based, massive, medium- to coarse-grained tabular sandstones. Locally, lenses of pebbles and conglomerate are found (0.3–0.7 m thick). Beds contain thin laminae or layers of plant material, seen either as small lumps of coalified material, or disseminated carbonaceous layers, which are sometimes repeated towards the tops of the beds. The unit has an overall thickness of 5–5.5 m. Unit A displays evidence for the development of large- and small-scale dipping lateral accretion surfaces (Fig. 11). The surfaces extend from the top to the bottom of Unit A, as massive 1.4–2 m thick sandstone beds. Each individual dipping surface may extend several tens of metres along the exposed section. Each clinoform comprises alternating beds of medium- to coarse-grained sandstones with 'floating' quartz pebbles, and draping 0.1–0.25 m thick shale beds. The clinoforms are traced throughout Unit A in all exposed sections of the Solitary Channel (e.g. Fig. 11) and, in contrast to the interpretation of Pickering et al. (2001), have a number of orientations between west and north-east (Cronin, 1994, 1995). The larger west-dipping surfaces were interpreted incorrectly as downstream-dipping clinoforms by Cronin (1995), but the other dipping surfaces (which are oblique to the trend of the Solitary Channel) were correctly interpreted as being lateral accretion surfaces, which is currently the accepted hypothesis for these smaller-scale packages.

The low-angle cross-stratified bundles observed at high angles to the inferred trend of the Solitary Channel are therefore interpreted as LADs. Most bundles are underlain by obvious erosive or very sharp bases. The bundles are sigmoidal in shape, originating from the right of the channel (south) either as isolated thin beds or as a thin bed over a thicker, underlying bed; they then progressively thicken, and then thin, towards the left (north). The bundles all shingle, usually in both directions. Dip angles may be up to 15° in the centre of an individual bundle (Cronin, 1994), which flattens out in the direction of shingling. The youngest beds in each bundle may have a more aggradational character on the left-hand side. Each of these bundles corresponds to the fill of a small-scale channel within the larger Solitary Channel. These small channels show clear evidence for lateral migration, and thus these channel forms are interpreted as small, sinuous channel elements (Fig. 12). They are usually thin (2–4 m), and only occasionally display a fining-upwards character. They rarely show evidence for tractional bedforms such as dunes, which are so typical of the basal lower parts of fluvial point bars.

2.2.3. *Ainsa Channels, Hecho Basin, northern Spain*

There are many excellent examples of submarine channel fills and related deposits exposed in the south-central

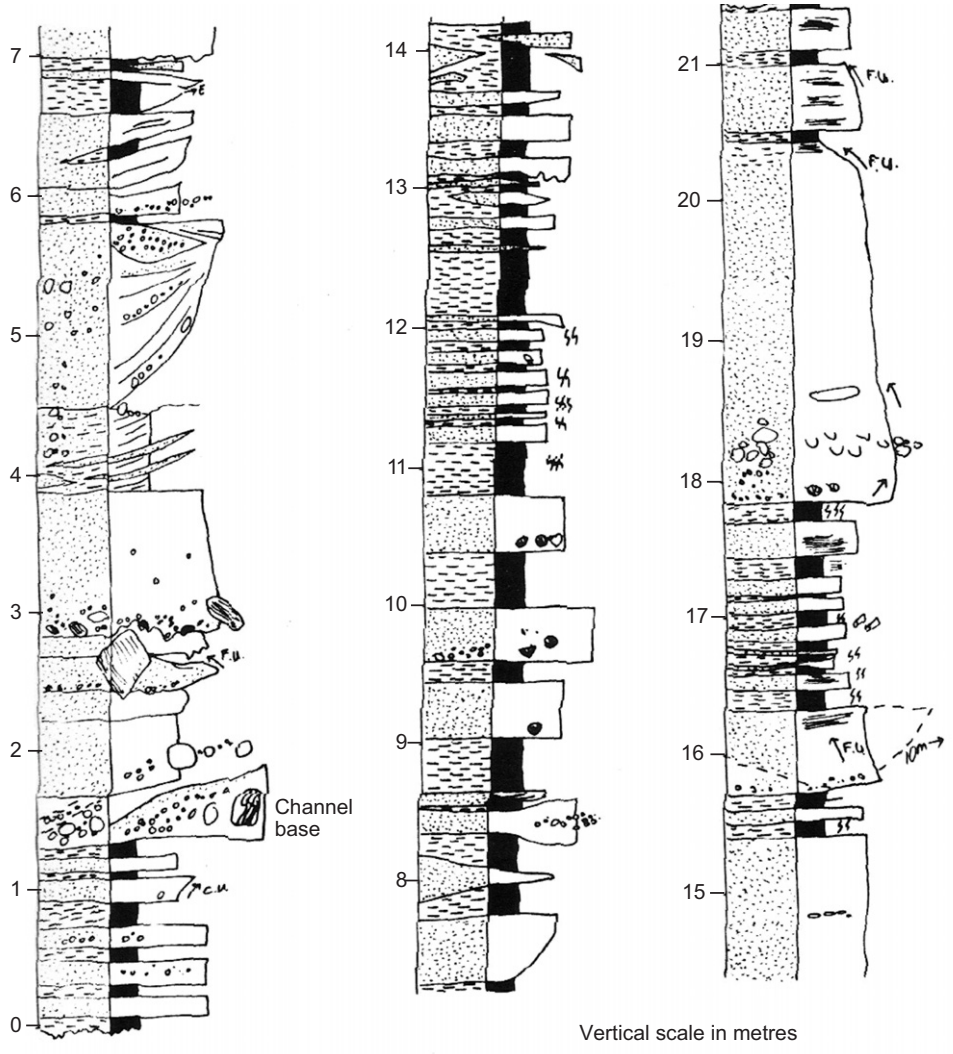


Fig. 11. Sedimentary log through a clinoform unit of the Solitary Channel, Tabernas Basin (from Cronin, 1994), showing upwards thinning from 1.3 m (base of channel) to 14.2 m, through Units A (0–8.6 m) and B (8.6–13.7 m). Within Unit A there are several bundles of sediment with inclined stratification towards the north, highly oblique to channel trend (e.g. 3.8–4.5 m; 4.5–5.8 m; 6.6–7.0 m; 7.0–7.7 m). These are interpreted as small-scale lateral accretion packages (1.5–3 m thick), in contrast to the larger scale cross-stratification which is thought to be formed by channel back-filling processes (Haughton, 2000). A line drawing of some of these packages is shown in Fig. 12.

Pyrenean foreland basin of the Spanish Pyrenees. The depositional setting of the basin was reconstructed from geological maps of Seguret (1970) and Soler and Puigdefabregas (1970), and subsequent work by Mutti and co-workers at the University of Parma (Mutti et al., 1985, 1988; Mutti, 1977). The basin fill through Cuisian to Lutetian time intervals consisted of a delta complex to the east that fed, via submarine channels incised onto a delta slope, a deeper turbidite basin to the west. There were three stages of evolution recognised within this period of basin filling. The first phase saw the development of fluvio-deltaic sequences to the east, the second phase then saw both shallow marine and deep-water sequences, when most of the turbidites were deposited in the deep basin to the west (Mutti et al., 1985). The third phase is represented by the deposition of the Ainsa Sequence, which is the focus of this case study. This sequence developed during a period of dramatic and marked synsedimentary deformation, which saw the deltaic shelves and alluvial plains being involved in severe structural uplift along the frontal thrust zone of the Pyrenees. Some thrusts propagated under the basin as it became progressively incorporated with the thrust front as a piggyback basin, and these growth-thrust sheet tips formed growing anticlinal features on the basin floor, e.g. the Boltana and Mediano Anticlines, which diverted sediment transport pathways (Mutti et al., 1988; Marzo et al., 1998). East of the Boltana Anticline, the sequences are dominated by submarine channel-fill turbidite bodies (Mutti et al., 1988), which are separated predominantly by upper slope-derived MTDs (Cronin et al., 1998; Pickering and Corregidor, 2005). Westwards from the Boltana Anticline, the succession is characterised by non-channelised sandstone lobes (Mutti and Ricci Lucchi, 1972; Mutti, 1977; Remacha et al., 2005).

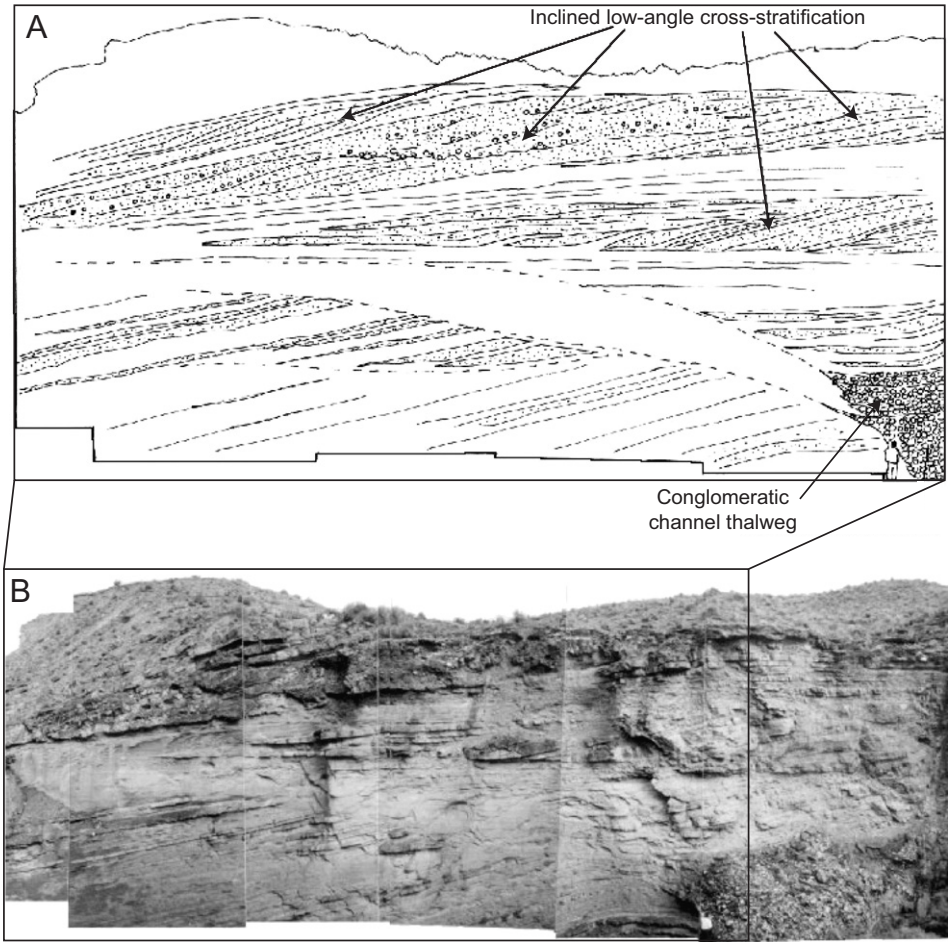


Fig. 12. Line drawing (A) and photomosaic (B), showing axial section through the Solitary Channel at Rambla Lanujar, Tabernas Basin. Palaeoflow is obliquely into the cliff. Several phases of channel activity are observed. Also visible is the geometry of low-angle cross-stratified bundles of interbedded sandstones, mudstones and, locally, pebbly sandstones. At least three such packages are observed in this image. Individual for scale (1.8 m high, bottom right).

Documentation of channels in the Ainsa Sequence, the last of the three phases of basin development, has included general characteristics of each channel section (Clark and Pickering, 1996) and more detailed studies of specific channel locations (e.g. Schuppers, 1993; Cronin, 1994; Clark and Pickering, 1996). Documentation of earlier channel fills, particularly of the Gerbe channels of the Santa Liestra Sequence, has not yet led to an equivalent proliferation of papers, and is largely restricted to the work of Mutti et al. (1988). In this section, we focus on the documentation of two channel sections, the Gerbe 1 Channel of the Santa Liestra Sequence, and the Ainsa 1 Channel of the younger Ainsa Sequence.

The Gerbe 1 Channel fill deposits are well documented by Mutti et al. (1988), and the vertical succession is shown in Fig. 13. The Gerbe channel-fill deposits have an overall thickness of about 45 m and are overlain by finer-grained thin-bedded turbidites. The succession consists of four fining-upwards sequences, with each sequence including basal clast-supported conglomerates, and pebbly cross-stratified sandstones, overlain by finer-grained facies. These sequences were interpreted as phases of channel incision, activity and abandonment (Mutti, 1985). The uppermost part of the channel-fill succession above these four fining-upwards sequences records the final abandonment of the Gerbe 1 Channel, and is dominated by finer-grained facies. Thin-bedded turbidite sandstones and mudstones encase thicker sandstone beds which are graded and have water escape features. Two of these thicker sandstone beds contain conglomeratic lenses. The units display abrupt lateral erosional terminations, and well developed lateral accretion surfaces. They have been interpreted as shallow sinuous channels found in the late stages of the larger channel system, corresponding to the abandonment phase (Mutti, 1985). This was one of the first documented examples of a sinuous submarine channel at outcrop.

The Ainsa 1 Channel has been described in some detail (Schuppers, 1993; Cronin, 1994; Clark and Pickering, 1996) as a mixed erosional–depositional channel. It is preceded and overlain by thick sections of upper slope/outer shelf-derived muddy slumps, which include pebbly and cobbly mudstones with extrabasinal clasts covered in *Lithophaga*

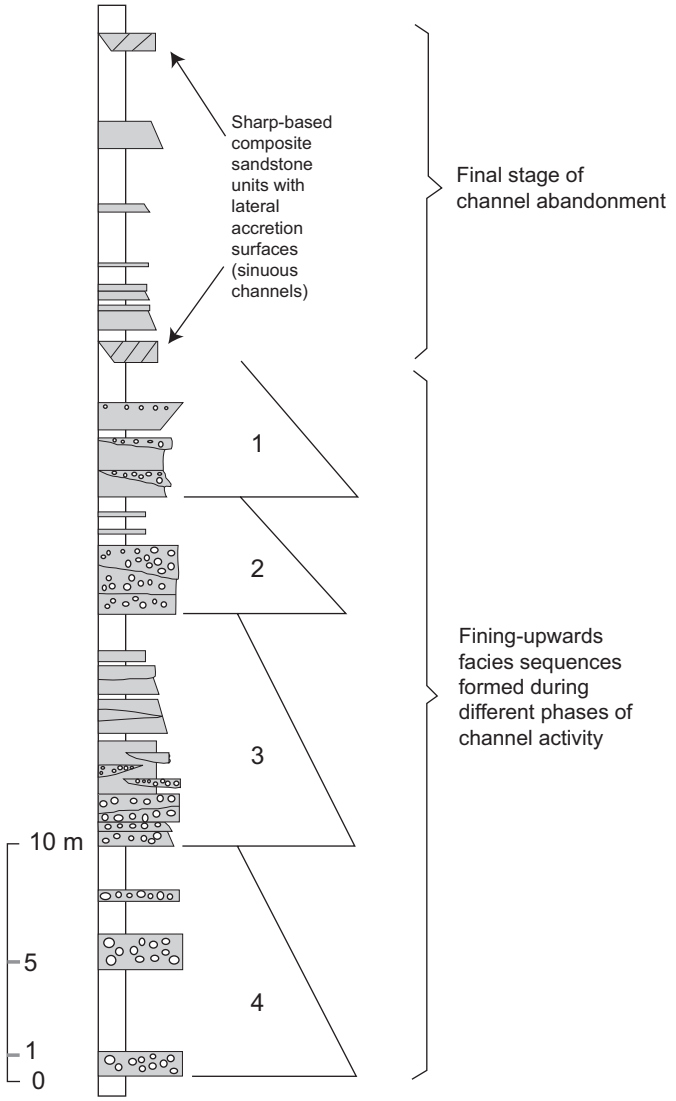


Fig. 13. Vertical facies distribution within the Gerbe channel-fill deposits (Santa Liestra Sequence). Note four main fining-upwards sequences in the lower part of the succession. These basal, residual deposits are overlain by finer-grained facies. The latter record the final phase of channel abandonment (modified from Mutti et al., 1985).

borings. The succession is interpreted as a deep-water slope interval which was frequently disturbed by earthquake-triggered collapse, blanketing the lower slope sector with MTDs (Cronin et al., 1998). Channels were developed between these slope collapse events, and pass down-dip into confined sheet-turbidite bodies, which ponded against the growing Boltana Anticline (Mutti et al., 1985). The Ainsa 1 Channel is best exposed in a quarry south of Ainsa (Fig. 14). Cronin (1994) interpreted the channel as having a restored width of approximately 850 m and a fill thickness of 30 m, with the fill recording polyphase history of erosional and depositional cycles, five in total, with packages of amalgamated sandstones, localised intraformational conglomerates, and interbedded sandstones and shales. Cronin (1994) documented the occurrence within the channel fill of lateral accretion surfaces, also recognised by Clark and Pickering (1996). Within fill sequence 2, which comprises much of the sandstones that occur directly above the channel base on the southern margin, beds are observed to swale, thicken and thin, and onlap the channel margin. The majority of sandstone beds are up to 1 m thick, with thinner sandstones uncommon. Beds commonly have thin coalified layers towards their tops, associated with a small change in grain size (typically from fine-grained sandstone to coarse siltstone). Sometimes these layers are more disseminated and diffuse, or repeated several times. These layers or laminae are composed of plant material, usually non-descript but locally recognisable plant leaves or bark can be seen.

Smaller scale (1–3 m across) channelised elements occur at the southern margin, with gravel-rich lags. Amalgamation of sandstone beds is common at the margin and not restricted to the main channel axis as suggested by Mutti et al. (1988). Sandstones are separated by thin shale interbeds, which regularly pinch out and laterally are sub-parallel to major bed boundaries. In the Peira-Cava region of the south-east Maritime Alps (France) similar bed contacts are seen (Bouma and Coleman, 1985), although the dipping internal contacts exposed so well on the southern margin of the Ainsa 1 Channel are not as clear in the French examples.

The lateral accretion surfaces described from the Hecho Basin are associated with underfit channel elements, related to variable energy of flows within a widened channel fairway. The vertical sequences exhibit variability in gravity flow energy, with alternation in erosion (small-scale channel cuts and amalgamation), sustained flow (growth of lateral accretion surfaces) and surge-type turbidity currents (graded beds) (*sensu* Mutti et al., 1999). Thinning- and thickening-upwards cycles are not recognised in the channel fill, and most beds are continuous from margin to margin, suggesting a dominance of back-filling processes within the channel body. The LAPs are thus associated with relatively 'passive' phases of channel activity.

2.2.4. Hasret Mountain Channels, Elazig Basin, eastern Turkey

A series of entrenched, multiphase occupancy, deep-water slope–channel complexes form a planform tributary network on the northern slope of the Eocene–Oligocene backarc Elazig Basin in eastern Turkey (Cronin et al., 2000a, b, 2005, in press, a, b). The lower 60% of the slope–channel-complex fills are characterised by coarse-grained sediments and the upper 40% by heterolithic facies. The latter drape a syn-sedimentary faulting phase of activity that saw reactivation of the slope–channel complexes after their main phases of filling. The lower part of this draping facies, which thickens towards the axes of the slope–channel complexes, is dominated by slumped shales and local thin-bedded turbidite sandstones and siltstones. The upper part of the draping facies comprises sheet and

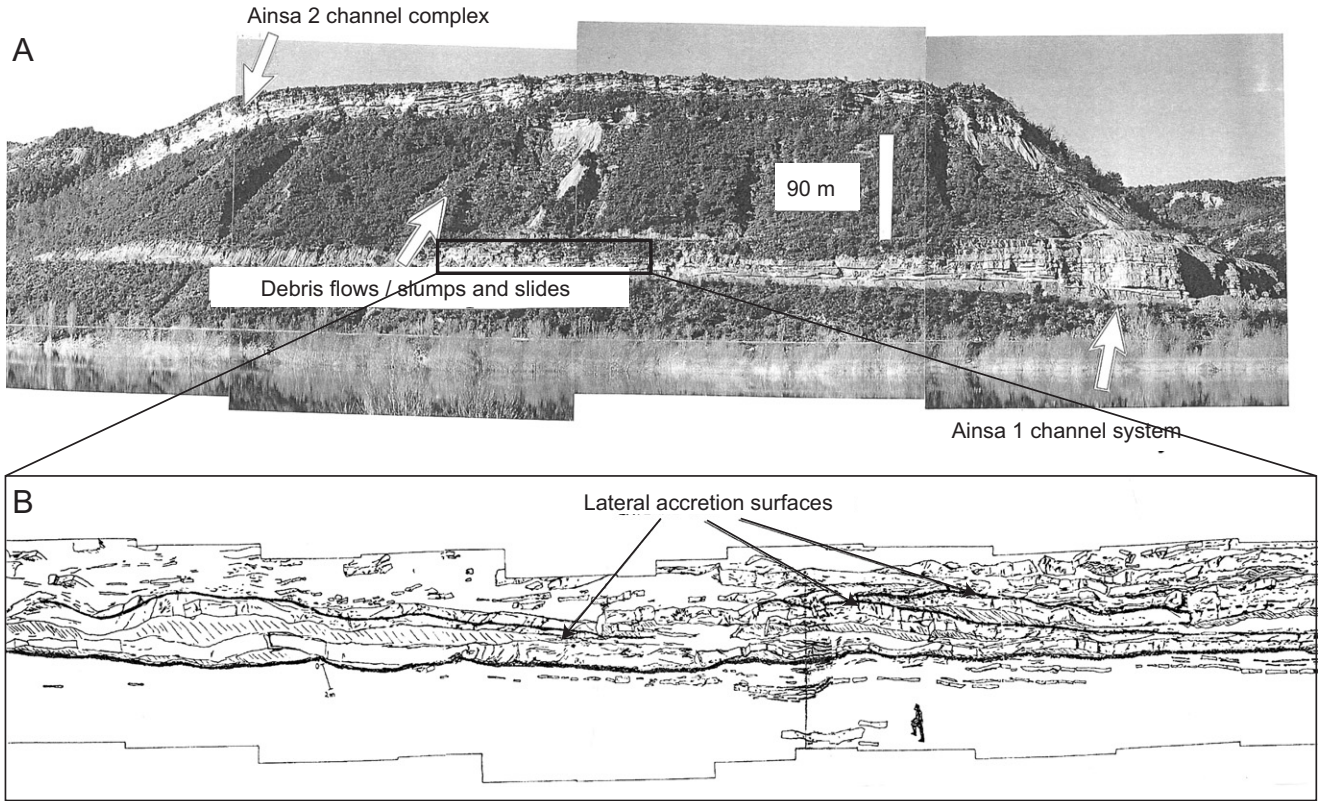


Fig. 14. Photomosaic (A) and enlarged line drawing (B) showing Ainsa 1 Channel quarry exposure. Note location, on the southern margin, of prominent lateral accretion surfaces associated with sinuous, sand-prone channel elements. Scale on lower image indicated by individual at bottom right.

lenticular pebbly sandstones and sandstones, interbedded with rippled sandstones and siltstones. They are associated with channelised sediment body geometries. This latter interval is also characterised by lateral accretion surfaces, where beds have a clearly asymptotic and shingling character, an association with sedimentary structures such as trough cross-bedding, and where palaeocurrents infer sinuosity of the channel elements. The sinuous channels are up to 3 m thick and 10–40 m in width. Interleaving shales have abundant and diverse deep-water and shelfal ichnofacies, and deep-water benthic/planktonic foraminiferal assemblage ratios. The sand-prone portions of these sinuous channel bodies are dislocated, and usually confined to the accretionary margins and channel floors. The exceptional exposure allows the channel elements to be tracked for 7 km in a series of dip and strike sections above four separate canyons.

Channel elements are overlain by a 1–2 m section of pelagic fauna-rich mudstone, which has a marked red tinge and is exposed throughout the area above the clastic-rich sections at Hasret Mountain. This interval is interpreted to reflect complete cessation of input of sediment to the slope from the source area, thought to reflect regional maximum flooding. These late-stage sinuous channel elements, and their association with entrenched deep-water slope–channel complexes, are therefore shown here as an example of confined late-stage sinuous channels.

Channel bodies are clearly recognisable in aerial photographs as shoestring-shaped bodies of coarse sediment, nested in finer-grained facies. Their axes, margins, confining levees and overbank complexes are readily mapped downslope and away from the channel bodies. The typical cross-sectional geometry of the channels resembles a ‘moose head’ in cross-sectional profile, with a low aspect ratio, a deep and occasionally asymmetric axial portion, succeeded by a more laterally extensive and mud-filled upper portion with a high aspect ratio (corresponding to the ‘antlers’ of the moose). This last architectural element is the focus of this case study.

The planform expression of the largest and most laterally extensive entrenched deep-water slope–channel complex, the Main Channel, is linear. All other channel complexes described from the area are tributary to the Main Channel. It is at least 1.2 km wide, and 200 m thick, making it much larger than the other channel complexes. The southern margin and overall orientation of the Main Channel are clearly controlled by the ENE–WSW orientation of the tilted fault block of basement rocks which confines it to the south, and forces palaeocurrents to run oblique to palaeoslope. Fig. 15 schematically illustrates the architecture of channels seen in Hasret Mountain.

The Main Channel is located above the buried axis of the earlier conglomerate-filled channel complex. The lower part of the channel element is characterised by slumped,

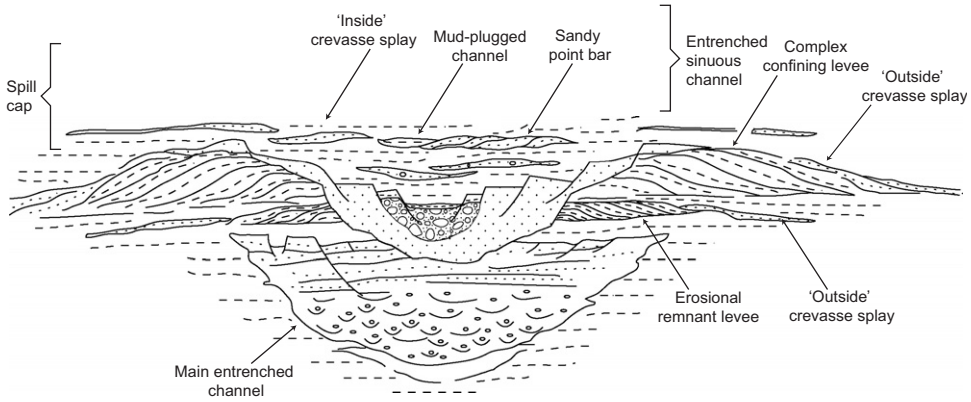


Fig. 15. Stylised model for entrenched deep-water slope–channel complexes, developed from the channel complexes of Hasret Mountain, Eocene, eastern Turkey. The different phases of channel-complex activity are clearly visible. A number of architectural elements are of particular interest: (1) outside crevasse splay: this corresponds to fill phases of early periods of channel occupancy, which have subsequently been aggraded over and then eroded by later phases of channel activity; these features are largely found as erosional remnants; (2) complex confining levee: the later aggradational phase of channel complex development which forms the obvious levee 'envelope' seen on seismic sections; (3) spill cap: the uppermost phase of channel complex fill, including the underfit late-stage sinuous channels and crevasse splays seen outside the main channel complex. Reproduced from Cronin et al. (in press, a) with permission of AAPG.

channel-margin, thin-bedded turbidites and mudstones. There are highly discordant bedding angles in some of these sediment bundles. This disturbed interval is underlain by sand-free slope mudstones, particularly evident in the left-hand side of the image shown in Fig. 16. The disturbed interval is overlain by a prominent set of low-angle cross-stratified turbidite sandstones, which shingle to the left and are truncated at their tops. The bases of some of these beds are covered with sole marks, and trough cross-bedding is common in the sandstones and oriented to the west and south-west, oblique (but not quite orthogonal to) the lateral accretion surfaces. Palaeocurrents are obliquely out of the exposure in this cut, and this varies in the many exposures to the left, allowing the channel elements to be mapped for several kilometres. Subsequent beds are ripple cross-laminated, interbedded, thin-bedded and thicker-bedded turbidites with prominent sole marks. These beds are broadly tabular, rather than low-angle cross-stratified.

The overall architecture of the section is thus: (1) erosive cut into slope mudstones; (2) slumped, channel margin, thin-bedded turbidites; (3) LAP with tractional bedforms (Fig. 17); (4) tabular channel-fill sandstones; (5) ripple cross-laminated thin-bedded turbidites; and (6) slope mudstones. As with the previous case studies, deep-water point bars in late-stage sinuous channels of entrenched slope–channel complexes are dissimilar in many ways to fluvial channel point bars, with variations in energy, fewer tractional features, and alternations in sustained sedimentation (growth of lateral accretion surfaces) and surge-type (*sensu* Mutti et al., 1999) turbidity currents (tabular, graded beds).

2.2.5. *Outcrop synthesis and working models*

Additional to the outcrop case studies documented above, special mention should be made of the study of Arnott (this issue) from the Isaac Channel of the Windermere Group, Canada. This channel is composed of LADs, which are up to 13 m thick with dips of 7–12° and lengths of 120–140 m. The lateral extent of entire LADs is 400 m. The lower parts of LADs are characterised by thicker, amalgamated sandstones and mudstone breccias with no tractional features, and the upper part by thinner-bedded turbidites which are truncated down their slopes. There is poorly developed upwards fining, although thinning is seen, and there is simultaneous vertical and lateral aggradation. These deep-water point bars appear to be similar to those observed in the Rehy Cliffs section of the Ross Formation (Fig. 10).

Drawing together all of the above examples, we have summarised the range of lateral accretion complexity observed in deep-water channel outcrops (Fig. 18). This summary is presented as a model for deep-water point bars, to be tested using other field examples, and for comparison with fluvial point bars. The following characteristics are listed which are common to all variations:

(1) Deep-water point bars may or may not be associated with a master erosional surface. Case 1 (Hasret Main Channel, Turkey) is associated with such a surface, with point-bar development over slumped, channel margin, thin-bedded turbidite facies in a channel cut. Case 2 (Ainsa Channel 1, Spain) has a basal surface which is predefined by topographically irregular seafloor, which is largely controlled by MTDs; point-bar development occurs above this surface. Case 3 (Solitary Channel, Spain) has isolated point-bar development within a much larger channel complex, with the active sinuous-channel element migrating laterally and stopping against the master confining channel-complex surface. Case 4 (Rehy Channel 5, Ireland) displays point-bar development above unconfined basin-floor sheet sandstones.

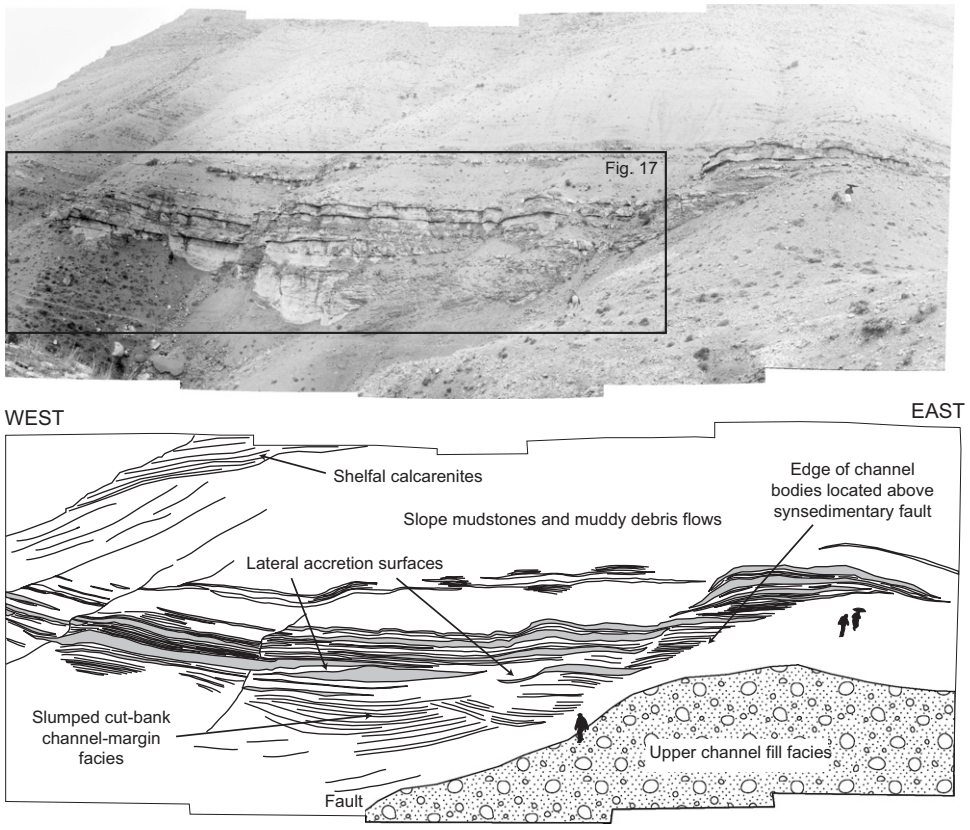


Fig. 16. Photomosaic and line drawing, showing close-up view of lens body 2 above the dip-section through the Hasret Mountain Main Channel. This lens body is a strike section through a sinuous channel element which has both laterally accreting (low-angle cross-stratified, shingled, and trough-cross-stratified, channel-fill sandstones) and vertically accreting (stacked, tabular and graded channel fill sandstones) elements within the main lens. Abundant tool and flute marks and other sole marks indicate that palaeoflow direction was out of the cliff towards the south, in stark contrast to the west and southwest palaeoflow directions observed in underlying phases of conglomerate and turbidite sandstones within the main channel complex. Sediments underlying the main lens are slumped channel margin mudstones. The entire section is full of bathyal depth benthic foraminifera. Individuals for scale. Reproduced from Cronin et al. (in press, a) with permission of AAPG.

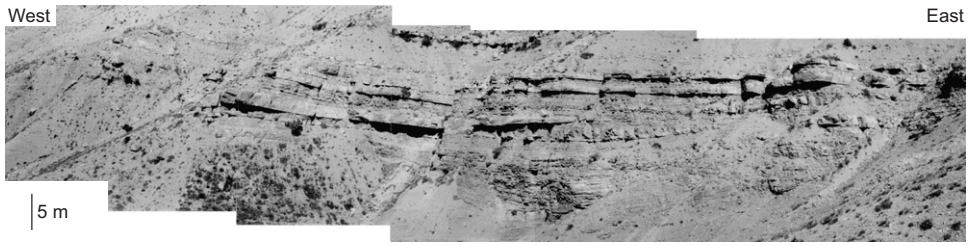


Fig. 17. Enlarged photomosaic of the Hasret Mountain Main Channel late-stage sinuous-channel element, showing detail of lateral accretion surfaces seen in Fig. 16.

(2) Deep-water point-bar growth shows fluctuations in activity. Case 1 shows lateral accretion occurring in several steps, with tractional bedforms common and evidence for sustained flow to allow this bar form growth; point-bar development stopped, and was then succeeded by, normal gravity flow deposition. Case 2 shows lateral accretion occurring episodically, with interruption by erosional episodes. Case 3 exhibits lateral accretion occurring continuously, followed by underfit gravity flows that led to aggradation within the channel. Case 4 exhibits lateral accretion of the point bar, with much small-scale complexity in flow energy, leading to erosion, local scouring and collapse of the point bar, and then reactivation of lateral accretion.
(3) Deep-water point bars are typically broadly fining-upwards, however, they do not show systematic fining-upwards profiles like those seen in fluvial point bars.
(4) Deep-water point bars are associated with the late stages of activity of each of the case studies documented

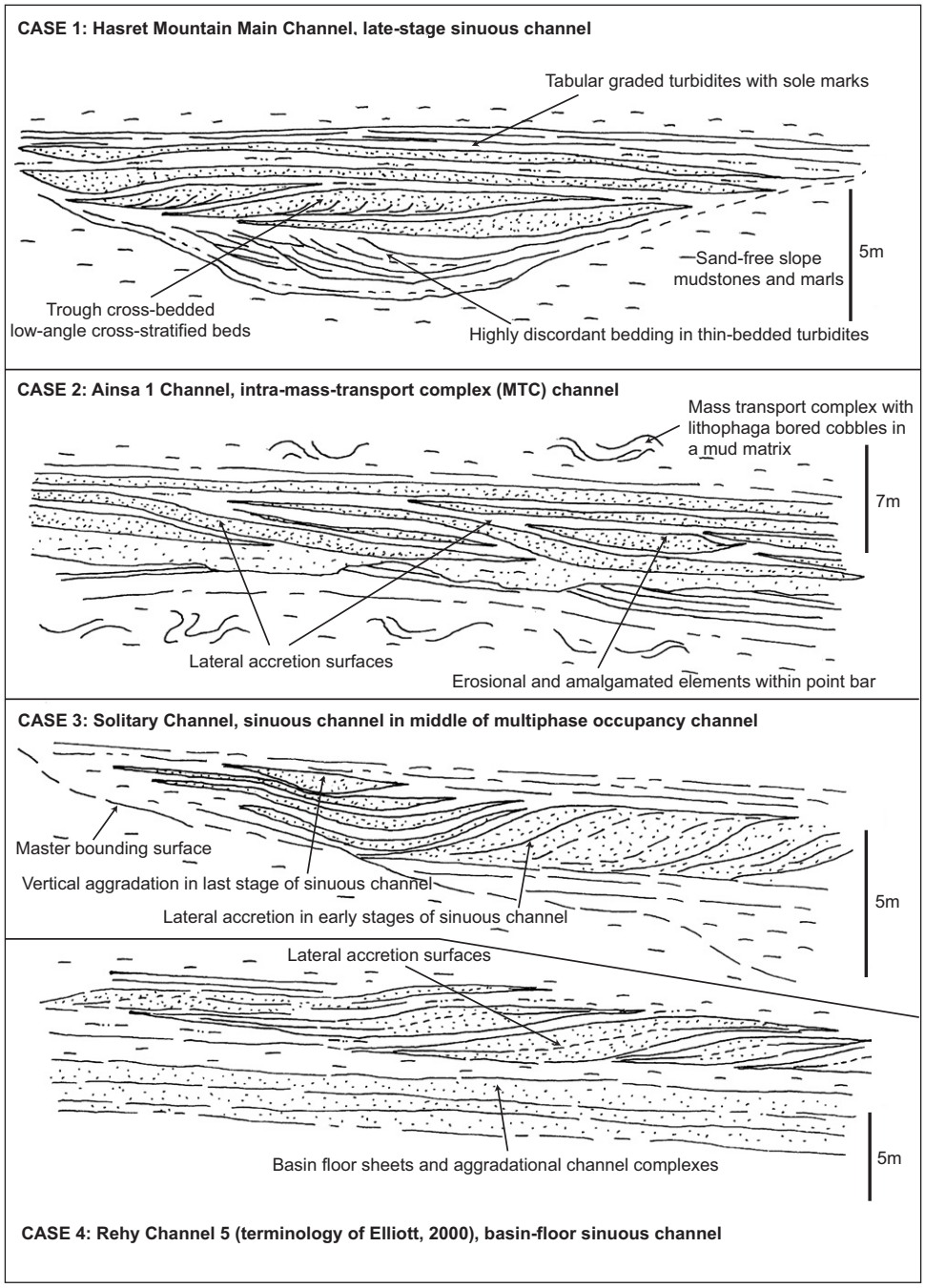


Fig. 18. Range of deep-water point-bar architecture observed at outcrop, as documented in this paper: Case 1: Hasret Mountain Main Channel late-stage sinuous channel element, Elazig Basin, eastern Turkey; Case 2: Ainsa 1 Channel, Tremp-Graus Basin, Spanish Pyrenees; Case 3: Solitary Channel, Tabernas-Sorbas Basin, south-east Spain; and Case 4: Rehy Channel 5, Ross Formation, western Ireland.

here. Cases 1 and 4 in particular are overlain by marine bands associated with maximum flooding surfaces.

(5) Deep-water point bars are thin relative to channel depth. For example, Abreu et al. (2003) document a LAP ~20 cm thick from the Jackfork Group, Arkansas (their Fig. 21) and Arnott (this issue) shows such a relationship in the Windermere Group, Canada. The reason for this is thought to be due to intra-channel topography having reduced lateral gradients (Das et al., 2004) (see also Section 3.1).

(6) It is difficult to draw dimensional associations between point-bar width and channel size, as documented LADs may be associated with second-order channels, rather than the master bounding surfaces of channel complexes (e.g. Clark and Pickering, 1996).

(7) Many deep-water point bars are associated with an increase in silt and mud in the system. This is

interpreted to be a consequence of the nature of the feeder system, and most likely an increase in suspended load within the fluvial feeder system. Rapidly migrating distributary fluvial channels in the source area, associated with mixed bed load and suspended load sediment transportation, would also explain the large amount of coalified plant material found in several of the case studies, and may also have implications for the presence of hyperpycnal flows in the late stages of these systems. The occurrence of coalified material is of course not evident from the classic Windermere Group LADs (Arnott, this issue) due to the age of the sediments (Proterozoic) nor was it documented in the other key study on LAPs (Abreu et al., 2003).

2.3. Subsurface deep-water sinuous channels

Tertiary slope deposits, originating from gravity flow deposition, have proven to be spectacularly successful hydrocarbon reservoirs, particularly on the west African margin. Coupled with advances in deep-water drilling technology, improved 3D seismic resolution, and recent increases in exploration and production activity in these areas, our knowledge of sedimentary architecture in deep-water slope settings has also significantly advanced. In fact, subsurface data sets, particularly from planform images such as seismic amplitude extraction displays, have driven outcrop workers back to the outcrop to go on 'elephant hunts' of their own for elusive architectural elements. Some of the most elusive elements are deep-water point bars and their related channels, as discussed in Section 2.2. Here we review some of the best-documented examples of deep-water sinuous channels from the west African margin to compare with modern and outcrop examples.

2.3.1. Confined sinuous channels, Lower Miocene, offshore Gabon

The Lower Miocene Baliste-Crecerelle canyon fill is a confined deep-water channel complex supplying two oil fields, the Baudroie Marine and Baliste fields, located about 20 km offshore from the modern Ogooue delta (Wonham et al., 2000). This study of a slope–channel complex/canyon is one of relatively few published examples presenting well data (wire line and core) alongside 3D seismic data. These subsurface data allow documentation of canyon evolution, including confined sheet sands, erosional surfaces, extensive mud drapes, and prominent sinuous channels, particularly in Baliste 2 (the upper part of the canyon fill). The filling of the canyon is related to long-term Lower Miocene sea-level rise, with the canyon being fed directly from a delta. Since delta-fed systems are classically dominated by fine-grained material, this is thought to have had potential for hyperpycnal flow regimes to prevail, and thus the development of sinuous deep-water channels. Successive channels are observed to be offset stacked, with different channel erosion-deposition cycles attributed to either autocyclic switching or relative changes in sea level.

Wonham et al. (2000) analysed channel bodies using amplitude maps from thin intervals (40 m thick). A vertical transition from straight to sinuous channels was observed. At the scale of the seismic data, lateral accretion surfaces were not recognised, although from the outcrop examples shown in Section 2.2, where LADs ranged in thickness from 2.5 to 13 m, this is not surprising. Even with the well data available, there was insufficient material to undertake a comprehensive calibration of sediment facies to architectural element (this also true for the majority of other subsurface sinuous channel studies), so planform analysis was instead undertaken. One of the key findings was that relationships observed in planform from fluvial and modern seafloor sinuous channels, e.g. straight line relationships seen in log-log plots of sinuous loop wavelength versus channel width or radius of curvature, were not observed to be the same. The subsurface Baliste 2 sinuous channels are also an order of magnitude smaller than modern Amazon and Mississippi examples (discussed in Section 2.1 above). It was noted that deep-water submarine channels are both wider and have a greater radius of curvature of sinuous loops than river channels with the same wavelength (Wonham et al., 2000).

2.3.2. Confined sinuous channels, Lower Miocene, offshore Angola

The Dahlia M9 Upper Field, Block 17, Angola, is a classic example of subsurface laterally migrating submarine channels (Abreu et al., 2003). The Green Channel Complex was documented to assist with characterisation of reservoir connectivity, and two outcrop examples were used to illustrate analogous architecture at outcrop, and to forward model the outcrop using seismic and well data from the Dahlia field.

The Green Channel Complex has been further subdivided into channel complex sets, each containing a number of individual channels (terminology of Sprague et al., 2002 and Abreu et al., 2003). The channel complexes are clearly recognised on amplitude extraction maps (Fig. 19) where they display an overall moderate to high sinuosity. Each channel complex starts with a relatively straight channel that becomes more highly sinuous over time. Active channels are 300 m wide and 40 m thick, and are located within the wider fairway of the channel complex (Abreu et al., 2003).

Detailed mapping of the Green Channel Complex (Abreu et al., 2003), over a series of successive bends in the channel, reveals consistencies in the internal geometry of reflections around bends. The reflections were found to be (1) shingled, (2) parallel to the edge of the channel on the inner bend, (3) showing bidirectional downlap in sections parallel to the trend of the channel on inner bends, and (4) generally preserved. The shingled reflections dip towards the channel along which they were formed and

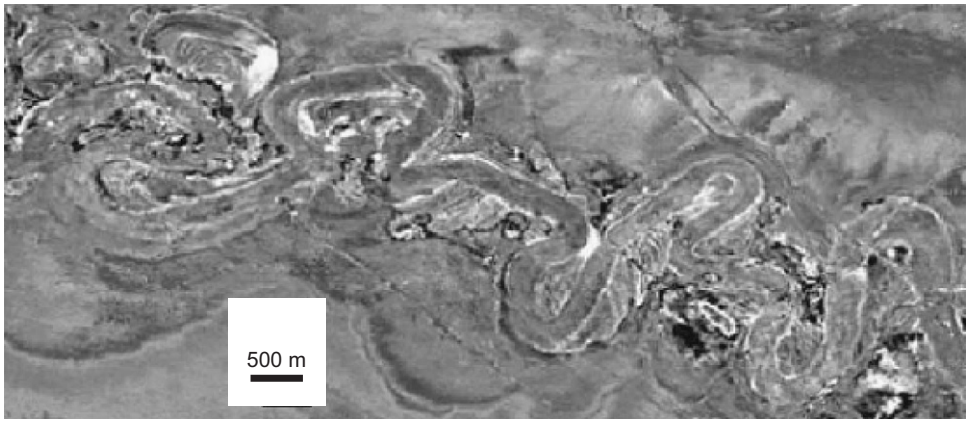


Fig. 19. Horizon slice from 3D seismic, 26 ms below the top of the Green Channel Complex, offshore Angola, showing moderate to high channel sinuosity. Reproduced from Abreu et al. (2003) with permission of Elsevier.

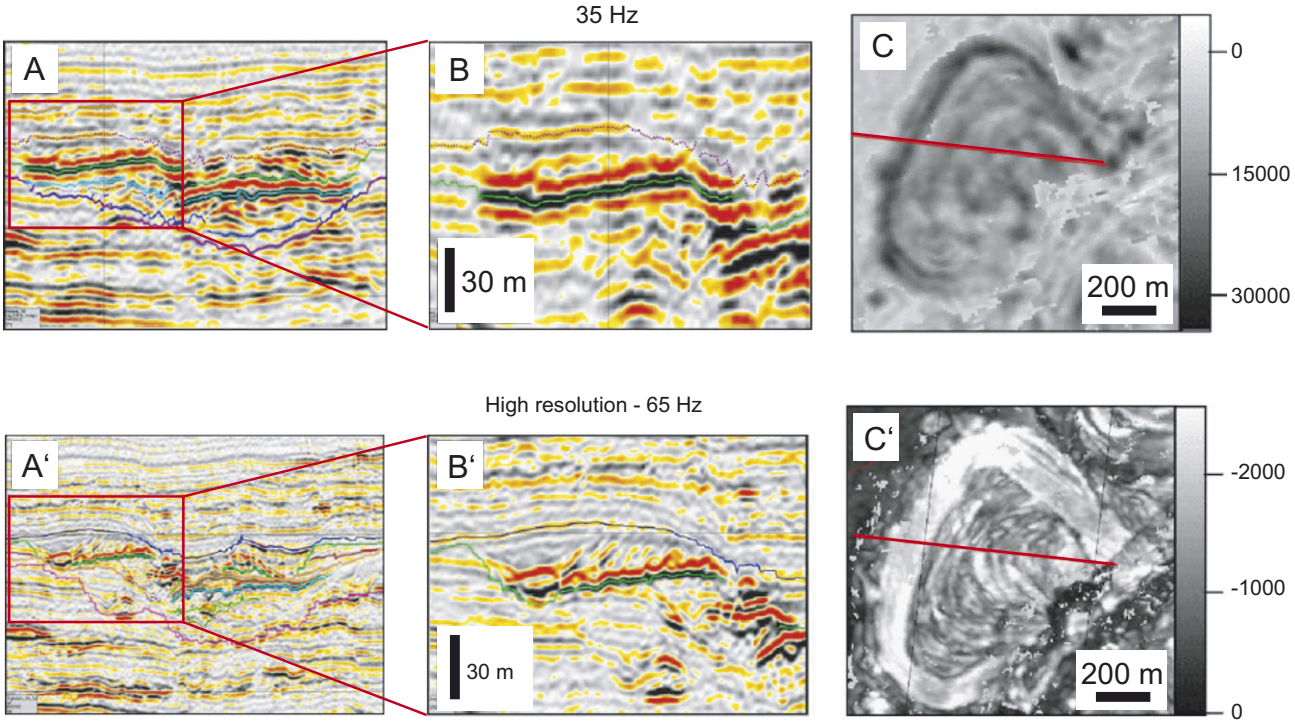


Fig. 20. High-resolution 3D seismic data from Block 17, offshore Angola. Image shows conventional resolution (35 Hz) and high-resolution (65 Hz) seismic examples of (1) a cross-sectional view of the Dahlia field (A and A′), (2) a 'zoomed-in' cross-sectional view of the Green Channel Complex (B and B′), and (3) an amplitude map at the base of the Green Channel Complex (C and C′). Amplitude extractions are from the green horizon at the base of the channel shown in B–B′. Red squares in A and A′ and red lines in C and C′ indicate position of cross-sections B and B′. Shingled reflectors at channel margins are visible in the higher-resolution data in cross-section B′, showing a characteristic 'scroll bar' pattern in map view C′. Reproduced from Abreu et al. (2003) with permission of Elsevier.

occasionally show a downdip component in the lateral migration of the channel (Fig. 20). These reflections are arranged in packages and this is where the term 'LAP' was introduced. The length of individual LAPs is five times the active channel width, and LAPs are thinner than the depth of the active channel. Core data from the Dahlia, and nearby Girassol Fields (which has a greater number of cored intervals), show a pronounced thinning- and fining-upwards of sedimentary facies, from conglomeratic channel lags and associated amalgamated sandstone beds, to deterioration in reservoir quality towards the top of LAPs. Such a vertical association of facies is very comparable with fluvial channel point bars (with the exception of the preponderance of graded beds in these deep-water examples and tractional features in the fluvial).

Other examples of sinuous channel belts offshore Angola show clear fining-upwards patterns within channels, and the combination of a few well penetrations and detailed seismic attribute analysis has led to relationships being drawn between seismic expression and reservoir quality

(Sikkema and Wojcik, 2000). In summary, sinuous channel belts contain three distinct units within the fining-upwards sequence, over an interval typically up to 200 m thick: (1) basal debrite sands, (2) amalgamated channel sands and (3) aggradational sinuous channels with overbank deposits. This scale of description would be comparable to the entrenched slope–channel complexes referred to above and in other studies, e.g. Mayall and Stewart (2000). The sandy debrites are not associated with sinuous channel forms, although rare low-sinuosity channel reaches are found where sandy debrite facies are interbedded with normal turbidites. Amalgamated channel sands are found associated with higher sinuousity patterns, including solitary sinuous channels. These prominent moderate- to high-sinuousity channel forms represent combinations of amalgamated channel sands and thin beds organised in multilateral systems, with lower sand content than the basal sandy debrite reservoirs (Sikkema and Wojcik, 2000).

Aggradational channels with levees have lower sand content, show classic 'gull-wing' geometry and have lower sinuosity than the truly sinuous forms present within the amalgamated channel sand units (Fig. 21). Some highly sinuous forms with low reflectivity and amorphous fill represent mud-filled bypass channels. These channel forms are interpreted to reflect changes in slope gradient (Sikkema and Wojcik, 2000).

2.3.3. *Sinuous channels from the Gulf of Mexico subsurface*

A number of deep-water channel–levee fields are in production in the central and eastern parts of the Gulf of Mexico, e.g. Ram Powell (Kendrick, 2000) and Tahoe (Clemenceau et al., 2000; Kendrick, 1998, 2000). These depositional systems are described as structurally unconfined slope channels in the form of ribbons, some 5 km wide and 10s of kilometre's long. They show classic 'gull-wing' geometry on seismic profiles, with overbank levees flanking a submarine channel (e.g. Tahoe, Kendrick, 2000). Somewhat surprisingly, production rates from the overbank thin-bedded units were far higher than expected (Shew et al., 1994). However, clear documentation of channel sinuosity is sparse. Clemenceau et al. (2000) described in some detail the production histories and architectures of Ram/Powell, and the 'L' and 'M' sands

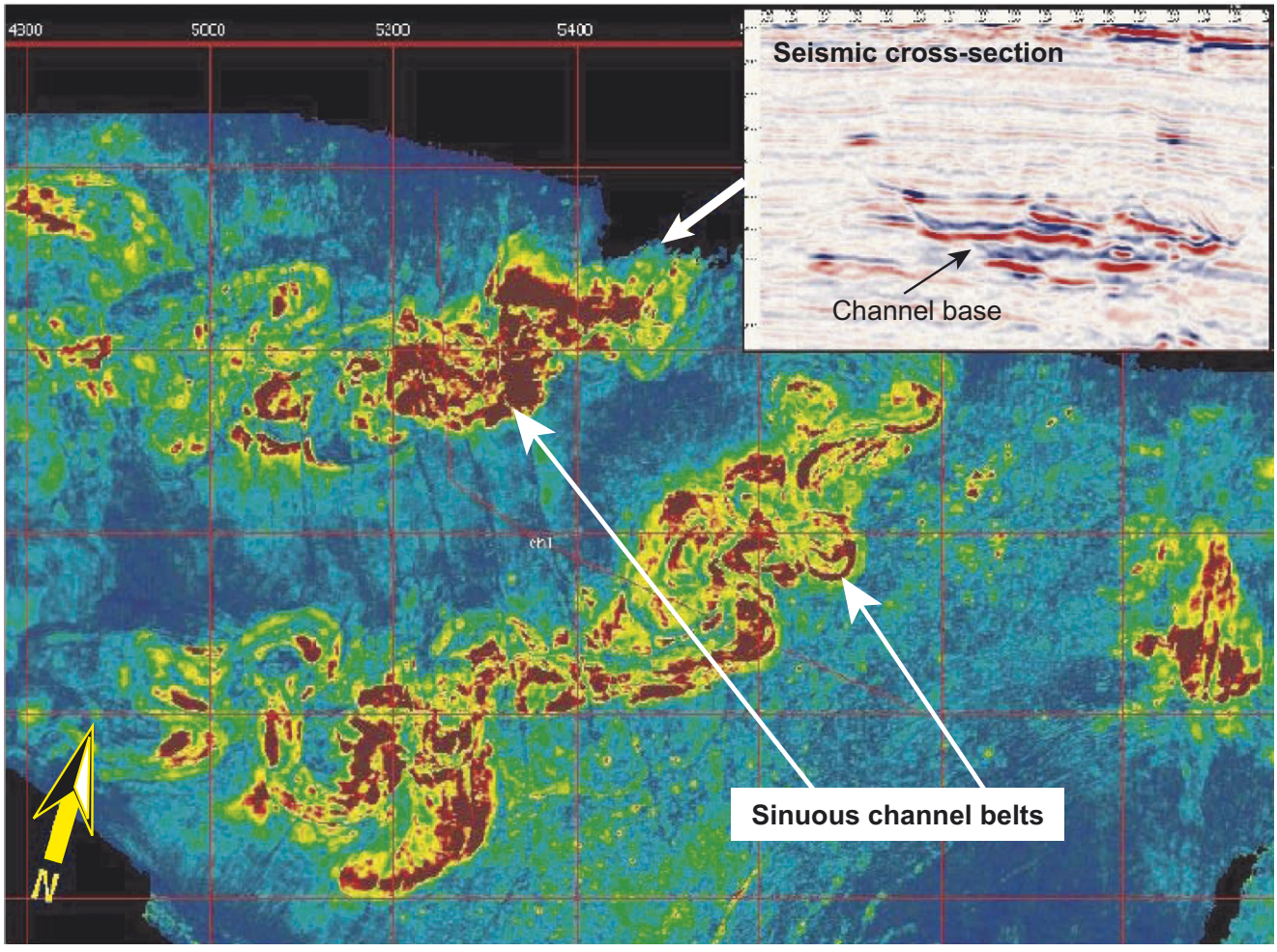


Fig. 21. Gated amplitude map with accompanying seismic section, illustrating seismic geometries of a Miocene sinuous channel complex in Block 18, Angola. Red = high amplitude. Reproduced from Sikkema and Wojcik (2000) with permission of GCSSEPM.

were described as being aggradational channel–levee complexes. The 'L' sand in particular contains much of the heterogeneity within the field and has been the focus of more detailed analysis. The overall character of the channel fill facies is of a very subtle fining-upwards character. Although the planform architecture has been imaged on seismic, only the oil-charged sands allowed imaging of architecture as water-filled sands are poorly imaged on seismic in this area. The channel is ~500–700 m wide and 10–30 m thick, with channel-fill sands unconnected to overbank sands. Other channel complexes have more convincing sinuous planform (e.g. Roberts and Compani, 1996), but few have been documented as comprehensively as those from west Africa.

2.3.4. Summary of subsurface observations

Most of the 'classic' papers describing highly sinuous deep-water channels in the subsurface are from offshore west Africa (e.g. Stephens et al., 1996; Kolla et al., 2001; Abreu et al., 2003; Mayall et al., 2006; Deptuck et al., this issue; Kolla, this issue). From these papers, and those discussed above, the following observations may be summarised:

(1) Gross planform characteristics of deep-water channels (sinuosities, sinuous loop wavelengths, avulsions) show many similarities with fluvial channels (Kolla et al., 2001). The Dahlia Green Channel Complex (Abreu et al., 2003) displays strong lateral and downdip migration with LADs on every channel bend and frequent cut-off loops. However, the nature of sinuosity evolution is thought to be due to repeated channel aggradation and subsequent lateral migration, rather than lateral migration alone as seen in fluvial channels (Peakall et al., 2000a; Kolla et al., 2001).
(2) Channel complexes show a broad fining-upwards of sedimentary facies, with a corresponding decrease in bed amalgamation.
(3) Sinuous deep-water channels are often found towards the top of confined slope–channel complexes, and this is interpreted to reflect changes in slope gradient and sediment supply, as discussed earlier (example shown in Fig. 22).
(4) Deep-water point-bar deposits (LAPs of Abreu et al., 2003) may be sand-rich or mud-rich.

2.4. Modelling of flows in sinuous channels

The physical and numerical modelling of sinuous submarine channels is a relatively recent research field, with the earliest numerical work on flow dynamics dating to 1999 (Imran et al., 1999) and experimental studies of channel processes dating to 2000 (Peakall et al., 2000a). Earlier numerical models did, however, examine the mean velocities of flow through submarine channel bends, through analysis of flow super-elevation (Komar, 1969;

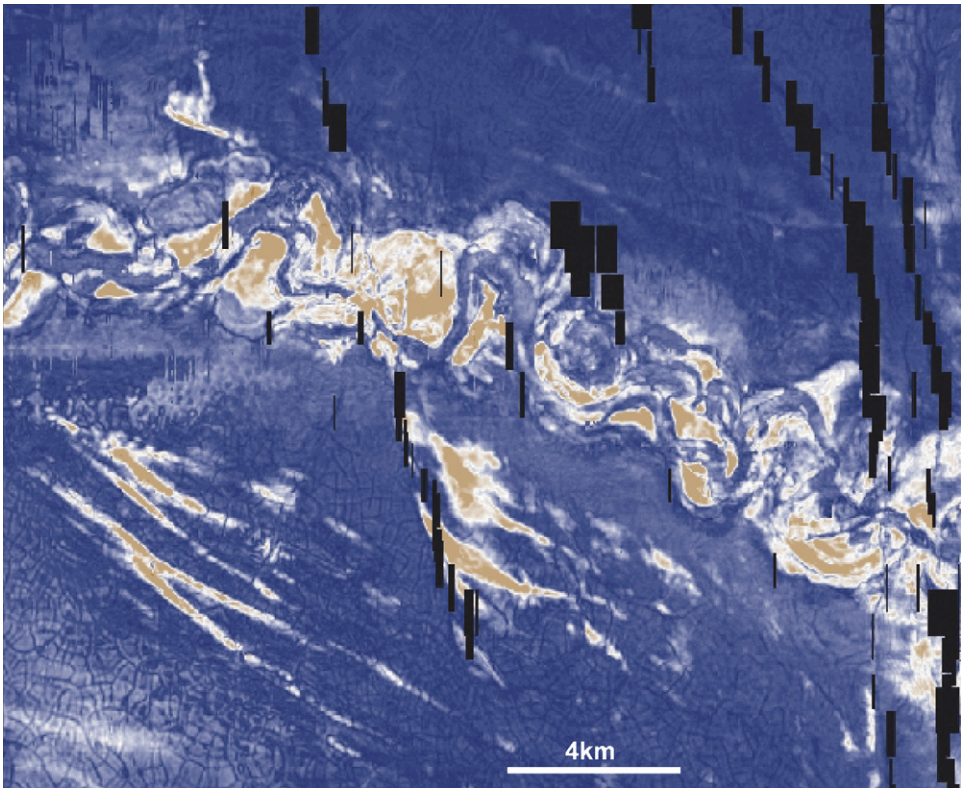


Fig. 22. Detail of 3D seismic horizon slice, showing a sinuous channel from the West African subsurface. High amplitudes are shown in red and low amplitudes in blue. Note how many of the channel cuts have low-amplitude fills, and how many of the higher amplitude areas are erosional remnants (Cronin, unpublished data courtesy of Eni Agip S.p.A.).

Bowen et al., 1984). Although the modelling of sinuous submarine channels is relatively new, it has built upon an extensive literature on gravity currents in straight experimental channels and associated numerical models (e.g. Middleton, 1966, 1993; Komar, 1977; Stacey and Bowen, 1988; García and Parker, 1993).

There has been a rapid expansion of the sinuous channel modelling field over the last few years, with progress made in three key areas: (1) channel initiation and development, (2) intra-channel processes, and (3) overbank processes, each of which are explored here.

2.4.1. Channel initiation and development

Sinuous submarine channel initiation and development has proved to be extremely difficult to model in the laboratory, with early work producing incipient channels, although these were neither longitudinally extensive nor sinuous (Imran et al., 2002; Parsons et al., 2002; Baas et al., 2004). Métivier et al. (2005) succeeded in producing erosive low-sinuosity channels in low-density cohesionless sediment (Fig. 23). The experiments inputted continuous brine currents that were approximately 1 cm thick and consequently laminar. Sinuous channels were found to form at the highest slopes ($>13^{\circ}$) and at the lowest discharges ($\leqslant 4$ ml/s), this minimising the spreading angle from the initial jet and encouraging channel erosion through bedload transport and progressive confinement (see also Lancien et al., 2006). The channels were associated with terraces but did not form bars (Métivier et al., 2005). Yu et al. (2006) also produced weakly sinuous channels, but from low-concentration (estimated at 1–2% volumetric concentration), low discharge (15–50 ml/s), clay-rich particulate flows. These channels formed on a slope of 4° and showed a downslope change from erosive channels to fully depositional channels with micro-levee relief of 1–2 mm. As with the Métivier et al. (2005) experiments, the flows forming the depositional channels were approximately 1 cm thick, were laminar (Reynolds numbers ~500), and did not form bars. Similarly, increasing the discharge resulted in a loss of channelisation. Instabilities within flows whose discharge is insufficient to cover the whole surface appear to be the key to channelisation within the experiments (Yu et al., 2006).

Comparisons with the modelling of meandering rivers suggest that the realistic physical modelling of active sinuous deep-water channels is an extremely difficult problem (e.g. Schumm and Khan, 1972; Smith, 1998; Peakall et al., 2007). This is in sharp contrast to making fluvial braided channels, which has been described as 'child's play' (Paola, 2001). The key problem in achieving realistic active sinuous channels is the adequate modelling of cohesion at laboratory scale (Peakall et al., 2007). The work on river meandering suggests that materials with cohesive properties are required to support significant sinuosity, but that the cohesive properties of clays restrict bend evolution and active migration.

Numerical modelling studies have examined both channel initiation and channel development, but are restricted to just a handful of examples. Incipient 3D channelisation has been simulated (Imran et al., 1998, 2002) and shows good agreement with experimental results (Imran et al., 2002), but, as with the early physical experiments, numerical modelling cannot simulate longer, more sinuous channels. Channel evolution itself has been examined using a depth-averaged analytical model incorporating deposition and erosion (Das et al., 2004). The model simulated flows through sine-generated channels with fixed model boundaries. Analysis of velocity patterns and deposition and erosion within the channel enabled some aspects of channel migration to be explored. Critically, two different equations were used for deposition, (1) the García (1990) similarity condition where deposition rate is a function of the mean concentration and independent of velocity and (2) the Rouse equation (Rouse, 1937), known from fluvial shear flow theory where deposition is related to velocity. The two equations give very different results, with the similarity criterion and Rouse equations predicting dominant sedimentation on the outside and inside of bends, respectively (Das et al., 2004). In terms of channel evolution, channels could either increase (Rouse) or decrease (similarity criterion) in bend amplitude and sinuosity, depending on which set of equations are used. The study concluded that erosional currents may be more favourable for channel migration, as these showed higher near-bank velocities and therefore greater outer bank erosion (Das et al., 2004). Furthermore,

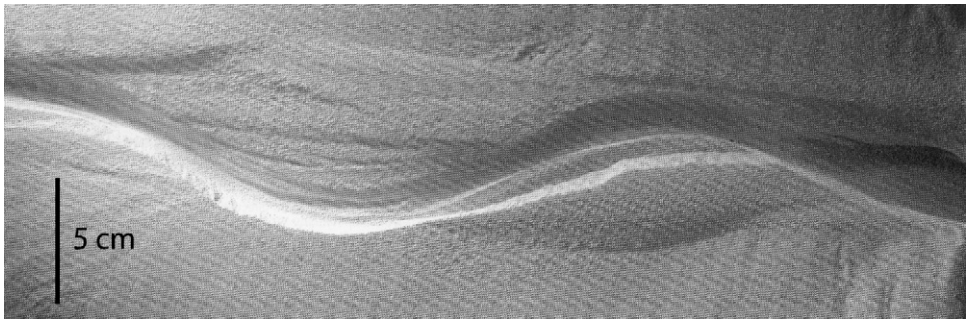


Fig. 23. Sinuous incisional channel formed in cohesionless sediment. Erosional terraces are present on the inside of channel bends (cf. Fig. 5). Reproduced from Métivier et al. (2005) with permission of SEPM.

channels would always increase in sinuosity with time if net erosional, since the differing depositional models would have no affect.

2.4.2. Intra-channel processes

Intra-channel processes can be sub-divided into flow processes and deposits, though clearly the two are intimately linked and feedback on one another.

2.4.2.1. Flow processes. Physical experiments have examined the nature of the 3D flow field within fixed-form sinuous channels, and have found that in the majority of modelled cases this differs greatly to fluvial experiments at the same scale, and to flow in meandering rivers (Fig. 24; Corney et al., 2006; Imran et al., 2007; Keevil et al., 2006a, this issue; Peakall et al., this issue). The two key forces affecting flow around bends are the centrifugal force and the pressure force. In sinuous rivers, velocity is high at the surface, and water moves towards the outer bank where it causes the surface of the flow to rise (super-elevate). The super-elevation causes increased pressure forces at the outer bank that then move water towards the inner bank at the base of the flow (Fig. 24). These flows combine to produce secondary circulation, which when added with the downstream-orientated flow, produces a helical (spiral) flow. The vertical profile of downstream velocity is quite different for gravity currents with maximum velocities and therefore high centrifugal forces close to the bed, leading to a reversed sense of secondary circulation relative to meandering rivers (Corney et al., 2006). Computational fluid dynamic (CFD) simulations and solutions of the Dean equations also demonstrate that the bodies of gravity currents exhibit reversed circulation with basal flow towards the outer bank (Corney, 2005).

In contrast to all other physical modelling experiments, Imran et al. (2007) show that for very low-concentration, low-velocity gravity currents exhibiting a velocity maximum of 0.55 of the flow depth, secondary currents do mimic those of rivers. This transition in the orientation of secondary flow with the position of the velocity maximum was previously shown by Corney (2005). Corney (2005) showed that flows with a velocity maximum less than or equal to ~0.4–0.45 of the flow height would all show a reversed secondary flow relative to rivers. The position of the velocity maximum in natural channelised turbidity flows (Xu et al., 2004), continuous input laboratory currents (e.g. Tesaker, 1969; Buckee et al., 2001), and numerical simulations of natural-sized flows (e.g. Felix, 2002, 2004) are in the range of 0.1–0.2 of the flow depth. Consequently, the data suggest that submarine channel flows will predominantly show a reversed secondary circulation relative to rivers (e.g. Corney et al., 2006). When they have slowed and deposited most of their sediment this secondary circulation may change to mimic fluvial systems (Imran et al., 2007), however, currents will be very weak and these late-stage secondary flows would be expected to have very little influence on sedimentation.

Experiments on particulate-rich flows through sinuous channels, while not directly recording the 3D flow fields, have identified the importance of inertial dominated run-up of gravity currents at the outer bank of sinuous channel bends (Straub et al., in press). The combination of centrifugal forces and run-up appears to account for the detailed experimental flow fields reported by Keevil et al. (2006a, this issue). Importantly, run-up of the higher-concentration basal flow component will further enhance the secondary circulation-induced movement of basal flow

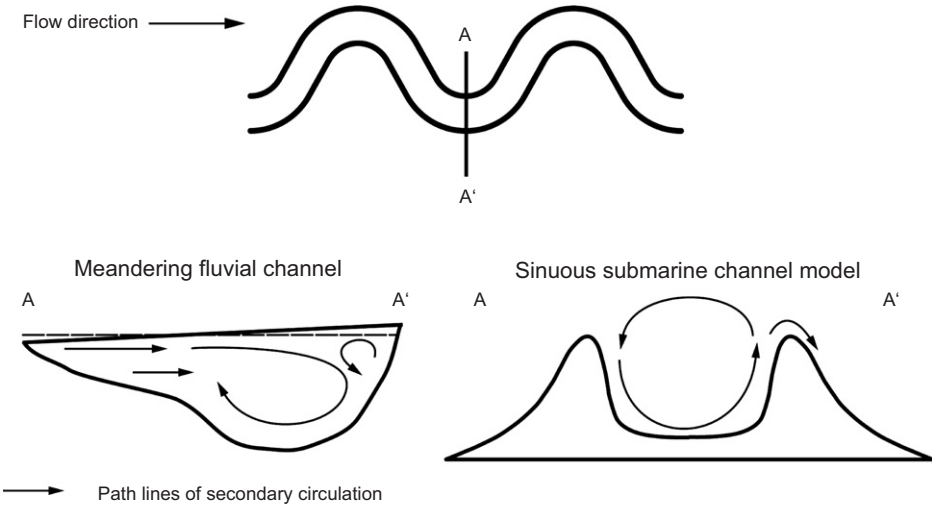


Fig. 24. Schematic comparison of secondary flow in subaerial and subaqueous channels. Note the reversal in orientation of the secondary flow cell, and enhanced overbank flow at the outer bank, in the submarine case relative to that in the river channel. No basal laterally tilting surface is drawn for the submarine case since this is poorly known. The topography is most likely subdued relative to subaerial channels and the orientation (dip towards the inner or outer banks) may vary as a function of channel evolution (see Section 2.4.2). The fluvial channel figure is adapted from Knighton (1998).

towards the outer bank in the upstream part of channel bends.

The physical, analytical, and CFD models described above are in contrast to the CFD modelling of Kassem and Imran (2004) who describe secondary flow in the normal sense of rivers, with basal flows towards the inner bank, and for positions of the velocity maximum above the bed of ~0.17–0.28. It is not clear why the approaches produce different results. However, the Kassem and Imran (2004) simulations *critically* do not display super-elevation at the top of the flow at channel bends as seen in the experiments and in natural channels (with the exception of the strongly unconfined flow (H/h ~2; see Section 2.4.3)). They also exhibit a notable return flow at the top of the current, and a very diffuse density boundary between the downstream- and upstream-directed flow, neither of which is seen in laboratory experiments. These factors may affect the combination of fluidal forces. Intriguingly, a physical experiment with the same width:depth ratio, rectangular cross-section and similar planform to one of the channels simulated by Kassem and Imran (2004) showed an opposite sense of movement to that in Kassem and Imran (2004), with a reversal of the secondary flow cell (Keevil et al., this issue).

Understanding the nature of the 3D flow field is critical to predictive modelling, as seen in the modelling of meandering rivers (e.g. Smith and McLean, 1984; Johannesson and Parker, 1989; Bridge, 1992; Darby and Delbono, 2002). It may well be the case that different bend geometries and quite clearly different flow characteristics control the nature and orientation of secondary circulation. In particular, the relative influence of secondary flow and run-up will differ with bend geometry and flow density. Future research is needed to examine these parameters and assess whether such different fields exist.

Super-elevation of flow is a prominent feature of submarine channel experiments and is believed to account for the levee height differences that occur on submarine channel bends (e.g. Pirmez and Imran, 2003). Komar (1969) first addressed the question of super-elevated flow at submarine channel bends, enabling the mean velocity–concentration relationship of channelised flow to be calculated. In order to actually ascertain one of these parameters, the other is commonly assumed; typically the concentration is assumed enabling velocity estimates to be made. Bowen et al. (1984) modified Komar's equation by introducing a densiometric Froude number, enabling velocity to be estimated independent of concentration. More recently, a generalised analytical approach to modelling submarine channel flows utilising both linear and non-linear layer-averaged equations has been developed (Imran et al., 1999). This approach predicts much higher concentrations, by a factor of ~2–5, for a given velocity than the Komar approach. However, a further complication is that (at least under certain circumstances) the assumption that the transverse bed surface and transverse super-elevated slope are not coupled, implicit in Imran et al. (1999), may be false (Parker et al., 2001). Finally, Straub et al. (in press) have shown, experimentally, that run-up of high-concentration material can significantly increase the super-elevation relative to that predicted by Komar (1969), leading to a 30% reduction in estimated within-channel flow velocities. These studies illustrate the difficulty and uncertainty in obtaining velocity and concentration data from submarine channels, and the need for further modelling.

Sinuous channel flow also differs from straight channels in a number of other key ways. Secondary flow leads to cross-channel variation in turbulence intensities, and consequently there does not appear to be a zone of restricted vertical sediment movement as postulated for straight channels (García and Parker, 1993; Buckee et al., 2001; Keevil et al., 2006a). Secondly, the presence of flow separation, as frequently seen in rivers (e.g. Bagnold, 1960), has been identified in sine-generated bends downstream of bend apices (Straub et al., in press). Lastly, Straub et al. (in press) have shown the importance of a small number of upstream bends in regulating channelised flow, with larger flows losing increased amounts of fluid at channel bends. This regulation may explain how sinuous submarine channels exhibit clear wavelength spectra, rather than a mixture of different wavelength bends (such as those observed in misfit river channels (e.g. Dury, 1965)) that over-print one another, each caused by a different flow size.

2.4.2.2. Sedimentation in sinuous channels. Physical experiments have only recently been used to examine sedimentation within sinuous submarine channels, and have resulted in markedly different models (Mohrig and Buttles, 2007; Peakall et al., this issue; Straub et al., in press). Similarly, numerical modelling has produced very different models of intra-channel sedimentation (Das et al., 2004; Salles, 2006). Here these studies are reviewed and a new integrative model proposed that solves these apparent paradoxes.

Saline flows over a mobile bed have been run through fixed-form fibreglass channels with a sinuosity of 1.36 (Peakall et al., this issue). These experiments produced inner bank accretions, equivalent to the 'point bars' of fluvial channels, that were located just downstream of bend apices. The sedimentation patterns can be explained in terms of the flow fields produced in identical but sediment-free channels (Keevil et al., 2006a). They are also in close agreement with analogous studies of sedimentation within compound fluvial channels of similar planform geometry (Wormleaton et al., 2004, 2005; Peakall et al., this issue). Such compound channels exhibit reversed bend circulation, albeit caused by a different process to the primary mechanism identified by Corney et al. (2006) and Keevil et al. (2006a). Shanmugam (2006, p. 270) has ascribed importance to the failure of experiments to produce point bars in subaqueous meanders. However the experiments of Peakall et al. (this issue) demonstrate that such forms,

albeit with differences in their characteristics, can form in physical experiments.

A second set of experiments have been undertaken using pre-formed channels (sinuosity 1.32), but with particulate-rich saline currents rather than pure saline flows (Straub et al., in press). These experiments were dominated by suspended load fallout and, while strongly depositional across the whole channel, predominantly deposited material on the outside of channel bends, resulting in a small net decrease (3%) in sinuosity with time (Straub et al., in press). Sedimentation at the outer bend was located both upstream and downstream of bend apices. Since bends grow in amplitude through erosion of the outer bank, Straub et al. (in press) concluded that sinuosity production occurs through either net-erosional or non-depositional flows.

Numerical models also show deposition on either the inner or outer bank, depending on the modelling approach adopted and the equations chosen. As discussed earlier, Das et al. (2004) found enhanced outer bank deposition when using a similarity equation for sedimentation, and inner bank accumulation when using a Rouse transport model. A novel recent approach is the use of cellular automata modelling for the simulation of sinuous submarine channels (Salles, 2006). Fluvial models, most notably in braided river dynamics have made considerable use of this approach (e.g. Murray and Paola, 1994, 1997), however, this is the first time such an approach has been tried for subaqueous channels. The cellular automata approach consists of a set of rules, of which the chosen sedimentation equation (Salles, 2006) again utilises the similarity criteria of García (1990). Flows through pre-defined sinuous channels displayed coarse-grained deposition on the outer bank and associated fine-grained deposition on the inner bank (Salles, 2006).

The differing physical and numerical models appear to conflict with each other for the case of dominantly depositional channels, yet can be integrated into a coherent whole. When channels first initiate they appear to grow rapidly in bend amplitude while undergoing relatively little aggradation (e.g. Peakall et al., 2000a; Kolla et al., this issue). During this phase, bypass of sediment is favoured and intra-channel deposition may be dominated by bedload or gradual suspension fall out. Inner-bank sediment accumulations form, with corresponding outer bank erosion and bend amplitude growth (Fig. 25). Later, as channels begin to shut down, strongly depositional flows with high suspended fall-out rates dominate. When this happens, sediment preferentially accumulates on outer banks as a result of inertial-dominated run-up forces (Fig. 25). The resulting deposits may therefore show outward-dipping surfaces ('lateral accretion surfaces') in bedload-dominated periods, and inward-dipping accumulations during relatively high-rates of suspended-sediment-dominated flows.

After initial bend growth, many aggradational submarine channels reach a point where there is a near cessation of planform movement (ossification), and growth is dominated by vertical aggradation (Peakall et al., 2000a). Explanations for this planform ossification have included clay hysteresis and climate-induced flow size reduction (Peakall et al., 2000a). However, this ossification may be related to parity between the forces promoting inner and outer bank accumulation respectively. As the channel develops, the growth in sinuosity, coupled to levee growth and channel confinement, collectively lead to a progressive

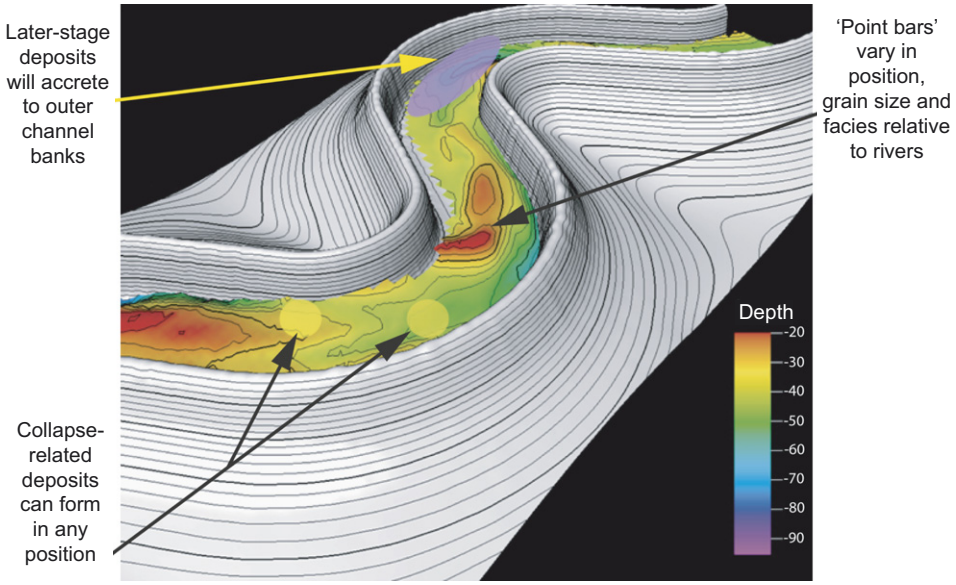


Fig. 25. A schematic model of intra-channel sedimentation in sinuous submarine channels. The base map shows inner-bank accumulations or 'point bars' and outer bank pools from bedload-dominated transport at times of sediment bypass (from the experiments of Peakall et al., this issue). Later-stage deposits form on outer banks and may show inward-directed dipping surfaces; these form from collapsing currents with high suspended-load fallout rates. Nested mounds can form at any point as a result of channel levee/bank collapse, though these may preferentially form at outer banks.

increase in both the strength of secondary flow cells and the importance of inertial run-up effects. Flow type may also alter, with progressive changes in the relative dominance of suspended load fall out rate to tractional forces. A point may be reached where the forces promoting inner- and outer-bank accumulation reach a balance, resulting in a cessation of both outer-bank erosion and inner-bank deposition. Consequently, the channel planform would ossify and be dominated solely by vertical aggradation.

Importantly, the physical experiments undertaken so far have failed to observe some sedimentary features recognised in sinuous submarine channels, such as nested mounds (Timbrell, 1993; Clark and Pickering, 1996), and this despite large-scale overspill at outer channel bends (Straub et al., in press). This suggests that such features are not formed by the broad-scale flow dynamics of such channels. Instead nested mounds probably form in response to bank collapse (Fig. 25; Peakall et al., 2000b, this issue).

2.4.3. Overbank processes

The nature and extent of overbank flow in sinuous submarine channels has been much debated, with models arguing for both very thin overbank flow (a few per cent of the in-channel depth; Hiscott et al., 1997) and much thicker overbank flow (Peakall et al., 2000a). Mohrig and Buttles (2007) have examined this issue using physical experiments and show that 'channelised' flow thicknesses (H) are less than 1.3 times the height of the channel depth (h). Although part of the flow can be overbank (up to 30%), there is very limited lateral spreading. This is primarily because the relative gravitational driving force is low, and because the within-channel flow drags (tows) the overbank component along (Peakall et al., 2000a; Mohrig and Buttles, 2007). Presumably the value of flow thickness to channel depth (H/h) that marks the boundary of 'channelised' flow is a function of the vertical stratification of the flow, since this controls the relative strength of the lateral spreading versus longitudinal drag forces. In many natural systems flow stratification may be considerably greater than that typically produced in the laboratory (Peakall et al., 2000a; Felix, 2002), suggesting that 'channelised' flows in some natural systems may have H/h values greater than 1.3. Coupled to observations of, and evidence for, thick overbank flows (e.g. Piper and Normark, 1983; Normark, 1989; Peakall et al., 2000a), Mohrig and Buttles' (2007) work strongly suggests that submarine channels frequently exhibit a considerable overbank component.

In addition to the towing mechanism through which in-channel flow influences overbank flow (Peakall et al., 2000a; Mohrig and Buttles, 2007), overbank flow can also influence within-channel flow. Physical experiments have shown that overbank fluid, if partially aligned with the downslope direction, can shear the in-channel fluid creating enhanced secondary flow that is reversed relative to meandering river channels (Keevil et al., this issue). Reversal of secondary flow by either formative mechanism, plus inertial dominated run-up, all act to enhance the movement of fluid overbank at outer channel bends (Corney et al., 2006; Keevil et al., 2006a, this issue; Mohrig and Buttles, 2007; Straub et al., in press). These processes have been observed in experiments to produce sediment waves (Keevil et al., 2006b; Peakall et al., this issue) and coarse-grained deposition on outer bank channel levees that is as coarse as sedimentation on the channel floor (Straub et al., in press). These grain-size distributions are inconsistent with previous field-based and theoretical models that suggest that only the upper parts of flow are lost at channel bends (Piper and Normark, 1983; Peakall et al., 2000a; Straub et al., in press). They agree, however, at least in part with the CFD simulations of Kassem and Imran (2004), who claim that the whole flow depth contributes to flow stripping.

Coarse-grained deposits such as spillover lobes and crevasse splays have been observed on outer bend levees (e.g. Dutton et al., 2003; Posamentier and Kolla, 2003). However, it is not clear that these are as coarse-grained as equivalent channel thalweg deposits, nor that outer bend channel levees generally are as coarse-grained as channel deposits. The generally smaller stratification of experimental flows and the relatively small width:depth ratios lead to strong secondary flow and accompanying large run-up effects. Consequently, the relative magnitude of the observed processes may be partially over-estimated in the laboratory. These initial physical and numerical models of overbank flow show great promise for assessing such processes (Kassem and Imran, 2004; Corney et al., 2006; Keevil et al., 2006a, this issue; Mohrig and Buttles, 2007; Straub et al., in press). However, they illustrate the need for further research on these enhanced overbank flow processes and their magnitude and influence on overbank deposition.

2.4.4. Physical and numerical modelling: conclusions

Physical and numerical modelling of sinuous submarine channels, although still in its relative 'infancy', has already contributed a wealth of insights, many of which have challenged existing ideas based on fluvial systems:

(1) The recognition of inertial run-up and reversed secondary flows demonstrate that the 3D flow field in deep-water sinuous channels is very different from rivers (e.g. Corney et al., 2006; Straub et al., in press). This flow field then controls deposition, with further evidence that both intra-channel and overbank sedimentation may be significantly different from models based on meandering rivers (Peakall et al., this issue; Straub et al., in press). Physical experiments of overbank flow have also revealed new insights into the magnitude and processes of these flows (Keevil et al., this issue; Mohrig and Buttles, 2007).
(2) Real progress has already been made in reproducing self-forming sinuous channels in the laboratory (Métivier et al., 2005; Yu et al., 2006). Numerical

modelling has also made great advances, with pioneering work conducted using three different approaches; layer-averaged modelling, full CFDs modelling, and cellular automata modelling (Imran et al., 1999; Das et al., 2004; Kassem and Imran, 2004; Salles, 2006).

(3) Future research must seek to integrate physical and numerical models to further investigate flow dynamics and event scale sedimentation.

(4) Finally, the cellular automata approach shows promise for investigating channels over much longer geological timescales, but this requires knowledge of both small-scale dynamics and comparison against detailed 3D data from natural systems (Salles, 2006).

3. Discussion

3.1. Fluvial versus deep-water channels

Sinuous submarine channels have drawn strong analogies with meandering river channels, most notably in terms of channel planforms, and geomorphological features such as point bars and bend cut-offs (Lonsdale and Hollister, 1979; Flood and Damuth, 1987; Clark et al., 1992; Klaucke and Hesse, 1996). This prevailing view was summarised in Leeder's (1999) leading sedimentology textbook as: '*Submarine fan channels are closely analogous to river channels*'.

There is indeed a considerable degree of similarity between fluvial and submarine channels in terms of planform morphometrics, particularly if channel thalweg width is used rather than levee width (Clark et al., 1992; Pirmez and Imran, 2003). However, there is also a large degree of similarity between submarine channel planforms and those of many other types of sinuous channels and flows, for instance Martian channels (Bellaiche et al., 1986b) and the Gulf Stream (Pirmez and Imran, 2003; their Table 1). The development of sinuosity is a fundamental property of fluids (Peakall et al., 2000a), and therefore while there are considerable similarities between planform data from different types of channel and flow, it need not imply broader similarities in terms of processes and deposits.

Morphologically, submarine channels exhibit a number of distinct differences, most spectacularly, the highly aggradational nature of some systems, with levees hundreds of metres high. In all systems, channel widths and depths decrease downstream (Normark, 1985). The nature of the channel conduit is also quite different, with low-angle channel banks and smooth floors, relative to rivers (e.g. Babonneau et al., 2002). The smoothness of many deep-water channels may have important implications for fluid flow within them relative to rivers (cf. Parsons et al., 2007).

Submarine channels have long been known to exhibit a number of processes that differ from rivers, including greatly enhanced flow super-elevation at bends (Komar, 1969), the significant influence of Coriolis force on flow, the formation of nested mounds within the channel (Timbrell, 1993; Clark and Pickering, 1996), flow stripping at channel bends (Piper and Normark, 1983), and continuous flow overspill along considerable channel reaches (Peakall et al., 2000a). More recently, sinuous submarine channels have been shown to have very different 3D flow patterns to rivers, with a reversed sense of helical (spiral) flow through bends (Corney et al., 2006; Keevil et al., 2006a). Submarine channels also show important inertial dominated run-up effects on outer bends (Straub et al., in press). These two processes will combine to produce enhanced fluid and sediment transport at the outer banks of bends, enabling features such as coarse-grained spillover lobes to form (see Section 2.4.3).

Submarine channels show a range of different migration patterns. Erosive-dominated channels may show greatest similarity with meandering rivers, with significant downstream migration and bend cut-offs (Abreu et al., 2003). In contrast, fine-grained aggradational channels exhibit very different channel migration patterns relative to meandering rivers, as shown by the greatly reduced frequency of bend cut-off in most systems (Peakall et al., 2000a), although the Bengal Fan is a notable exception (Schwenk et al., 2003). Aggradational channels display prominent increases in bend amplitude but only exhibit limited downstream sweep. While sweep is frequently noted (e.g. Deptuck et al., 2003; Posamentier and Kolla, 2003; Kolla et al., this issue) it is typically only on the order of 2–3 times channel width, which explains why channel cut-off is comparatively rare (wavelength is ~12 times width; Pirmez and Imran, 2003). Similarly, lateral migration in submarine channels typically occurs solely through bend amplitude growth, rather than migration of a whole channel (Peakall et al., 2000a). External forcing such as salt tectonics and tectonics can, however, cause submarine channels to migrate (e.g. Weimer, 1991; Posamentier and Kolla, 2003), as is also observed for fluvial channels (e.g. Alexander et al., 1994; Peakall et al., 2000c).

The deposits of submarine channels, while still poorly understood, exhibit a number of important differences. Most prominently, levees are much larger and sand units within them can be very extensive, enabling them to form hydrocarbon reservoirs (Clemenceau et al., 2000; Kendrick, 1998, 2000; Peakall et al., 2000b). Inner-bank accumulations (or point bars in fluvial terminology) are present in submarine channels but do show a number of key differences. They appear to be located further downstream relative to bend apices than in rivers and to only form during periods when sediment bypass is dominant (Abreu et al., 2003; Arnott, this issue; Peakall et al., this issue). Evidence is also emerging that intra-channel topography may show reduced lateral gradients (Das et al., 2004) and, consequently, inner-bank point bars and their associated lateral accretion surfaces may be thinner (Arnott, this issue). Other smaller bar forms such as migrating unit bars which are common in many meandering rivers, notably in coarser-grained rivers, have not been recognised in sinuous deep-water channels

(e.g. Lewin, 1978; Bridge, 2003; Peakall et al., 2007). In contrast to rivers, other features such as nested mounds and outer bank accretion further complicate deep-water intra-channel architecture (see Section 2.4.2).

These differences in terms of processes, channel migration and deposits reflect the significant differences in the physics of gravity currents and the open-channel shear flows of fluvial channels. Gravity currents have significant upper boundary friction, much reduced effective gravity, and ongoing entrainment of surrounding fluid (e.g. Peakall et al., 2000a). These collectively lead to major differences in the vertical distribution of downstream velocity, and associated parameters such as turbulence and sediment concentration distributions (e.g. Stacey and Bowen, 1988; Keevil et al., 2006a). Since the driving force of turbidity currents is the sediment suspended within the flow, suspension-related transport dominates relative to bedload apart from when flows are dominantly bypassing. This factor may lead to very high suspended sediment fallout rates and relatively high basal concentrations during deposition, which may partially account for the greatly reduced incidence of larger bedforms such as dunes (Arnott, this issue; Cronin et al., in press, a). As finer-grained gravity currents decelerate they may also undergo deposition by exceeding the capacity of the flow to carry the sediment, rather than the competence of individual grain-size classes, in sharp contrast to river channels (Hiscott, 1994).

Given our increasing recognition of the sheer range of differences between submarine and subaerial sinuous channels, in terms of morphology, processes, channel migration and deposits, it seems timely to suggest that the prevailing view that the two forms are strongly analogous should be overturned. There are areas where the two channel types do show a degree of analogy, but these are outweighed by those areas which show strong differences. It would be fairer to rewrite the overview statement of Leeder (1999) to state '*submarine fan channels are not closely analogous to river channels*'.

3.2. Braiding and sinuous channels

Braiding, or braid-like features, have been reported from a number of modern deep-water channels, mostly at channel mouths/confluences and channel–lobe transition zones (Belderson et al., 1984; Kenyon and Millington, 1995; Klaucke and Hesse, 1996; Ercilla et al., 1998; Hesse et al., 2001). They appear to be related to rapid deposition of sand-rich sediments, resulting from abrupt changes in turbidity current flow parameters, e.g. zones where gradient and degree of confinement rapidly decrease leading to reduced flow thickness and velocity. Features resembling braid bars have also occasionally been observed within channels (e.g. Cronin et al., 1995; Kenyon and Millington, 1995). However, in all of the above examples, the channels are not truly sinuous, i.e. they do not exhibit minimum average sinuosities >1.2. In addition, published examples of intra-channel 'braid bars' are lacking integrated high-resolution planform and cross-sectional data; some may actually be erosional remnants bounded by incisional thalwegs (e.g. Cronin et al., 1995). We therefore conclude that well-constrained examples of channel braiding or intra-channel depositional braid bars have yet to be reported from truly sinuous modern deep-water channels.

Braided channel forms at outcrop are common in gravel-prone submarine canyon fills, where high-energy stream flow and avalanching/gravely debris flows predominate. There are many examples of braided morphology within canyon fills in slope settings with narrow or non-existent shelves and elevated hinterland (Gerbe-Cotefablo system, Eocene, Spanish Pyrenees, Mutti, 1985; Palaeocene Point Lobos Canyon, California, USA, Cronin and Kidd, 1998; other Californian examples, Walker, 1975; Adana Basin, Turkey, Satur et al., 2004a, b, 2005). In all of these examples, the interpreted braided morphology is only observed in proximal, high gradient settings. Braided channels have not been interpreted from an open slope environment.

3.3. Future research directions

A major target of future sinuous channels research should be improved integration of different methodologies and datasets, in order to address key questions. An example is the calibration of high-quality planform and cross-sectional geophysical data (e.g. 3D seismic and side-scan sonar/multibeam bathymetry) using well core or shallow core data (e.g. Flood et al., 1995; Wonham et al., 2000). There are currently very few accessible studies of this nature, and those which are in the public domain have already yielded some surprises, e.g. the widespread character of debris flows on distal Mississippi Fan (Nelson et al., 1992; Schwab et al., 1996). Targeted coring of specific intra-channel architectures, e.g. point bars, in modern sinuous channels would also be particularly valuable. There are obvious limitations to shallow piston- and gravity-coring techniques when it comes to recovering sand-rich sediments from spatially restricted targets. However, improved technologies such as vibracoring are now capable of recovering sand-dominated sediments down to 2 km WD from ships equipped with dynamic positioning. An additional aim must be to continue applying high-resolution geophysical techniques, e.g. 100 kHz side-scan sonar, to active sinuous channels on the modern seafloor; this will provide further insights into the distribution and character of small-scale (10s of centimetres to 10s of metres) channel floor features such as scours and bedforms. Existing medium-and high-resolution side-scan sonar datasets have already shown the value of this technique for resolving detailed intra-channel architecture (e.g. O'Connell et al., 1991a; Twichell et al., 1992; Cronin et al., 1995; Babonneau et al., 2002).

In the subsurface, more efficient transfer of 'non-sensitive' industry 3D seismic to the academic community would be welcome. Although there are often significant commercial issues to overcome, this would undoubtedly lead to major advances in understanding. Industry 3D datasets are already providing unprecedented insights into geomorphic evolution of deep-water sinuous channels (e.g. Deptuck et al., 2003, this issue; Heinio and Davies, this issue), but very few are calibrated by shallow coring, which is a relatively inexpensive activity compared to deeper drilling.

In the modelling realm, an obvious target is to incorporate real sinuous channel morphologies (e.g. those extracted from multibeam bathmetry or surficial 3D seismic data) into experimental runs (cf. Peakall et al., this issue; Struab et al., in press). It is also expected that there will be increased research effort into self-forming channels and some aspects of numerical modelling, e.g. the cellular automata approach (Salles, 2006). A major step forward would be to improve our ability to monitor natural flows in modern sinuous channels. This would require equipment to be anchored to the seafloor within an active channel, and designed to withstand the intense forces placed upon it. There are some indications that this methodology is capable of yielding valuable data, e.g. Zaire Fan, Khripounoff et al. (2003), and further attempts in other suitably 'active' systems are already in progress or at the planning stage. Another possible monitoring technique is for some kind of tracer to be entrained and transported by the flow and its location monitored remotely; this method is currently restricted by technological limitations, e.g. tracer size and the problems of generating significant acoustic signal strength in a turbid sediment-laden flow or its subsequent deposit.

Finally, the introduction of new technologies, e.g. ground-penetrating radar (Young et al., 2003), are revolutionising our approach to outcrop-based studies. These techniques can provide better constraints on some of the classic outcrop geometries, and may help determine whether certain features, e.g. LAPs/LADs (Abreu et al., 2003; Arnott, this issue), are always diagnostic of sinuous channel planform.

4. Summary

This overview paper has drawn together examples of deep-water sinuous channel geometries, process and deposits from a variety of settings, both natural and experimental. In addition to the brief summaries of previous research presented above, we have introduced a new process model for sinuous channel evolution and discussed some of the key topics in this fast-moving research field. The main conclusions from this latter section are as follows:

(1) We recommend that the long-held notion that fluvial and deep-water sinuous channels are similar, largely based upon gross planform morphologic characteristics, is discontinued. We propose here that *differences* between river and submarine channels are of far greater importance, in terms of geometry, flow processes, migration style and deposit character.
(2) Braiding does not appear to be an important process within sinuous channels; published examples are exclusively related to low-sinuosity canyons or channels and/or marked changes in channel cross-sectional area, e.g. channel mouths.
(3) Future research should focus on integration and calibration of geophysical and sedimentological datasets, and exploitation of new technologies, in order to better understand detailed architecture, geomorphic evolution and flow processes of deep-water sinuous channels.

Acknowledgements

This paper, and the accompanying special issue volume, originated from a meeting held at the National Oceanography Centre, Southampton in 2005, which was co-sponsored by the UK Turbidite Architecture and Process Studies group (UK-TAPS) and the Marine Studies Group of the Geological Society, London. We are grateful to Vikki Gunn for administrative support during the meeting, and to all attendees for their scientific input, which resulted in a lively and constructive exchange of ideas. David Roberts, Editor of Marine and Petroleum Geology, has been fully supportive from conception to conclusion of this special issue, and we appreciate his patience during production of this introductory paper. Finally, Gareth Keevil is thanked for his help with several figures, and for the use of Fig. 23.

References

Abreu, V., Sullivan, M., Pirmez, C., Mohrig, D., 2003. Lateral accretion packages (LAPs): an important reservoir element in deep water sinuous channels. Marine and Petroleum Geology 20, 631–648.

Alexander, J., Bridge, J.S., Leeder, M.R., Collier, R.E.L.l., Gawthorpe, R.L., 1994. Holocene meander-belt evolution in an active extensional basin, southwestern Montana. Journal of Sedimentary Research B 64, 542–559.

Antobreh, A.A., Krastel, S., 2006. Morphology, seismic characteristics and development of Cap Timiris Canyon, offshore Mauritania: a newly discovered canyon preserved off a major arid climatic region. Marine and Petroleum Geology 23, 37–59.

Arnott, R.W.C., this issue. Stratal architecture and origin of lateral accretion deposits (LADs) and conterminuous inner-bank levee deposits in a base-of-slope sinuous channel, Lower Isaac Formation (Neoproterozoic), East-Central British Columbia, Canada. Marine and Petroleum Geology, doi:10.1016/j.marpetgeo.2007.01.006.

Baas, J.H., Van Kesteren, W., Postma, G., 2004. Deposits of depletive high-density turbidity currents: a flume analogue of bed geometry, structure and texture. Sedimentology 51, 1053–1088.

Babonneau, N., Savoye, B., Cremer, M., Klein, B., 2002. Morphology and architecture of the present canyon and channel system of the Zaire deep-sea fan. Marine and Petroleum Geology 19, 445–467.

Babonneau, N., Savoye, B., Cremer, M., Bez, M., 2004. Multiple terraces within the deep incised Zaire Valley (ZaïAngo Project): are they confined levees? In: Lomas, S.A., Joseph, P. (Eds.), Confined Turbidite Systems. Geological Society, London, Special Publication, vol. 222, pp. 91–114.

Bagnold, R.A., 1960. Some aspects of the shape of river meanders. US Geological Survey Professional Paper 282E, pp. 135–144.

Beaubouef, R.T., Rossen, C., Zelt, F.B., Sullivan, M.D., Mohrig, D.C., Jennette, D.C., 1999. Deep-water Sandstones, Brushy Canyon Formation, West Texas: Field Guide, AAPG Hedberg Field Research Conference.

Belderson, R.H., Kenyon, N.H., Stride, A.H., Pelton, C.D., 1984. A 'braided' distributary system on the Orinoco deep-sea fan. Marine Geology 56, 195–206.

Bellaiche, G., Droz, L., Aloisi, J.-L., Bouye, C., Got, H., Monaco, A., Maldonado, A., Serra-Raventos, J., Mirabile, L., 1981. The Ebro and the Rhone deep-sea fans: first comparative study. Marine Geology 43, M75–M85.

Bellaiche, G., Droz, L., Coutellier, V., Berthon, J.-L., Orsolini, P., Ravenne, C., Aloisi, J.-C., Got, H., Monaco, A., 1984. Detailed morphology, structure and main growth pattern of the Rhône deep-sea fan. Marine Geology 55, 181–193.

Bellaiche, G., Coutellier, V., Droz, L., 1986a. Seismic evidence of widespread mass transport deposits in the Rhone deep-sea fan: their role in the fan construction. Marine Geology 71, 327–340.

Bellaiche, G., Coutellier, V., Droz, L., Masson, P., 1986b. Deep-sea and Martian channels. Deep-Sea Research 33, 973–980.

Bellaiche, G., Coutellier, V., Droz, L., Le Cann, C., 1990. Mass-gravity deposits on the Provençal continental rise (northwestern Mediterranean Sea). Oceanologica Acta 13, 121–125.

Bonnel, C., Dennielou, B., Droz, L., Mulder, T., Berné, S., 2005. Architecture and depositional pattern of the Rhône Neofan and recent gravity activity in the Gulf of Lions (western Mediterranean). Marine and Petroleum Geology 22, 827–843.

Bouma, A.H., Coleman, J.M., 1985. Peira-Cava turbidite system, France. In: Bouma, A.H., Barnes, N.E., Normark, W.R. (Eds.), Submarine Fans and Related Turbidite Sequences. Springer, Berlin, pp. 217–222.

Bouma, A.H., Stelting, C.E., Coleman, J.M., 1984. Mississippi Fan: internal structure and depositional processes. Geo-Marine Letters 3, 147–153.

Bouma, A.H., Coleman, J.M., DSDP Leg 96 Shipboard Scientists, 1985a. Mississippi Fan: Leg 96 program and principal results. In: Bouma, A.H., Normark, W.R., Barnes, N.E. (Eds.), Submarine Fans and Related Turbidite Systems. Springer, New York, pp. 247–252.

Bouma, A.H., Stelting, C.E., Coleman, J.M., 1985b. Mississippi Fan: Gulf of Mexico. In: Bouma, A.H., Barnes, N.E., Normark, W.R. (Eds.), Submarine Fans and Related Turbidite Sequences. Springer, Berlin, pp. 143–150.

Bouma, A.H., Coleman, J.M., Stelting, C.E., Kohl, B., 1989. Influence of relative sea level changes on the construction of the Mississippi Fan. Geo-Marine Letters 9, 161–170.

Bowen, A.J., Normark, W.R., Piper, D.J.W., 1984. Modelling of turbidity currents on Navy Submarine Fan, California Continental Borderland. Sedimentology 31, 169–186.

Bridge, J.S., 1992. A revised model for water flow, sediment transport, bed topography, and grain-size sorting in natural river bends. Water Resources Research 28, 999–1013.

Bridge, J.S., 2003. Rivers and Floodplains; Forms, Processes and Sedimentary Record. Blackwell, Oxford, UK, 491pp.

Bruschi, R., Bughi, S., Spinazzè, M., Torselletti, E., Vitali, L., 2006. Impact of debris flows and turbidity currents on seafloor structures. Norwegian Journal of Geology 86, 317–337.

Buckee, C., Kneller, B., Peakall, J., 2001. Turbulence structure in steady solute-driven gravity currents. In: McCaffrey, W.D., Kneller, B.C., Peakall, J. (Eds.), Particulate Gravity Currents. International Association of Sedimentologists, Special Publication, vol. 31, pp. 173–188.

Chapin, M.A., Davies, P., Gibson, J.L., Pettingill, H.S., 1994. Reservoir architecture of turbidite sheet sandstones in laterally extensive outcrops, Ross Formation, Western Ireland. In: Weimer, P., Bouma, A.H., Perkins, B.F. (Eds.). Submarine Fans and Turbidite Systems: Sequence Stratigraphy, Reservoir Architecture and Production Characteristics. GCSSEPM Foundation 15th Annual Research Conference, 4–7 December 1994, pp. 53–68.

Clark, J.D., Pickering, K.T., 1996a. Submarine Channels: Process and Architecture. Vallis Press, London, 231pp.

Clark, J.D., Pickering, K.T., 1996b. Architectural elements and growth patterns of submarine channels: applications to hydrocarbon exploration. Bulletin of the American Association of Petroleum Geologists 80, 194–221.

Clark, J.D., Kenyon, N.H., Pickering, K.T., 1992. Quantitative analysis of the geometry of submarine channels: implications for the classification of submarine fans. Geology 20, 633–636.

Clemenceau, G.R., Colbert, J., Eddens, J., 2000. Production results from levee-overbank turbidite sands at Ram/Powell field, deepwater Gulf of Mexico. In: Weimer, P., et al. (Eds.) Turbidite Reservoirs of the World. 20th Annual Gulf Coast Section SEPM Proceedings, pp. 241–251.

Clift, P.D., Shimizu, N., Layne, G.D., Blusztajn, J.S., Gaedicke, C., Schlüter, H.-U., Clark, M.K., Amjad, S., 2001. Development of the Indus Fan and its significance for the erosional history of the Western Himalaya and Karakoram. Geological Society of America Bulletin 114, 1039–1051.

Collinson, J.D., Martinsen, O., Bakken, B., Kloster, A., 1991. Early fill of the Western Irish Namurian Basin: a complex relationship between turbidites and deltas. Basin Research 3, 223–242.

Cook, T.W., 1993. Facies architecture of deep-water channel deposits, Brushy Canyon Formation, West Texas, and Jackfork Group, Arkansas. Unpublished M.S. Thesis, Lousiana State University, 108pp.

Cook, T.W., Bouma, A.H., Chapin, M.A., Zhu, H., 1994. Facies architecture and reservoir characterization of a submarine fan channel complex, Jackfork Formation, Arkanas. In: Weimer, P., Bouma, A.H., Perkins, B.F. (Eds.), Submarine Fans and Turbidite Systems: Sequence Stratigraphy, Reservoir Architecture and Production Characteristics. GCSSEPM Foundation 15th Annual Research Conference, 4–7 December 1994, pp. 69–81.

Corney, R.K.T., 2005. Numerical, analytical and experimental modelling of channelised gravity currents. Unpublished Ph.D. thesis, University of Leeds, Leeds, 314pp.

Corney, R.K.T., Peakall, J., Parsons, D.R., Elliott, L., Amos, K.J., Best, J.L., Keevil, G.M., Ingham, D.B., 2006. The orientation of helical flow in curved channels. Sedimentology 53, 249–257.

Cronin, B.T., 1994. Channel-fill architecture in deep-water sequences: variability, quantification and applications. Unpublished Ph.D. thesis, University of Wales, 332pp.

Cronin, B.T., 1995. Structurally-controlled deep-sea channel courses: examples from the Miocene of south-east Spain and the Alboran Sea, south-west Mediterranean. In: Hartley, A.J., Prosser, D.J. (Eds.), Characterisation of Deep Marine Clastic Systems. Geological Society, London, Special Publication, vol. 94, pp. 113–133.

Cronin, B.T., Kidd, R.B., 1998. Heterogeneity and lithotype distribution in ancient deep-sea canyons: point Lobos deep-sea canyon as a reservoir analogue. Sedimentary Geology 115, 315–349.

Cronin, B.T., Kenyon, N.H., Woodside, J., den Bezemer, T., van der Wal, A., Millington, J., Ivanov, M.K., Limonov, A., 1995. The Almeria Canyon: a meandering channel system on an active margin, Alboran Sea, western Mediterranean. In: Pickering, K.T., Hiscott, R.N., Kenyon, N.H., Lucchi, F.R., Smith, R.D.A. (Eds.), Atlas of Deep-water Environments: Architectural Styles in Turbidite Systems. Chapman & Hall, London, pp. 84–88.

Cronin, B.T., Hartley, A.J., Owen, D., Kneller, B., 1998. Slumps, debris flows and sandy deep-water channel systems: implications for the application of sequence stratigraphy to deep water clastic sediments. Journal of the Geological Society of London 155, 429–432.

Cronin, B.T., Hartley, A.J., Çelik, H., Hurst, A., Türkmen, I., Kerey, E., 2000a. Equilibrium profile development in graded deep-water slopes:

Eocene, Eastern Turkey. Journal of the Geological Society of London 157, 943–955.
Cronin, B.T., Hurst, A., Çelik, H., Türkmen, I., 2000b. Superb exposure of a channel levee and overbank complex in an ancient deep-water slope environment. Sedimentary Geology 132, 205–216.
Cronin, B.T., Çelik, H., Hurst, A., Türkmen, I., 2005. Mud prone entrenched deep-water slope channel complexes from the Eocene of eastern Turkey. In: Hodgson, D.M., Flint, S.S. (Eds.), Submarine Slope Systems: Processes and Products. Geological Society, London, Special Publication, vol. 244, pp. 155–180.
Cronin, B.T., Çelik, H., Hurst, A., Gul, M., Gürbüz, K., Mazzini, A., Overstolz, M., in press, a. Deep-water slope channel complex fill and overbank architecture of the Tinker Channel, Kirkgecit Formation, Turkey. In: Studlick, J., et al. (Eds.), Atlas of Deep-Water Turbidite Systems, AAPG Special Issue.
Cronin, B.T., Çelik, H., Hurst, A., in press, b. Hasret Mountain Main Channel, Eocene, eastern Turkey: sinuous channels in late stages of entrenched deep-water channel complexes. In: Studlick, J., et al. (Eds.), Atlas of deep-water turbidite systems, AAPG Special Issue.
Curray, J.R., Moore, D.G., 1971. Growth of the Bengal deep-sea fan and denudation in the Himalayas. Geological Society of America Bulletin 82, 563–572.
Curray, J.R., Emmel, F.J., Moore, D.G., 2003. The Bengal Fan: morphology, geometry, stratigraphy, history and processes. Marine and Petroleum Geology 19, 1191–1223.
Curtin, T.B., 1986. Physical observation in the plume region of the Amazon river during peak discharge—II. Water masses. Continental Shelf Research 6, 53–71.
Damuth, J.E., Embley, R.W., 1981. Mass-transport processes on Amazon Cone: Western Equatorial Atlantic. Bulletin of the American Association of Petroleum Geologists 65, 629–643.
Damuth, J.E., Flood, R.D., 1984. Morphology, sedimentation processes, and growth pattern of the Amazon deep-sea fan. Geo-Marine Letters 3, 109–117.
Damuth, J.E., Flood, R.D., 1985. Amazon Fan, Atlantic Ocean. In: Bouma, A.H., Normark, W.R., Barnes, N.E. (Eds.), Submarine Fans and Related Turbidite Systems. Springer, New York, pp. 97–106.
Damuth, J.E., Kumar, N., 1975. Amazon Cone: morphology, sediments, age and growth pattern. Geological Society of America Bulletin 86, 873–878.
Damuth, J.E., Kolla, V., Flood, R.D., Kowsmann, R.O., Monteiro, M.C., Gorini, M.A., Palma, J.J.C., Belderson, R.H., 1983a. Distributary channel meandering and bifurcation patterns on Amazon deep-sea fan as revealed by long-range side-scan sonar (GLORIA). Geology 11, 94–98.
Damuth, J.E., Kowsmann, R.O., Flood, R.D., Belderson, R.H., Gorini, M.A., 1983b. Age relationships of distributary channels on Amazon deep-sea fan: implications for fan growth pattern. Geology 11, 470–473.
Damuth, J.E., Flood, R.D., Kowsmann, R.O., Belderson, R.H., Gorini, M.A., 1988. Anatomy and growth pattern of Amazon deep-sea fan as revealed by long-range side-scan sonar (GLORIA) and high resolution seismic studies. Bulletin of the American Association of Petroleum Geologists 72, 885–911.
Damuth, J.E., Flood, R.D., Pirmez, C., Manley, P.L., 1995. Architectural elements and depositional processes of Amazon Deep-sea Fan: imaging by long-range sidescan sonar (GLORIA), bathymetric swath-mapping (Sea Beam), high-resolution seismic and piston-core data. In: Pickering, K.T., Hiscott, R.N., Kenyon, N.H., Lucchi, F.R., Smith, R.D.A. (Eds.), Atlas of Deep-water Environments: Architectural Styles in Turbidite Systems. Chapman & Hall, London, pp. 105–121.
Darby, S.E., Delbono, I., 2002. A model of equilibrium topography for meander bends with erodible banks. Earth Surface Processes and Landforms 27, 1057–1085.
Das, H.S., Imran, J., Pirmez, C., Mohrig, D., 2004. Numerical modeling of flow and bed evolution in meandering submarine channels. Journal of Geophysical Research 119, C10009.
Davies, D.K., 1972. Deep sea sediments and their sedimentation, Gulf of Mexico. Bulletin of the American Association of Petroleum Geologists 56, 2212–2239.
Deep Sea Drilling Project, Leg 96 Scientific Party, 1983. On the Mississippi fan. Nature 306, 736–737.
Dennielou, B., Huchon, C., Beaudouin, C., Berné, S., 2006. Vertical grain-size variability within a turbidite levee: autocyclicity or allocyclicity? A case study from the Rhône neofan, Gulf of Lions, Western Mediterranean. Marine Geology 234, 191–213.
Deptuck, M.E., Steffens, G.S., Barton, M., Pirmez, C., 2003. Architecture and evolution of upper fan channel-belts on the Niger Delta slope and in the Arabian Sea. Marine and Petroleum Geology 20, 649–676.
Deptuck, M.E., Sylvester, Z., Pirmez, C., O'Byrne, C., this issue. Migration-aggradation history and 3-D seismic geomorphology of submarine channels in the Pleistocene Benin-major Canyon, western Niger Delta slope. Marine and Petroleum Geology, doi:10.1016/j.marpetgeo.2007.01.005.
D'Heilly, P., Millot, C., Monaco, A., Got, H., 1988. Hydrodynamic study of the furrow of the Petit-Rhone Canyon. Deep-Sea Research 35, 465–471.
Droz, L., Bellaiche, G., 1985. Rhone Deep-Sea Fan: morphostructure and growth pattern. Bulletin of the American Association of Petroleum Geologists 69, 460–479.
Droz, L., Bellaiche, G., 1991. Seismic facies and geologic evolution of the central portion of the Indus Fan. In: Weimer, P., Link, M.H. (Eds.), Seismic Facies and Sedimentary Processes of Submarine Fans and Related Systems. Springer, New York, pp. 383–402.
Droz, L., Rigaut, F., Cochonat, P., Tofani, R., 1996. Morphology and recent evolution of the Zaire turbidite system (Gulf of Guinea). Geological Society of America Bulletin 108, 253–269.
Droz, L., Kergoat, R., Cochonat, P., Berné, S., 2001. Recent sedimentary events in the western Gulf of Lions (western Mediterranean). Marine Geology 176, 23–37.
Droz, L., Marsset, T., Ondréas, H., Lopez, M., Savoye, B., Spy-Anderson, F.-L., 2003. Architecture of an active mud-rich turbidite system: the Zaire Fan (Congo-Angola margin southeast Atlantic): results from ZaïAngo 1 and 2 cruises. Bulletin of the American Association of Petroleum Geologists 87, 1145–1168.
Dury, G.H., 1965. Theoretical implications of underfit streams. United States Geological Survey Professional Paper, 454-C, 40pp.
Dutton, S.P., Flanders, W.A., Barton, M.D., 2003. Reservoir characterization of a Permian deep-water sandstone, East Ford field, Delaware Basin, Texas. Bulletin of the American Association of Petroleum Geologists 87, 609–627.
Elliott, T., 2000a. Depositional architecture of a sand-rich, channelized turbidite system: the Upper Carboniferous Ross Sandstone Formation, western Ireland. In: Weimer, P., et al. (Eds.) Turbidite Reservoirs of the World. 20th Annual Gulf Coast Section SEPM Proceedings, pp. 342–373.
Elliott, T., 2000b. Megaflute erosion surfaces and the initiation of turbidite channels. Geology 28, 119–122.
Elliott, T., Pulham, A.J., Davies, S.J., 2000. Sedimentology, sequence stratigraphy and spectral gamma ray expression of turbidite, slope, and deltaic depositional systems in an Upper Carboniferous basin-fill succession, western Ireland. In: Graham, J.R., Ryan, A. (Eds.), International Association of Sedimentologists Dublin 2000 Field Trip Guidebook, pp. 1–40.
Emmel, F.J., Curray, J.R., 1981a. Channel piracy on the lower Bengal Fan. Geo-Marine Letters 1, 123–127.
Emmel, F.J., Curray, J.R., 1981b. Dynamic events near the upper and mid-fan boundary of the Bengal Fan. Geo-Marine Letters 1, 201–205.
Emmel, F.J., Curray, J.R., 1984. The Bengal submarine fan, northeastern Indian Ocean. Geo-Marine Letters 3, 119–124.
Emmel, F.J., Curray, J.R., 1985. Bengal Fan, Indian Ocean. In: Bouma, A.H., Normark, W.R., Barnes, N.E. (Eds.), Submarine Fans and Related Turbidite Systems. Springer, New York, pp. 107–112.
Ercilla, G., Alonso, B., Baraza, J., Chiocci, F.L., Estrada, F., Farrán, M., Gonthier, E., Perez-Belzuz, F., Pirmez, C., Reeder, M., Torres, J.,

Urgeles, R., 1998. New high-resolution acoustic data from the 'braided system' of the Orinoco deep-sea fan. Marine Geology 146, 243–250.
Ercilla, G., Alonso, B., Estrada, F., Chiocci, F.L., Baraza, J., Farran, M., 2002. The Magdalena Turbidite System (Caribbean Sea): present-day morphology and architecture model. Marine Geology 185, 303–318.
Estrada, F., Ercilla, G., Alonso, B., 2005. Quantitative study of a Magdalena submarine channel (Caribbean Sea): implications for sedimentary dynamics. Marine and Petroleum Geology 22, 623–635.
Feeley, M.H., Buffler, R.T., Bryant, W.R., 1985. Depositional units and growth pattern of the Mississippi Fan. In: Bouma, A.H., Normark, W.R., Barnes, N.E. (Eds.), Submarine Fans and Related Turbidite Systems. Springer, New York, pp. 253–257.
Felix, M., 2002. Flow structure of turbidity currents. Sedimentology 49, 397–419.
Felix, M., 2004. The significance of single value variables in turbidity currents. Journal of Hydraulic Research 42, 323–330.
Fildani, A., Normark, W.R., Kostic, S., Parker, G., 2006. Channel formation by flow stripping: large-scale scour features along the Monterey East Channel and their relation to sediment waves. Sedimentology 53, 1265–1287.
Flood, R.D., 1987. Side echoes from a sinuous fan channel obscure the structure of submarine fan channel/levee systems, Amazon Fan. Geo-Marine Letters 7, 15–22.
Flood, R.D., Damuth, J.E., 1987. Quantitative characteristics of sinuous distributary channels on the Amazon deep-sea fan. Geological Society of America Bulletin 98, 728–738.
Flood, R.D., Manley, P.L., Kowsmann, K.O., Appi, C.J., Pirmez, C., 1991. Seismic facies and late quaternary growth of Amazon submarine fan. In: Weimer, P., Link, M.H. (Eds.), Seismic Facies and Sedimentary Processes of Submarine Fans and Turbidite Systems. Springer, New York, pp. 415–434.
Flood, R.D., Piper, D.J.W., Klaus, A., et al., 1995. Proceedings of the ODP, Initial Reports, 155. College Station, TX (Ocean Drilling Program).
Flood, R.D., Piper, D.J.W., Klaus, A., Peterson, L.C. (Eds.), 1997. Proceedings of the ODP, Scientific Results, 155. College Station, TX (Ocean Drilling Program).
Franzinelli, E., Potter, P.E., 1983. Petrology, chemistry, and texture of modern river sands, Amazon River system. Journal of Geology 91, 23–39.
García, M., 1990. Depositing and eroding turbidity sediment driven flows: turbidity currents. Project Report 306, St. Anthony Falls Hydraulic Laboratory, University of Minnesota, Minneapolis, Minnesota.
García, M., Parker, G., 1993. Experiments on the entrainment of sediment into suspension by a dense bottom current. Journal of Geophysical Research 98, 4793–4807.
Garrison, L.E., Kenyon, N.H., Bouma, A.H., 1982. Channel systems and lobe construction in the Mississippi Fan. Geo-Marine Letters 2, 31–39.
Gaullier, V., Antonini, E., Benkhelil, J., Got, H., 1998. Recent gravity-driven sedimentary bodies in the North Balearic Basin: geometry and quantification. Comptes Rendus de l'Academie des Sciences, Serie II. Sciences de la Terre et des Planetes 327, 677–684.
Gervais, A., Mulder, T., Savoye, B., Migeon, S., Cremer, M., 2001. Recent processes of levee formation on the Zaire deep-sea fan. Comptes Rendus de l'Academie des Sciences, Serie II. Sciences de la Terre et des Planetes 332, 371–378.
Ghibaudo, G., 1980. Deep-sea fan deposits in the Macigno formation (Middle-Upper Oligocene) of the Gordana Valley, Northern Apennines, Italy. Journal of Sedimentary Petrology 50, 723–0742.
Gill, W.D., 1979. Synsedimentary sliding and slumping in the West Clare Namurian Basin, Ireland. Geological Survey of Ireland Special Paper, 4.
Gill, W.D., Keunen, P.H., 1958. Sand volcanoes on slumps in the Carboniferous of County Clare, Ireland. Quarterly Journal of the Geological Society London 113, 441–460.
Hagen, RA., Bergersen, D.D., Moberly, R., Coulbourn, W.T., 1994. Morphology of a large meandering submarine canyon system in the Peru-Chile forearc. Journal of Marine Geology 119, 7–38.
Haughton, P.D.W., 2000. Evolving turbidite systems on a deforming basin floor, Tabernas, south-east Spain. Sedimentology 47, 497–518.
Heezen, B.C., Ewing, M., Granelli, N.C.L., Menzies, R.J., Schneider, E.D., 1964. Congo submarine canyon. Bulletin of the American Association of Petroleum Geologists 48, 1126–1149.
Heinio, P., Davies, R.J., this issue. Knickpoint migration in submarine channels in response to fold growth, western Niger Delta. Marine and Petroleum Geology, doi:10.1016/j.marpetgeo.2006.09.002.
Hesse, R., Klaucke, I., Khodabakhsh, S., Piper, D.J.W., Ryan, W.B.F., NAMOC Study Group, 2001. Sandy submarine braid plains: potential deep-water reservoirs. Bulletin of the American Association of Petroleum Geologists 85, 1499–1521.
Hiscott, R.N., 1980. Depositional framework of sandy mid-fan complexes of Tourelle Formation, Ordovician, Quebec. Bulletin of the American Association of Petroleum Geologists 64, 1052–1077.
Hiscott, R.N., 1994. Loss of capacity, not competence, as the fundamental process governing deposition from turbidity currents. Journal of Sedimentary Research 64, 209–214.
Hiscott, R.N., Hall., F.R., Pirmez, C., 1997. Turbidity-current overspill from the Amazon channel: texture of the silt/sand load, paleoflow from anisotropy of magnetic susceptibility and implications for flow processes. In: Flood, R.D., Piper, D.J.W., Klaus, A., Peterson, L.C. (Eds.), Proceedings of the Ocean Drilling Program, Scientific Results, 155. College Station, Texas, Ocean Drilling Program, pp. 53–78.
Hodson, G., 1954. The beds above the Carboniferous Limestone of County Clare, Eire. Quarterly of the Geological Society of London 109, 259–283.
Huang, T.C., Goodell, H.G., 1970. Sediments and sedimentary processes of eastern Mississippi Cone, Gulf of Mexico. Bulletin of the American Association of Petroleum Geologists 54, 2070–2100.
Hübscher, C., Spieß, V., Breitzke, M., Weber, M.E., 1997. The youngest channel–levee system of the Bengal fan: results from digital sediment echosounder data. Marine Geology 141, 125–145.
Imran, J., Parker, G., Katopodes, N., 1998. A numerical model of channel inception on submarine fans. Journal of Geophysical Research 103, 1219–1238.
Imran, J., Parker, G., Pirmez, C., 1999. A nonlinear model of flow in meandering submarine and subaerial channels. Journal of Fluid Mechanics 400, 295–331.
Imran, J., Parker, G., Harff, P., 2002. Experiments on incipient channelization of submarine fans. Journal of Hydraulic Research 40, 21–32.
Imran, J., Islam, M.A., Huang, H., Kassem, A., Dickerson, J., Pirmez, C., Parker, G., 2007. Helical flow couplets in submarine gravity underflows. Geology 35, 659–662.
Johannesson, H., Parker, G., 1989. Linear theory of river meanders. In: Ikeda, S., Parker, G. (Eds.), River Meandering, vol. 12. American Geophysical Union, Water Resources Monograph, Washington, DC, pp. 181–214.
Kassem, A., Imran, J., 2004. Three-dimensional modeling of density current, II. flow in sinuous confined and unconfined channels. Journal of Hydraulic Research 42, 591–602.
Kastens, K.A., Shor, A.N., 1985. Depositional processes of a meandering channel on Mississippi Fan. Bulletin of the American Association of Petroleum Geologists 69, 190–202.
Kastens, K.A., Shor, A.N., 1986. Evolution of a channel meander on the Mississippi Deep-Sea Fan. Bulletin of the American Association of Petroleum Geologists 71, 165–175.
Keevil, G.M., Peakall, J., Best, J.L., Amos, K.J., 2006a. Flow structure in sinuous submarine channels: velocity and turbulence structure of an experimental submarine channel. Marine Geology 229, 241–257.
Keevil, G.M., Peakall, J., Best, J.L., 2006b. Flow dynamics of sinuous submarine channels. AAPG Annual Meeting, 9–12 April 2006, Houston, Texas.
Keevil, G.M., Peakall, J., Best, J.L., this issue. The influence of scale, slope and channel geometry on the flow dynamics of submarine channels. Marine and Petroleum Geology, doi:10.1016/j.marpetgeo.2007.01.009.

Kendrick, J.W., 1998. Turbidite reservoir architecture in the Gulf of Mexico, insights from field development: In: Developing and managing turbidite reservoirs, case histories and experiences. In: EAGE/AAPG Third Research Symposium, Almeria, Spain.

Kendrick, J.W., 2000. Turbidite reservoir architecture in the northern Gulf of Mexico deep water: insights from the development of Auger, Tahoe and Ram/Powell Fields. In: Weimer, P. et al. (Eds.) Turbidite Reservoirs of the World. 20th Annual Gulf Coast Section SEPM Proceedings, pp. 450–468.

Kenyon, N.H., Millington, J., 1995. Contrasting deep-sea depositional systems in the Bering Sea. In: Pickering, K.T., Hiscott, R.N., Kenyon, N.H., Ricci Lucchi, F., Smith, R.D.A. (Eds.), Atlas of Deep-water Environments: Architectural Style in Turbidite Systems. Chapman & Hall, London, pp. 196–201.

Kenyon, N.H., Stride, A.H., Belderson, R.H., 1975. Plan views of active faults and other features on the lower Nile cone. Geological Society of America Bulletin 86, 1733–1739.

Kenyon, N.H., Amir, A., Cramp, A., 1995a. Geometry of the younger sediment bodies of the Indus Fan. In: Pickering, K.T., Hiscott, R.N., Kenyon, N.H., Lucchi, F.R., Smith, R.D.A. (Eds.), Atlas of Deep-water Environments: Architectural Styles in Turbidite Systems. Chapman & Hall, London, pp. 89–93.

Kenyon, N.H., Millington, J., Droz, L., Ivanov, M.K., 1995b. Scour holes in a channel–lobe transition zone on the Rhône cone. In: Pickering, K.T., Hiscott, R.N., Kenyon, N.H., Ricci Lucchi, F., Smith, R.D.A. (Eds.), Atlas of Deep-water Environments: Architectural Style in Turbidite Systems. Chapman & Hall, London, pp. 212–215.

Khripounoff, A., Vangriesheim, A., Babonneau, N., Crassous, P., Dennielou, B., Savoye, B., 2003. Direct observation of intense turbidity current activity in the Zaire submarine valley at 4000 m water depth. Marine Geology 194, 151–158.

Klaucke, I., Hesse, R., 1996. Fluvial features in the deep sea: new insights from the glacigenic submarine drainage system of the Northwest Atlantic Mid-Ocean channel in the Labrador Sea. Sedimentary Geology 106, 223–234.

Kleverlaan, K., 1982. Geologische onderzeokingen in het Tabernas bekken. Unpublished M.Sc. Thesis, University of Amsterdam, The Netherlands, 306pp.

Kleverlaan, K., 1989. Three distinctive feeder-lobe systems within one time-slice of the Tortonian Tabernas Fan, south-east Spain. Sedimentology 36, 25–45.

Kneller, B., 2003. The influence of flow parameters on turbidite slope channel architecture. Marine and Petroleum Geology 20, 901–910.

Knighton, A.D., 1998. Fluvial Forms and Processes: A New Perspective. Arnold, London, 383pp.

Kohl, B., DSDP Leg 96 Shipboard Scientists, 1985. Biostratigraphy and sedimentation rates of the Mississippi Fan. In: Bouma, A.H., Normark, W.R., Barnes, N.E. (Eds.), Submarine Fans and Related Turbidite Systems. Springer, New York, pp. 267–273.

Kolla, V., this issue. A review of sinuous avulsion patterns in some major deep-sea fans and factors controlling them. Marine and Petroleum Geology, doi:10.1016/j.marpetgeo.2007.01.004.

Kolla, V., Buffler, R.T., 1983/1984. Morphologic, acoustic, and sedimentologic characteristics of the Magdalena Fan. Geo-Marine Letters 3, 85–91.

Kolla, V., Coumes, F., 1984. Morpho-acoustic and sedimentologic characteristics of the Indus Fan. Geo-Marine Letters 3, 133–139.

Kolla, V., Coumes, F., 1987. Morphology, internal structure, seismic stratigraphy and sedimentation of Indus Fan. Bulletin of the American Association of Petroleum Geologists 71, 650–677.

Kolla, V., Schwab, A.M., 1995. Indus Fan: multi channel seismic reflection images of channel–levee-overbank complexes. In: Pickering, K.T., Hiscott, R.N., Kenyon, N.H., Ricci Lucchi, F., Smith, R.D.A. (Eds.), Atlas of Deep-water Environments: Architectural Style in Turbidite Systems. Chapman & Hall, London, pp. 100–104.

Kolla, V., Buffler, R.T., Ladd, J.W., 1984. Seismic stratigraphy and sedimentation of Magdalena Fan, Southern Colombian Basin, Caribbean Sea. Bulletin of the American Association of Petroleum Geologists 68, 316–332.

Kolla, V., Bourges, P., Urrity, J.M., Safa, P., 2001. Evolution of deep-water Tertiary sinuous channels offshore Angola (west Africa) and implications for reservoir architecture. Bulletin of the American Association of Petroleum Geologists 85, 1373–1405.

Kolla, V., Posamentier, H.W., Wood, L.J., this issue. Deep-water and fluvial sinuous channels—characteristics, similarities and dissimilarities, and modes of formation. Marine and Petroleum Geology.

Komar, P.D., 1969. Channelized flow of turbidity currents with application to Monterey deep-sea fan channel. Journal of Geophysical Research 74, 4544–4553.

Komar, P.D., 1977. Computer simulation of turbidity current flow and the study of deep-sea channels and fan sedimentation. In: Goldberg, E.D., McCave, I.N., O'Brien, J.J., Steele, J.H. (Eds.), The Sea; Ideas and Observations on Progress in the Study of the Seas, Volume 6, Marine Modeling. Wiley, New York, pp. 603–621.

Kottke, B., Schwenk, T., Breitzke, M., Wiedicke, M., Kudrass, H.R., Spieß, V., 2003. Acoustic facies and depositional processes in the upper submarine canyon Swatch of No Ground (Bay of Bengal). Deep-Sea Research, II 50, 979–1001.

Krastel, S., Hanebuth, T.J.J., Antobreh, A.A., Henrich, R., Holz, C., Kolling, M., Schulz, H.D., Wien, K., Wynn, R.B., 2004. Cap Timiris Canyon: a newly discovered channel system offshore of Mauritania. EOS 85, 417–423.

Lancien, P., Métivier, F., Lajeunesse, E., Cacas, M.C., 2006. Incision dynamics and shear stress measurements in submarine channel experiments. In: Parker, G., García, M. (Eds.), River, Coastal and Estuarine Morphodynamics: RCEM 2005. Taylor & Francis, London, pp. 527–533.

Leeder, M.R., 1999. Sedimentology and Sedimentary Basins; from Turbulence to Tectonics. Blackwell, Oxford, 592pp.

Lewin, J., 1978. Meander development and floodplain sedimentation: a case study from mid-Wales. Geological Journal 13, 25–36.

Lien, T., Walker, R.G., Martinsen, O.J., 2003. Turbidites in the Upper carboniferous Ross Formation, western Ireland: reconstruction of a channel and spillover system. Sedimentology 50, 113–148.

Lonsdale, P., Hollister, C.D., 1979. Cut-off at an abyssal meander, south of Iceland. Geology 7, 597–601.

Lopez, M., 2001. Architecture and depositional pattern of the quaternary deep-sea fan of the Amazon. Marine and Petroleum Geology 18, 479–486.

Manley, P.L., Flood, R.D., 1988. Cyclic sediment deposition within Amazon Deep-Sea Fan. Bulletin of the American Association of Petroleum Geologists 72, 912–925.

Martinsen, O.J., Lien, T., Walker, R.G., Collinson, J.D., 2003. Facies and sequential organization of a mudstone-dominated slope and basin floor succession: the Gull Island Formation, Shannon Basin, Western Ireland. Marine and Petroleum Geology 20, 789–807.

Marzo, M., Munoz, J.A., Verges, J., Lopez-Blanco, M., Arbués, P., Barbera, X., Cabrera, L., Columbo, F., Serra-Kiel, J., 1998. Sedimentation and tectonics: case studies from Paleogene, continental to deep water sequences of the South Pyrenean Foreland basin (NE Spain). Excursion B2: 15th International Congress of Sedimentology, International Association of Sedimentologists, Alicante, Spain.

Mascle, J., Zitter, T., Bellaiche, G., Droz, L., Gaullier, V., Loncke, L., Prismed Scientific Party, 2001. The Nile deep sea fan: preliminary results from a swath bathymetry survey. Marine and Petroleum Geology 18, 471–477.

Maslin, M., Mikkelsen, N., 1998. Timing of the late quaternary Amazon fan complex mass-transport deposits. In: Cramp, A., MacLeod, C.J., Lee, S.V., Jones, E.J.W. (Eds.), Geological Evolution of Ocean Basins: Results from the Ocean Drilling Program. Geological Society, London, Special Publication, vol. 131, pp. 129–150.

Maslin, M., Vilela, C., Mikkelsen, N., Grootes, P., 2005. Causes of catastrophic sediment failures of the Amazon Fan. Quaternary Science Reviews 24, 2180–2193.

May, J.A., Warme, J.E., Slater, R.A., 1983. Role of submarine canyons on shelfbreak erosion and sedimentation: modern and ancient examples. In: Stanley, D.J., Moore, G.T. (Eds.), The Shelfbreak: Critical Interface on Continental Margins. Society of Economic Paleontologists and Mineralogists, Special Publication, vol. 33, pp. 315–332.

Mayall, M., Stewart, I., 2000. The architecture of turbidite slope channels. In: Weimer, P., Slatt, R.M., Coleman, J.L., Rosen, N., Nelson, C.H., Bouma, A.H., Styzen, M., Lawrence, D.T. (Eds.), Global Deep-Water Reservoirs. Gulf Coast Section SEPM 20th Annual Conference, pp. 578–586.

Mayall, M., Jones, E., Casey, M., 2006. Turbidite channel reservoirs—key elements in facies prediction and effective development. Marine and Petroleum Geology 23, 821–841.

McHargue, T.R., 1991. Seismic facies, processes and evolution of Miocene inner fan channels, Indus Submarine Fan. In: Weimer, P., Link, M.H. (Eds.), Seismic Facies and Sedimentary Processes of Submarine Fans and Turbidite Systems. Springer, New York, pp. 402–413.

McHargue, T.R., Webb, J.E., 1986. Internal geometry, seismic facies and petroleum potential of canyons and inner fan channels of the Indus Submarine Fan. Bulletin of the American Association of Petroleum Geologists 70, 161–180.

Meade, R.H., Dunne, T., Richey, J.E., Santos, U.M., Salati, E., 1985. Storage and remobilization of suspended sediment in the lower Amazon River of Brazil. Science 228, 488–490.

Mear, Y., 1984. Séquences et unités sédimentaires du glacis rhôdanien (Méditerranée Occidentale). Unpublished Thesis (3rd cycle), University of Perpignan.

Menard, H.W., Smith, S.M., Pratt, R.M., 1965. The Rhône Deep-sea fan. In: Whittard, W.F., Bradshaw, R. (Eds.), Submarine Geology and Geophysics. Butterworth, London, pp. 271–284.

Métivier, F., Lajeunesse, E., Cacas, M.C., 2005. Submarine canyons in the bathtub. Journal of Sedimentary Research 75, 6–11.

Middleton, G.V., 1966. Experiments on density and turbidity currents: (Part 2) Uniform flow of density currents. Canadian Journal of Earth Sciences 3, 627–637.

Middleton, G.V., 1993. Sediment deposition from turbidity currents. Annual Review of Earth and Planetary Sciences 21, 89–114.

Migeon, S., Savoye, B., Babonneau, N., Spy-Anderson, F.-L., 2004. Processes of sediment-wave construction along the present Zaire deep-sea meandering channel: role of meanders and flow stripping. Journal of Sedimentary Research 74, 580–598.

Mohrig, D., Buttles, J., 2007. Deep turbidity currents in shallow channels. Geology 35, 155–158.

Moore, G.T., Starke, G.W., Bonham, L.C., Woodbury, H.O., 1978. Mississippi Fan, Gulf of Mexico—physiography, stratigraphy, and sedimentation patterns. American Association of Petroleum Geologists Studies in Geology 7, 155–191.

Mulder, T., Alexander, H., 2001. The physical character of submarine density flows and their deposits. Sedimentology 48, 269–301.

Mulder, T., Syvitski, J.P.M., Migeon, S., Faugeres, J.C., Savoye, B., 2003. Marine hyperpycnal flows: initiation, behaviour and related deposits. a review. Marine and Petroleum Geology 20, 861–882.

Murray, A.B., Paola, C., 1994. A cellular model of braided rivers. Nature 371, 54–57.

Murray, A.B., Paola, C., 1997. Properties of a cellular braided stream model. Earth Surface Processes and Landforms 22, 1001–1025.

Mutti, E., 1977. Distinctive thin-bedded turbidite facies and related depositional environments in the Eocene Hecho Group (South-Central Pyrenees, Spain). Sedimentology 24, 107–131.

Mutti, E., 1985. Hecho turbidite system, Spain. In: Bouma, A.H., Normark, W.R., Barnes, N.E. (Eds.), Submarine Fans and Related Turbidite Systems. Springer, New York, pp. 205–208.

Mutti, E., Normark, W.R., 1987. Comparing examples of modern and ancient turbidite systems: Problems and concepts. In: Legget, J.K., Zuffa, G.G. (Eds.), Deep Water Clastic Deposits: Models and Case Histories. Graham and Trotman, London, pp. 1–38.

Mutti, E., Ricci Lucchi, F., 1972. Le torbiditi del l'Apennino sttentrionale: introduzione all'analisi di facies. Memoir Societa Geologica Italiana 11, 161–199.

Mutti, E., Remacha, E., Sgavetti, M., Rosell, J., Valloni, R., Zamorano, M., 1985. Stratigraphy and facies characteristics of the Eocene Hecho Group turbidite systems, South-Central Pyrenees. In: Mila, M.D., Rosell, J. (Eds.), IAS 6th European Regional Meeting, Excursion Guidebook No. 12, Lerida, Spain.

Mutti, E., Seguret, M., Sgavetti, M., 1988. Sedimentation and deformation in the Tertiary sequences of the Southern Pyrenees. Field Trip Guide 7, AAPG Mediterranean Basins Conference, Nice, France, September 1988.

Mutti, E., Tinterri, R., Remacha, E., Mavilla, N., Angella, S., Fava, L., 1999. An introduction to the analysis of ancient turbidite basins from an outcrop perspective. AAPG Continuing Education Course Note Series 39.

Naini, B.R., Kolla, V., 1982. Acoustic character and thickness of sediments of the Indus Fan and the continental margin of western India. Marine Geology 47, 181–195.

Nelson, C.H., Twichell, D.C., Schwab, W.C., Lee, H.J., Kenyon, N.H., 1992. Upper Pleistocene turbidite sand beds and chaotic silt beds in the channelized, distal, outer-fan lobes of the Mississippi Fan. Geology 20, 693–696.

Nilsen, T.H., Imerato, D.P., Moore, D.W., 1994. Reservoir geometry and architecture of productive Upper Cretaceous mud-rich and sand-rich submarine-fan systems, Sacramento Basin, California. In: Weimer, P., Bouma, A.H., Perkins, B.F., (Eds.), Submarine Fans and Turbidite Systems: Sequence Stratigraphy, Reservoir Architecture and Production Characteristics, GCSSEPM Foundation 15th Annual Research Conference, 4–7 December 1994, pp. 269–280.

Normark, W.R., 1985. Local morphologic controls and effects of basin geometry on flow processes in deep marine basins. In: Zuffa, G.G. (Ed.), Provenance of Arenites, Reidel, Dordrecht, The Netherlands, pp. 47–63.

Normark, W.R., 1989. Observed parameters for turbidity-current flow in channels, Reserve Fan, Lake Superior. Journal of Sedimentary Petrology 59, 423–431.

Normark, W.R., Piper, D.J.W., 1991. Initiation processes and flow evolution of turbidity currents: implications for the depositional record. SEPM Special Publication 46, 207–229.

Normark, W.R., Barnes, N.E., Coumes, F., 1985. Rhone Fan, Mediterranean. In: Bouma, A.H., Normark, W.R., Barnes, N.E. (Eds.), Submarine Fans and Related Turbidite Systems. Springer, New York, pp. 151–156.

Normark, W.R., Piper, D.J.W., Posamentier, H., Pirmez, C., Migeon, S., 2002. Variability in form and growth of sediment waves on turbidite channel levees. Marine Geology 192, 23–58.

O'Connell, S., Stelting, C.E., Bouma, A.H., Coleman, J.M., Cremer, M., Droz, L., Meyer-Wright, A.A., Normark, W.R., Pickering, K.T., Stow, D.A.V., DSDP Leg 96 Shipboard Scientists, 1985. Drilling results on the lower Mississippi Fan. In: Bouma, A.H., Normark, W.R., Barnes, N.E. (Eds.), Submarine Fans and Related Turbidite Systems. Springer, New York, pp. 291–298.

O'Connell, S., Normark, W.R., Ryan, W.B.F., Kenyon, N.H., 1991a. An entrenched thalweg channel on the Rhône Fan: interpretation from a SeaBeam and SeaMARC 1 survey. SEPM Special Publication 46, 259–270.

O'Connell, S., Ryan, W.B.F., Normark, W.R., 1991b. Evolution of a fan channel on the surface of the outer Mississippi Fan: evidence from side-looking sonar. In: Weimer, P., Link, M.H. (Eds.), Seismic Facies and Sedimentary Processes of Submarine Fans and Turbidite Systems. Springer, New York, pp. 365–381.

O'Connell, S., McHugh, C., Ryan, W.B.F., 1995. Unique fan morphology in an entrenched thalweg channel on the Rhône Fan. In: Pickering, K.T., Hiscott, R.N., Kenyon, N.H., Ricci Lucchi, F., Smith, R.D.A. (Eds.), Atlas of Deep-water Environments: Architectural Style in Turbidite Systems. Chapman & Hall, London, pp. 80–83.

Paola, C., 2001. Modelling stream braiding over a range of scales. In: Mosley, M.P. (Ed.), Gravel-Bed Rivers V. Caxton Press, Christchurch, NZ, pp. 11–46.

Parker, G., Imran, J., Pirmez, C., 2001. Transverse slope of bed and turbid-clear water interface of channelized turbidity currents flowing around bends. In: Seminara, G., Blondeaux, P. (Eds.), River, Coastal and Estuarine Morphodynamics. Springer, Berlin, pp. 119–139.

Parsons, D.R., Best, J.L., Lane, S.N., Orfeo, O., Hardy, R.J., Kostaschuk, R., 2007. Form roughness and the absence of secondary flow in a large confluence-diffluence, Rio Parana, Argentina. Earth Surface Processes and Landforms 32, 155–162.

Parsons, J.D., Schweller, W.J., Stelting, C.W., Southard, J.B., Lyons, W.J., Grotzinger, J.P., 2002. A preliminary experimental study of turbidite fan deposits. Journal of Sedimentary Research 72, 619–628.

Parsons, J.D., Schweller, W.J., Stelting, C.W., Southard, J.B., Lyons, W.J., Grotzinger, J.P., 2003. A preliminary experimental study of turbidite fan deposits-reply. Journal of Sedimentary Research 73, 839–841.

Peakall, J., McCaffrey, W.D., Kneller, B.C., 2000a. A process model for the evolution, morphology, and architecture of sinuous submarine channels. Journal of Sedimentary Research 70, 434–448.

Peakall, J., McCaffrey, W.D., Kneller, B.C., Stelting, C.E., McHargue, T.R., Schweller, W.J., 2000b. A process model for the evolution of submarine fan channels: implications for sedimentary architecture. In: Bouma, A.H., Stone, C.G. (Eds.), Fine-grained Turbidite Systems. American Association of Petroleum Geologists, Memoir 72/SEPM, Special Publication, vol. 68, pp. 73–88.

Peakall, J., Leeder, M.R., Best, J., Ashworth, P., 2000c. River response to lateral tilting: a synthesis and some implications for the modelling of alluvial architecture in extensional basins. Basin Research 12, 413–424.

Peakall, J., Ashworth, P.J., Best, J.L., 2007. Meander-bend evolution, alluvial architecture, and the role of cohesion in sinuous river channels: a flume study. Journal of Sedimentary Research 77, 197–212.

Peakall, J., Amos, K.J., Keevil, G.M., Bradbury, P.W., Gupta, S., this issue. Flow processes and sedimentation in submarine channel bends. Marine and Petroleum Geology, this issue, doi:10.1016/j.marpetgeo.2007.01.008.

Pickering, K.T., Corregidor, J., 2005. Mass-transport complexes (MTCs) and tectonic control on basin-floor submarine fans, Middle Eocene, south Spanish Pyrenees. Journal of Sedimentary Research 75, 761–783.

Pickering, K.T., Coleman, J., Cremer, M., Droz, L., Kohl, B., Normark, W., O'Connell, S., Stow, D., Meyer-Wright, A., 1986. A high sinuosity, laterally migrating submarine fan channel–levee-overbank: results from DSDP Leg 96 on the Mississippi Fan, Gulf of Mexico. Marine and Petroleum Geology 3, 3–18.

Pickering, K.T., Hodgson, D.M., Platzman, E., Clark, J.D., Stephens, C., 2001. A new type of bedform produced by backfilling processes in a submarine channel, Late Miocene, Tabernas-Sorbas basin, south-east Spain. Journal of Sedimentary Research 71, 692–704.

Piper, D.J.W., Normark, W.R., 1983. Turbidite depositional patterns and flow characteristics, Navy submarine fan, California Borderland. Sedimentology 30, 681–694.

Piper, D.J.W., Normark, W.R., 2001. Sandy fans—from Amazon to Hueneme and beyond. Bulletin of the American Association of Petroleum Geologists 85, 1407–1438.

Pirmez, C., Flood, R.D., 1995. Morphology and structure of Amazon Channel. In: Flood, R.D., Piper, D.J.W., Klaus, A., et al. (Eds.), Proceedings of the Ocean Drilling Program, Initial Reports, 155, Ocean Drilling Program, College Station, TX, pp. 23–45.

Pirmez, C., Imran, J., 2003. Reconstruction of turbidity currents in Amazon Channel. Marine and Petroleum Geology 20, 823–849.

Pirmez, C., Beaubouef, R.T., Friedmann, S.J., Mohrig, D.C., 2000. Equilibrium Profile and base-level in submarine channels: Examples from Late Pleistocene systems and implications for the architecture of deepwater reservoirs. In: Weimer, P., et al. (Eds.) Turbidite Reservoirs of the World. 20th Annual Gulf Coast Section SEPM Proceedings, pp. 782–805.

Popescu, I., Lericolais, G., Panin, N., Wong, H.K., Droz, L., 2001. Late Quaternary channel avulsions on the Danube deep-sea fan, Black Sea. Marine Geology 179, 25–37.

Posamentier, H.W., 2003. Depositional elements associated with a basin-floor channel–levee system: case study from the Gulf of Mexico. Marine and Petroleum Geology 20, 667–690.

Posamentier, H.W., Kolla, V., 2003. Seismic geomorphology and stratigraphy of depositional elements in deep-water settings. Journal of Sedimentary Research 73, 367–388.

Prins, M.A., Postma, G., 2000. Effects of climate, sea level, and tectonics unravelled for last deglaciation turbidite records of the Arabian Sea. Geology 28, 375–378.

Prins, M.A., Postma, G., Cleveringa, J., Cramp, A., Kenyon, N.H., 2000. Controls on terrigenous sediment supply to the Arabian Sea during the late Quaternary: the Indus Fan. Marine Geology 169, 327–349.

Redbourn, L.J., Bull, J.M., Scrutton, R.A., Stow, D.A.V., 1993. Channels, echo character mapping and tectonics from 3.5 kHz profiles, distal Bengal Fan. Marine Geology 114, 155–170.

Remacha, E., Fernández, L.P., Maestro, E., 2005. The transition between sheet-like lobe and basin-plain turbidites in the Hecho Basin (south-central Pyrenees, Spain). Journal of Sedimentary Research 75, 798–819.

Rimington, N., Cramp, A., Morton, A., 2000. Amazon Fan sands: implications for provenance. Marine and Petroleum Geology 17, 267–284.

Roberts, M.T., Compani, B., 1996. Miocene example of a meandering submarine channel–levee system from 3D seismic reflection data, Gulf of Mexico Basin. GCSSEPM Foundation 17th Annual Research Conference, pp. 241–254.

Rouse, H., 1937. Modern conceptions of the mechanics of turbulence. Transactions of the American Society of Civil Engineers 102, 463–543.

Salles, T., 2006. Modélisation numérique du remplissage sédimentaire des canyons et chenaux sous-marins par approche génétique (Numerical modelling of the sedimentary fill of submarine canyons and channels using a genetic approach). Unpublished Ph.D. Thesis, University of Bordeaux, France, 215pp.

Satur, N., Cronin, B.T., Hurst, A., Kelling, G., Gürbüz, K., 2004a. Down-channel variations in stratal patterns within a conglomeratic, deep-water fan feeder system (Miocene, Adana Basin, Southern Turkey). In: Joseph, P., Lomas, S. (Eds.), Confined Turbidite Systems. Geological Society, London, Special Publication, vol. 222, pp. 241–260.

Satur, N., Hurst, A., Cronin, B.T., Kelling, G., Gürbüz, K., 2004b. Sand-body geometry in a sand-rich, deep-water clastic system, Miocene Cingoz Formation of Southern Turkey. Marine and Petroleum Geology 17, 239–252.

Satur, N., Kelling, G., Cronin, B.T., Hurst, A., Gürbüz, K., 2005. Sedimentary architecture of a canyon-style fairway feeding a deep-water clastic system, the Miocene Cingoz Formation, southern Turkey: significance for reservoir characterisation and modelling. Sedimentary Geology 173, 91–119.

Savoye, B., Cochonat, P., Apprioual, R., Bain, O., Baltzer, A., Bellec, V., Beuzart, P., Bourillet, J.-F., Cagna, R., Cremer, M., Crusson, A., Dennielou, B., Diebler, D., Droz, L., Ennes, J.-C., Floch, G., Guiomar, M., Harmegnies, F., Kerbrat, R., Klein, B., Kuhn, H., Landuré, J.-Y., Lasnier, C., Le Drezen, E., Le Formal, J.-P., Lopez, M., Loubrieu, B., Marsset, T., Migeon, S., Normand, A., Nouzé, H., Ondréas, H., Pelleau, P., Saget, P., Séranne, M., Sibuet, J.-C., Tofani, R., Voisset, M., 2000. Structure and recent evolution of the Zaire deep-sea fan: preliminary results of the Zaïango 1 and 2 cruises (Angola-Congo margin). Comptes Rendus de l'Academie des Sciences, Serie II. Sciences de la Terre et des Planetes 331, 211–220.

Schumm, S.A., Khan, H.R., 1972. Experimental study of channel patterns. Geological Society of America Bulletin 83, 1755–1770.

Schuppers, J.D., 1993. Quantification of turbidite facies in a reservoir-analogous submarine-fan channel sandbody, south-central Pyrenees, Spain. Special Publications of the International Association of Sedimentologists 15, 99–112.

Schwab, W.C., Lee, H.J., Twichell, D.C., Locat, J., Nelson, C.H., McArthur, W.G., Kenyon, N.H., 1996. Sediment mass-flow processes on a depositional lobe, outer Mississippi Fan. Journal of Sedimentary Research 66, 916–927.

Schwenk, T., Spieß, V., Hübscher, C., Breitzke, M., 2003. Frequent channel avulsions within the active channel–levee system of the middle Bengal Fan—an exceptional channel–levee development derived from Parasound and Hydrosweep data. Deep-Sea Research II 50, 1023–1045.

Schwenk, T., Spieß, V., Breitzke, M., Hübscher, C., 2005. The architecture and evolution of the Middle Bengal Fan in vicinity of the active channel–levee system imaged by high-resolution seismic data. Marine and Petroleum Geology 22, 637–656.

Seguret, M., 1970. Etude tectonique des nappes et series decolles de la partie centrale du versant sud des Pyrenees. Publications Ustela, Montepellier. Series Geologiques Structuraux 21, 1–155.

Shanmugam, G., 2003. A preliminary experimental study of turbidite fan deposits-discussion. Journal of Sedimentary Research 73, 838–839.

Shanmugam, G., 2006. Deep-Water Processes and Facies Models: Implications for Sandstone Petroleum Reservoirs. Elsevier, Amsterdam, 476pp.

Shanmugam, G., Moiola, R.J., 1988. Submarine fans: Characteristics, models, classification, and reservoir potential. Earth Science Reviews 24, 383–428.

Shepard, F.P., 1965. Types of submarine valleys. Bulletin of the American Association of Petroleum Geologists 49, 304–310.

Shepard, F.P., 1966. Meander in valley crossing a deep-ocean fan. Science 154, 385–386.

Shepard, F.P., Emery, K.O., 1973. Congo submarine canyon and fan valley. Bulletin of the American Association of Petroleum Geologists 57, 1679–1691.

Shew, R.D., Rollins, G.M., Tiller, G.M., Hackbarth, C.J., White, C.D., 1994. Characterization and modelling of thin-bedded turbidite deposits from the Gulf of Mexico using detailed subsurface and analog data. In: Weimer, P., Bouma, A.H., Perkins, B.F. (Eds.), Submarine Fans and Turbidite Systems. GCSSEPM Foundation 15th Annual Research Conference, pp. 327–334.

Sikkema, W., Wojcik, K.M., 2000. 3D visualisation of turbidite systems, lower Congo Basin, offshore Angola. In: Weimer, P., Slatt, R.M., Coleman, J.L., Rosen, N., Nelson, C.H., Bouma, A.H., Styzen, M., Lawrence, D.T. (Eds.), Global Deep-Water Reservoirs. Gulf Coast Section SEPM 20th Annual Conference, pp. 928–939.

Smith, C.E., 1998. Modeling high sinuosity meanders in a small flume. Geomorphology 25, 19–30.

Smith, J.D., McLean, S.R., 1984. A model for flow in meandering streams. Water Resources Research 20, 1301–1315.

Soler, M., Puigdefabregas, C., 1970. Lineas generales de la geologia del Alt Aragon Occidental. Pireneos 96, 5–20.

Sprague, A.R., Sullivan, M.D., Campion, K.M., Jensen, G.N., Goulding, F.J., Sickafoose, D.K., Jenette, D.C., 2002. The physical stratigraphy of deep-water strata: a hierarchial approach to the analysis of genetically related stratigraphic elements for improved reservoir prediction. AAPG Annual Meeting, Abstracts, Houston, pp. 10–13.

Stacey, M.W., Bowen, A.J., 1988. The vertical structure of density and turbidity currents: theory and observations. Journal of Geophysical Research 93, 3528–3542.

Stelting, C.E., DSDP Leg 96 Shipboard Scientists, 1985. Migratory characteristics of a mid-fan meander belt, Mississippi Fan. In: Bouma, A.H., Normark, W.R., Barnes, N.E. (Eds.), Submarine Fans and Related Turbidite Sequences. Springer, New York, pp. 283–290.

Stelting, C.E., Pickering, K.T., Bouma, A.H., Coleman, J.M., Cremer, M., Droz, L., Meyer-Wright, A.A., Normark, W.R., O'Connell, S., Stow, D.A.V., DSDP Leg 96 Shipboard Scientists, 1985. Drilling results on the middle Mississippi Fan. In: Bouma, A.H., Normark, W.R., Barnes, N.E. (Eds.), Submarine Fans and Related Turbidite Systems. Springer, New York, pp. 275–282.

Stephens, A.R., Monson, G.D., Reilly, J.M., 1996. The relevance of seismic amplitudes in exploring the Niger Delta. Offshore West Africa Conference papers, pp. 54–60.

Stow, D.A.V., Cochran, J.R., ODP Leg 116 Shipboard Scientific Party, 1989. The Bengal Fan: some preliminary results from ODP drilling. Geo-Marine Letters 9, 1–10.

Straub, K.M., Mohrig, D.C., Buttles, J., McElroy, B., Pirmez, C., in press. Interactions between turbidity currents and topography in aggrading sinuous submarine channels: a laboratory study. Geological Society of America Bulletin.

Stuart, C.J., Caughey, C.A., 1976. Form and composition of the Mississippi Fan. Gulf Coast Association of Geological Societies Transactions 26, 333–343.

Tesaker, E., 1969. Uniform turbidity currents. Unpublished doctoral thesis, Technical University of Norway, Trondheim

Timbrell, G., 1993. Sandstone architecture of the Balder Formation depositional system, UK Quadrant 9 and adjacent areas. In: Parker, J.R. (Ed.), Petroleum Geology of Northwest Europe, Proceedings of the 4th Conference. Geological Society of London, pp. 107–121.

Torres, J., Droz, L., Savoye, B., Terentieva, E., Cochonat, P., Kenyon, N.H., Canals, M., 1997. Deep-sea avulsion and morphosedimentary evolution of the Rhône Fan Valley and Neofan during the Late Quaternary (north-western Mediterranean Sea). Sedimentology 44, 457–477.

Twichell, D.C., Kenyon, N.H., Parson, L., McGregor, B.A., 1991. Depositional patterns of the Mississippi Fan surface: evidence from GLORIA II and high-resolution seismic profiles. In: Weimer, P., Link, M.H. (Eds.), Seismic Facies and Sedimentary Processes of Submarine Fans and Turbidite Systems. Springer, New York, pp. 349–363.

Twichell, D.C., Schwab, W.C., Nelson, C.H., Kenyon, N.H., Lee, H.J., 1992. Characteristics of a sandy depositional lobe on the outer Mississippi Fan from SeaMARC 1A sidescan sonar images. Geology 20, 689–692.

Twichell, D.C., Schwab, W.C., Kenyon, N.H., 1995. Geometry of sandy deposits at the distal edge of the Mississippi Fan, Gulf of Mexico. In: Pickering, K.T., Hiscott, R.N., Kenyon, N.H., Ricci Lucchi, F., Smith, R.D.A. (Eds.), Atlas of Deep-water Environments: Architectural Style in Turbidite Systems. Chapman & Hall, London, pp. 282–286.

Twichell, D.C., Cross, V.A., Paskevich, V.F., Hutchinson, D.R., Winters, W.J., Hart, P.E., 2005. GIS of selected geophysical and core data in the northern Gulf of Mexico continental slope collected by the US Geological Survey. US Geological Survey Open-File Report 2005-1071. DVD-ROM.

Van Weering, T.C.E., Van Iperen, J., 1984. Fine-grained sediment of the Zaire deep-sea fan, southern Atlantic Ocean. In: Stow, D.A.V., Piper, D.J.W. (Eds.), Fine-Grained Sediments: Deep-Water Processes and Facies. Geological Society, London, Special Publication, vol. 15, pp. 95–113.

Von Rad, U., Tahir, M., 1997. Late Quaternary sedimentation on the outer Indus shelf and slope (Pakistan): evidence from high-resolution seismic data and coring. Marine Geology 138, 193–236.

Walker, J.R., Massingill, J.V., 1970. Slump features on the Mississippi Fan, north-eastern Gulf of Mexico. Geological Society of America Bulletin 81, 3101–3108.

Walker, R.G., 1975. Generalised facies models for resedimented conglomerates of turbidite association. Geological Society of America Bulletin 86, 737–748.

Weber, M.E., Wiedicke, M.H., Kudrass, H.R., Hübscher, C., Erlenkeuser, H., 1997. Active growth of the Bengal Fan during sea-level rise and highstand. Geology 25, 315–318.

Weimer, P., 1989. Sequence stratigraphy of the Mississippi Fan (Plio-Pleistocene), Gulf of Mexico. Geo-Marine Letters 9, 185–272.

Weimer, P., 1990. Sequence stratigraphy, facies geometries, and depositional history of the Mississippi Fan, Gulf of Mexico. Bulletin of the American Association of Petroleum Geologists 74, 425–453.

Weimer, P., 1991. Seismic facies, characteristics and variations in channel evolution, Mississippi Fan (Plio-Pleistocene), Gulf of Mexico.

In: Weimer, P., Link, M.H. (Eds.), Seismic Facies and Sedimentary Processes of Submarine Fans and Turbidite Systems. Springer, New York, pp. 323–347.

Weimer, P., Buffler, R.T., 1988. Distribution and seismic facies of Mississippi Fan channels. Geology 16, 900–903.

Wen, R., Sinding-Larsen, R., Kenyon, N.H., 1995. Computer enhanced GLORIA sidescan sonar images of the surface of the Mississippi Fan. In: Pickering, K.T., Hiscott, R.N., Kenyon, N.H., Ricci Lucchi, F., Smith, R.D.A. (Eds.), Atlas of Deep-water Environments: Architectural Style in Turbidite Systems. Chapman & Hall, London, pp. 297–299.

Wetzel, A., 1993. The transfer of river load to deep-sea fans: a quantitative approach. Bulletin of the American Association of Petroleum Geologists 77, 1679–1692.

Wignall, P.B., Best, J.L., 2002. Reply to comment on 'The Western Irish Namurian Basin reassessed' by O.J. Martinsen and J.D. Collinson, Basin Research (2002), 12, 59–78. Basin Research 14, 531–542.

Wonham, J.P., Jayr, S., Mougamba, R., Chuilon, P., 2000. 3D sedimentary evolution of a canyon fill (Lower Miocene-age) from the Mandorove Formation, offshore Gabon. Marine and Petroleum Geology 17, 175–197.

Wormleaton, P.R., Sellin, R.H.J., Bryant, T., Loveless, J.H., Hey, R.D., Catmur, S.E., 2004. Flow structures in a two-stage channel with a mobile bed. Journal of Hydraulic Research 42, 145–162.

Wormleaton, P.R., Hey, R.D., Sellin, R.H.J., Bryant, T., Loveless, J., Catmur, S.E., 2005. Behavior of meandering overbank channels with graded sand beds. Journal of Hydraulic Engineering 131, 665–681.

Wuellner, D.E., James, W.C., 1989. Braided and meandering submarine fan channel deposits, Tesnus Formation, Marathon Basin, West Texas. Sedimentary Geology 62, 27–45.

Wynn, R.B., Stow, D.A.V., 2002. Classification and characterisation of deep-water sediment waves. Marine Geology 192, 7–22.

Wynn, R.B., Kenyon, N.H., Masson, D.G., Stow, D.A.V., Weaver, P.P.E., 2002a. Characterization and recognition of deep-water channel–lobe transition zones. Bulletin of the American Association of Petroleum Geologists 86, 1441–1462.

Wynn, R.B., Piper, D.J.W., Gee, M.J.R., 2002b. Generation and migration of coarse-grained sediment waves in turbidity current channels and channel–lobe transition zones. Marine Geology 192, 59–78.

Xu, J.P., Noble, M.A., Rosenfeld, L.K., 2004. In-situ measurements of velocity structure within turbidity currents. Geophysical Research Letters 31.

Young, R.A., Slatt, R.M., Staggs, J.G., 2003. Application of ground penetrating radar imaging to deepwater (turbidite) outcrops. Marine and Petroleum Geology 20, 809–821.

Yu, B., Cantelli, A., Marr, J., Pirmez, C., O'Byrne, C., Parker, G., 2006. Experiments on self-channelized subaqueous fans emplaced by turbidity currents and dilute mudflows. Journal of Sedimentary Research 76, 889–902.